Pedestrian - Level Wind Environment around Buildings

Hanqing Wu

A Thesis

in

The Centre

for Building Studies

Presented in Partial Fulfilment of the Requirements

for the Degree of Doctor of Philosophy at

Concordia University

Montreal, Quebec, Canada

April 1994

ISBN 0-315-90909-9

ABSTRACT

Pedestrian - level Wind Environment around Buildings

Hanqing Wu

Concordia University, 1994

In modern cities with more and more tall buildings, wind problems are becoming critical for the safety and comfort of pedestrians. Without general theory available to determine the wind conditions, these problems have to be studied experimentally on a case-by-case basis. General guidelines and specific advice are widely needed for city planning and building design. A systematic study has been carried out on the flow mechanism of building-induced winds, the knowledge generation and representation for application purposes as well as the development of measurement techniques for pedestrian-level wind flows.

Wind flow around building models has been investigated using various experimental techniques. For isolated buildings, a number of flow modules have been established to relate the building dimensions to wind speeds of the front vortex, corner streams, pass-through flows and wake turbulence. An influence scale has been proposed to describe the spatial extent of wind flows around buildings at the pedestrian level. Wind flows around two or multiple building models, such as two buildings in tandem, side-by-side and staggered positions, as well as building-enclosed courtyards have been examined by considering the interaction of flow modules around respective isolated buildings.

Regarding the effect of surrounding street blocks, a set of equations have been derived for estimating wind speeds by building parameters such as the blockage ratio and the height difference.

In addition, statistical models have been applied for analyzing local meteorological records with respect to wind speeds, directions and occurrence frequencies. Considering the features of upstream terrains and surrounding street blocks, a comprehensive procedure has been established to link the pedestrian-level wind conditions around buildings with the long-term weather data.

Results of the current study have been integrated with the literature information to develop a knowledge-based system that automates the preliminary assessment of pedestrian-level wind conditions. A multi-objective decision making process has also been implemented for the selection of remedial measures if required. The developed knowledge-based computer system is very effective to apply research findings in building design and city planning.

ACKNOWLEDGEMENTS

The author wishes to express his sincere gratitude to Dr. T. Stathopoulos for his supervision, guidance and encouragement throughout the course of this study, in particular, for his effort and time in reviewing this thesis and giving suggestions to improve the content.

Many thanks are due to Mr. H. Obermeir for his invaluable assistance in making experiment models and measurement devices, Dr. C. Bédard for his constructive advice on expert systems, Mr. S. Bélanger for his computer expertise, Dr. R. Mallidi for his help in using the infrared video camera, Dr. F. Haghighat for providing the uniform heat generator, and Dr. P. Saathoff for his encouragement and interest in this study. The friendship, assistance and advice of the rest of the staff and fellow graduate students at the Centre for Building Studies is also acknowledged.

Many researchers have generously contributed their up-to-date information along with valuable suggestions to this project. The author is most grateful to Dr. N. Isyumov and Ms. F. Livesey of the University of Western Ontario, Dr. P. Irwin of RWDI Inc., Dr. S. Murakami of Tokyo University, Dr. Y. Uematsu of Tohoku University, Dr. M. Bottema of Eindhoven University of Technology, and others.

The School of Graduate Studies at Concordia University is also appreciated for awarding the author the Concordia Graduate Student Fellowship and the Fee Remission for International Students.

A very special note of thanks is extended to the author's wife, Lilin, for her love, understanding, support and patience.

PEDESTRIAN-LEVEL WIND ENVIRONMENT AROUND BUILDINGS

TABLE OF CONTENTS

LIST OF FIGURES xii

LIST OF TABLES xvi

NOMENCLATURE xviii

CHAPTER 1

INTRODUCTION 1

1.1 GENERAL 1

1.2 OBJECTIVE 2

1.3 APPROACH 3

1.4 THESIS OUTLINE 4

CHAPTER 2

A BRIEF REVIEW OF EXISTING KNOWLEDGE 7

2.1 BACKGROUND 8

2.2 WIND FLOW AROUND BUILDINGS 10

2.3 CRITERIA FOR WIND CONDITIONS 14

2.4 DESIGN GUIDELINES AND REMEDIAL ACTIONS 16

2.5 SUMMARY 20

CHAPTER 3

EXPERIMENTAL TECHNIQUES 22

3.1 WIND-TUNNEL FACILITIES 22

3.2 REQUIREMENTS FOR PEDESTRIAN-LEVEL WIND MEASUREMENTS 24

3.3 THERMAL ANEMOMETER 26

3.4 IRWIN'S SURFACE PRESSURE SENSOR 27

3.5 LASER-DOPPLER ANEMOMETRY 30

3.6 FLOW VISUALIZATION 31

3.7 INFRARED THERMOGRAPHY 34

3.8 SUMMARY 37

CHAPTER 4

WIND FLOW AROUND ISOLATED BUILDING MODELS 39

4.1 FLOW MECHANISM OF ISOLATED BUILDINGS 39

4.2 INFLUENCE SCALE FOR AN ISOLATED RECTANGULAR BUILDING 43

4.3 FRONT VORTEX 45

4.3.1 Wind Speed in Front of Buildings 46

4.3.2 Ground Pressure Distribution 47

4.3.3 Relation between Wind Speeds and Building Dimensions . . . 48

4.4 CORNER STREAM 53

4.4.1 Flow Pattern and Speed Distribution 53

4.4.2 Wind Speed Variation 54

4.5 PASS-THROUGH FLOW 56

4.6 WAKE TURBULENCE 58

4.7 FLUCTUATION OF 3-D TURBULENT FLOW 61

4.8 EFFECT OF WIND DIRECTION 64

4.9 SUMMARY 70

CHAPTER 5

WIND FLOW AROUND TWO- AND MULTI-BUILDING MODELS 72

5.1 TWO BUILDINGS IN TANDEM POSITION 72

5.1.1 Effect of Building Height and Distance 74

5.1.2 Ground Pressure Distributions 76

5.1.3 Prediction of Wind Speed 78

5.2 TWO SIDE-BY-SIDE BUILDINGS 81

5.2.1 Wind Speed along Central Line 82

5.2.2 Effect of Building Dimensions and Distances 83

5.2.3 Speed Distribution over Gap 85

5.3 TWO STAGGERED TALL BUILDINGS 88

5.4 OTHER BUILDING COMBINATIONS 92

5.4.1 Two Buildings 92

5.4.2 Multiple Buildings 95

5.5 COURTYARDS ENCLOSED BY LOW BUILDINGS 96

5.5.1 Courtyard without Opening 97

5.5.2 Courtyard with Opening 99

5.6 STREET BLOCKS 101

5.6.1 Models and Instrumentations 101

5.6.2 Uniform Street Blocks 103

5.6.3 Tall Buildings above Uniform Surroundings 107

5.6.4 Other Considerations 111

5.7 SUMMARY 114

CHAPTER 6

URBAN MICROCLIMATIC WIND CONDITIONS 117

6.1 INFLUENCE ELEMENTS 118

6.2 METEOROLOGICAL DATA 119

6.3 TERRAIN ROUGHNESS 124

6.4 MAIN BUILDING AND IMMEDIATE SURROUNDINGS 129

6.5 ARCHITECTURAL DETAILS AND REMEDIAL ACTIONS 134

6.6 WIND DISCOMFORT CRITERIA 137

6.7 A CASE STUDY 141

6.8 SUMMARY 149

CHAPTER 7

A KNOWLEDGE-BASED SYSTEM 151

7.1 INTRODUCTION 151

7.2 GENERAL ARCHITECTURE OF DEWEN 153

7.3 DETAILED DESCRIPTION OF MAJOR COMPONENTS 155

7.3.1 Model Identification 155

7.3.2 Data Input 157

7.3.3 Combination with Meteorological Data 159

7.3.4 Conformance of Criteria 159

7.3.5 Suggestions and Report 160

7.3 A CASE STUDY 161

7.5 REMEDY SELECTION: MULTI-OBJECTIVE DECISION MAKING 166

7.5.1 Aerodynamic Weight and Utility 167

7.5.2 Non-aerodynamic Concerns 168

7.5.3 An Example for Remedy Selection 170

7.6 SUMMARY 172

CHAPTER 8

CONCLUSIONS AND RECOMMENDATIONS 174

8.1 CONCLUSIONS 174

8.2 SUMMARY OF CONTRIBUTIONS 179

8.3 RECOMMENDATIONS FOR FUTURE WORK 180

REFERENCES 184

APPENDICES

A. WIND EFFECTS ON PEOPLE 197

B. SUMMARY OF DISCOMFORT WIND CRITERIA 199

C. WIND ORDINANCE, CITY BY-LAWS AND GUIDELINES 204

D. EFFECT OF WIND DIRECTION 209

E. MODIFICATION FUNCTION FOR TANDEM BUILDINGS 212

F. WIND CONDITIONS INSIDE COURTYARDS AND OVER OPENINGS 214

G. EFFICIENCY OF TYPICAL REMEDIAL ACTIONS 218

LIST OF FIGURES

Figure	Title	Page
2.0.1	Three elements and their relations in pedestrian-level wind studies	8
2.2.1	Typical aerodynamic effects likely to induce high-speed winds, after Gandemer (1975)	11
2.3.1	Melbourne's criteria for daylight hours for a turbulence intensity of 30%, after Melbourne (1978)	17
2.4.1	Wind speed distributions around tall buildings of different cross sections, after Murakami et al (1979)	19
3.1.1	Profiles of mean wind speeds and turbulence intensity over a simulated suburban terrain	23
3.4.1	Irwin's surface wind sensors reproduced and used in the present study	27
3.4.2	Comparison of mean and rms wind speeds measured by a vertically-installed hot-film anemometer and surface wind sensors	29
3.5.1	3-D wind speeds in front of a tall building	31
3.6.1	Surface flow pattern around an isolated building	32
3.6.2	Vortex flow between two buildings in tandem position	33
3.7.1	Reduced temperatures around isolated tall buildings	35
4.1.1	Windy regions around isolated buildings, after Beranek (1984)	40
4.2.1	(a) Sketch of the flow pattern around a building base; and (b) Relation between the vortex size and the influence scale	44
4.3.1	Mean overspeed ratios in front of buildings	47
4.3.2	Distributions of ground pressure coefficients in front of buildings with different (a) heights; (b) widths; and (c) sizes	49

4.3.3 Schemes of front vortex system, pedestrian-level velocities and ground pressure distribution in front of a building 50

4.3.4 Comparison of front-vortex speeds derived from wind-tunnel experiments and empirical estimations 52

4.4.1 Mean overspeed ratios of corner streams 54

4.4.2 Maximum mean overspeed ratios of corner streams 56

4.5.1 Variation of maximum mean overspeed ratio of pass-through flow with building height 58

4 6.1 Effect of building height on the mean speeds behind buildings 60

4.6.2 Effect of along-wind depth on the mean speeds behind buildings 60

4.7.1 Mean and rms overspeed ratios near the side of a tall building 62

4.7.2 Effect of building height on the rms overspeed ratios behind buildings . . . 63

4.7.3 Effect of along-wind depth on the rms overspeed ratios behind buildings 63

4.8.1 Overspeed ratios around a slender building with different wind incidence 65

4.8.2 Overspeed ratios around a large building with different wind incidence . . 67

4.8.3 Mean and rms overspeed ratios behind buildings oblique to incident wind with θ=30° 68

4.8.4 Variation of wake turbulence with building height and wind direction . . . 69

5.1.1 Two buildings in tandem position 74

5.1.2 Maximum overspeed ratios of mean and rms speeds between two tandem buildings 75

5.1.3 Ground pressure distributions between two tandem buildings with various (a) heights of the front building and (b) distances between buildings 77

5.1.4 (a) Overspeed ratios and (b) modification functions for tandem buildings (data from several sources) 79

5.1.5 Contours of modification function for tandem building models, derived from literature information and the current study 80

5.2.1 Overspeed ratios in the gap between two identical buildings 83

5.2.2 Modification functions for the gap flow between two identical side-by-side buildings 85

5.2.3 Distributions of mean overspeed ratios over gaps between buildings 86

5.3.1 Overspeed ratios around corners of a slender building staggered to the other 89

5.3.2 Contours of overspeed ratios of corner streams around staggered buildings 91

5.3.3 Transversal wind drift caused by circuit short-cutting of pressure field around two slab-type buildings 92

5.4.1 Maximum overspeed ratios of the mean and rms wind speeds at their occurring positions in gaps between two tall buildings 93

5.4.2 Thermal images of reduced temperatures around two-building models . . . 94

5.5.1 Thermal images of reduced temperatures around courtyards enclosed by low buildings without openings 97

5.5.2 Thermal images of reduced temperatures around courtyards enclosed by low buildings with openings 100

5.6.1 A typical model arrangement with a tall building surrounded by uniform street blocks 102

5.6.2 Measurement points on streets 25 m wide 103

5.6.3 A sketch of simplified street blocks: dimensions and areas 104

5.6.4 Averaged wind speeds over the along-wind streets between uniform blocks. 106

5.6.5 Empirical relation between the average wind speeds and blockage ratios 106

5.6.6 Wind speed ratios distributed around tall buildings standing among uniform street blocks 108

5.6.7 Variation of maximum wind-speed amplification with the height difference 109

5.6.8 Comparison of measured and predicted wind speeds around tall buildings with uniform surroundings 110

5.6.9 Variation of wind speeds in front of tall buildings with height differences 110

5.6.10 Effect of wind incidence on speeds around uniform street blocks 112

5.6.11 Effect of tall building locations within a block on wind speeds along adjacent streets 113

6.1.1 Evolution of wind profiles influenced by numerous elements 118

6.2.1 Wind roses drawn from data recorded at Dorval Airport, Montreal 121

6.4.1 Boundary layer flow approaching the building of interest 132

6.7.1 Plan view of the building and its surrounding for the case study 142

6.7.2 Annual hourly maximum speeds around block corners, calculated from wind-tunnel measurements and weather station records for daylight hours 148

7.2.1 General architecture of the knowledge-based system DEWEN 154

7.3.1 Three basic building models in DEWEN 156

7.3.2 The main street block and surroundings for data input of Model B 158

7.3.3 General suggestions of remedies for wind-speed reduction 161

7.4.1 Building model evaluated in case study 162

7.4.2 Input data stored in a spreadsheet file 163

7.4.3 Comparison of average of wind speeds measured in wind tunnel and predicted by the computer system 166

7.5.1 General structure of decision making for remedy selections 167

7.5.2 A consulting case for the selection of remedies 171

LIST OF TABLES

Table	Title	Page
3.2.1	Point and area techniques for assessing pedestrian-level winds	25
3.8.1	Comparison of wind tunnel methods for the assessment of pedestrian-level winds	38
4.1.1	Flow mechanisms around isolated, rectangular buildings	42
5.0.1	Flow mechanisms around two and multiple building models	73
5.4.1	Overall impact values of the building models in Fig. 5.4.2	95
5.5.1	Normalized overall impact values of the courtyard models in Fig. 5.5.1	98
5.5.2	Normalized overall impact values of the courtyard models in Fig. 5.5.2	101
6.2.1	Numbers of observations of classified wind speeds in 16 compass directions	120
6.2.2	Weibull constants for three specific time periods estimated from meteorological records for 31 years at Dorval Airport, Montreal	123
6.3.1	Classification of terrains and roughness lengths, after Wieringa (1992)	126
6.5.1	Aerodynamic utility values of typical remedies for three flow mechanisms	137
6.6.1	Comfort criteria for windiness proposed by Davenport (1972)	138
6.6.2	Wind discomfort criteria for daylight hours, Melbourne (1978)	139
6.7.1	Measured wind speeds in m/s at 18 positions around building models for 6 wind directions	144
6.7.2	Estimated wind speeds with the exceedance frequency of 0.001	147
7.4.1	Modification factors estimated for four streets and 16 wind directions	163
7.4.2	Calculated exceedance frequencies in percent for different threshold speeds	

and time periods 164

7.5.1 Weight of aerodynamic factor (W_a) assigned for human activities and frequencies of exceedance of mean wind speeds higher than 5 m/s 168

NOMENCLATURE

A_e	courtyard area enclosed by buildings
A_L	area of building lot
A_R	area of building roofs in a street block
A_S	windward area of buildings in a street block
B_L	the larger of windward dimensions of a rectangular building
B_S	the smaller of windward dimensions of a rectangular building
b	measurement height of wind speeds at pedestrian level
C_i	constant
C_p	ground wind pressure coefficient
c_t	Weibull constant
D	along-wind length (depth) of a rectangular building
	diameter of the base hole of Irwin's sensor
d	depth of the upstream building in two tandem buildings
	external diameter of Irwin's sensor
d_i	internal diameter of Irwin's sensor
f_i	modification factor
g	gust factor
H	building height
$\bar{H}$	average height of buildings around a courtyard
h	height of Irwin's sensor

h	height of the upstream building of two tandem buildings
$\bar{h}$	general roof-top level or average height of obstacles
K	mean overspeed ratio
K_{CS}	maximum mean overspeed ratio of corner streams
K_{FV}	maximum mean overspeed ratio of front vortex
K_{GP}	maximum mean overspeed ratio of gap flow between buildings side by side
K_{PT}	maximum mean overspeed ratio of pass-through flow
K_{TD}	maximum mean overspeed ratio of vortex between tandem buildings
k	rms overspeed ratio
k_i	Weibull constant
L	distance between buildings
M	modification factor or function
$P(>V_o(\theta_i))$	probability of wind exceedance in angle sector θ_i recorded at a weather station
$P(>V_T)$	probability of wind exceedance of the threshold speed V_T for all sectors
p_i	Weibull constant: accumulated probability for angle sector θ_i
R_B	blockage ratio of uniform street blocks
S	influence scale of a building to pedestrian-level winds
S_V	vortex size observed in flow visualization around building base
U	mean wind speed in the direction of approaching wind
	utility value of a remedy
u_*	shear velocity
V	horizontal mean wind speed perpendicular to approach wind

V	horizontal mean wind speed
	instantaneous wind speed measured by Irwin's sensor
V_d	typical speed of down-washing flow
$\overline{V}_o$	average speed over along-wind streets between uniform blocks
$V_o(\theta_i)$	wind speed in angle sector θ_i recorded at a weather station
V_T	threshold wind speed
W	cross-wind length (width) of rectangular building
	inside length of building-enclosed courtyard
	vertical mean wind speed
	weight in the selection of remedies
w	width of the upstream building of two tandem buildings
X, x	coordinator or distance in the direction of approach wind
Y, y	horizontal coordinator or distance perpendicular to approach wind
Z, z	vertical coordinator, height above ground
z_o	surface roughness length
z_d	vertical displacement of zero plane of wind profile
Z_r	reference height

Greek Symbols

α	index of power law of boundary-layer wind profile
	constant
β	constant
ΔP	pressure difference between two inlets of Irwin's sensor

δ	gradient height of boundary-layer flow
$\delta T(x,y)$	reduced temperature detected by infrared thermography
θ	wind angle of incidence
θ_i	wind angle sector in a 16-direction compass
κ	von Kármán constant
ρ	air density
$\varphi(bldg)$	function of building dimensions and geometry
Ω	overall wind impact calculated by the integration of δT

Subscripts

a	in the absence of building
	along wind
	aerodynamic
e	effective (speed)
	enclosed (area)
i	*i*th sector in a 16-direction compass
G	at gradient height of atmospheric boundary layer
H	at building height
h	(function) relevant to front building height
L	(function) relevant to distance between buildings
M	maximum value of
m, *mean*	mean value of
n	non-aerodynamic

o	overall value of
p	peak value of (wind speed)
rms	rms value of
X, x	in direction of approach wind
Y, y	perpendicular to approach wind, horizontal
Z, z	at the height above ground

Abbreviations

3-D	three dimension(al)
BRE	Building Research Establishment, U.K.
DEWEN	Discomfort Evaluation of Wind ENvironment
KBS	Knowledge-Based System
LDA	Laser Doppler Anemometer
rms	root-mean-square

CHAPTER 1

INTRODUCTION

1.1 GENERAL

It has long been recognized that buildings may create inhospitable or even dangerous wind environmental conditions at ground level. In Roman times, Vitruvius recommended that streets be oriented diagonally to the prevailing winter winds in order to maximize the wind shelter for pedestrians (Aynsley, 1989). In Chinese, *feng-shui*, meaning literally *wind-water*, is the word to appraise the location and orientation of a house, that is supposed to have an influence on the fortune of the family.

In modern cities with more and more tall buildings, wind problems are becoming critical for city planning and building design. Among the effects created by winds in the vicinity of buildings, the most significant is the impact on safety and comfort of pedestrians. Note that two elderly ladies died from skull injuries in the United Kingdom after being blown over by winds near high-rise buildings (Penwarden, 1973). Several accidents caused by building-induced winds in cities were also reported by Melbourne and Joubert (1971), Jackson (1978), Aynsley (1989) and others.

With growing awareness of the wind problems, both field measurements and laboratory tests have progressed around the world in the last 30 years. More and more city authorities are in the process of establishing city bylaws and acceptance criteria for the wind conditions around buildings. Demonstration of satisfactory wind environment is required to obtain a permit for new projects in a number of cities, such as Boston, Calgary, London, Montreal, San Francisco, Tokyo etc (Stathopoulos and Saathoff, 1989).

Wind environmental conditions around a building at a built-up site are influenced by the building geometry, surroundings, upstream terrain and local meteorological records as well. During the process of building design and city planning, decisions made at preliminary stages have the most significant impact on the wind environment. It is thus desired to take the wind problems into consideration at the earliest stages when most contributing elements are allowed to be altered. Unfortunately, there is no general theory available to determine the wind environment or to provide remedial suggestions for unacceptable wind conditions. Actual problems have to be investigated on a case-by-case basis, traditionally by boundary-layer wind tunnel experiments. Therefore, it is highly desirable to carry out a systematic study on the major contributing elements for understanding the fundamental mechanisms involved and for generating guidelines and rules of thumb accessible to the practitioners in city planning and building design.

1.2 OBJECTIVE

The literature information on pedestrian-level wind studies had thoroughly been reviewed when the current research project started. A general impression received from the review was that there were clear gaps between laboratory studies and building applications. Research outcomes were either too specific to provide general guidance or too idealized for practical circumstances.

This project aims at a comprehensive understanding of the pedestrian-level wind flow around buildings. The major components influencing local wind behaviours are investigated extensively through experimental measurements and theoretical analyses. It is also attempted to automate the procedures for evaluating the wind environment around buildings and for providing suggestions to cure unacceptable wind conditions. The general objective can be briefly stated as follows:

(1) Re-evaluation of literature information relevant to pedestrian-level winds;

(2) Understanding of aerodynamics contributing to the wind conditions around buildings;

(3) Classification, generalization and integration of research findings; and

(4) Presentation of knowledge via a user-friendly interface for design and planning.

1.3 APPROACH

In order to attain the desired goals, a unique research approach has been adopted in the current study.

Although most previous studies were devoted to specific building cases, some basic principles or rules of thumb may be drawn out by a detailed analysis and a thorough synthesis of the literature data. The organized knowledge has formed a solid foundation for advanced investigations.

Several wind-tunnel techniques have been applied for capturing details of the wind flow around buildings at the pedestrian level. These consist of some well-established methods like the Laser Doppler anemometer, thermal anemometers, surface pressure sensors and surface flow visualization. A new technique based on infrared thermography has been developed for assessing the variation of pedestrian-level wind flows around buildings.

More fundamental studies can provide further insight into problems. Appropriate models have been established for those elements responsible for the wind environmental conditions at the pedestrian level. Building complexes, for example, are classified into several simple building models, in which isolated, rectangular buildings serve as a bench-mark model. Flows around building groups, such as twin towers, building-enclosed courtyards and street blocks, are thus considered as the variations or modifications of wind flows around respective isolated buildings. To establish the relations between wind conditions and building models, wind-tunnel measurements are carried out for a range of building configurations.

Research outcomes from the present study are then integrated with the literature information to constitute the knowledge base for a computer system. The technique of knowledge-based system has been remarkable for linking academic research to engineering practice. It has been applied here as a tool to represent the organized knowledge via a user-friendly interface. The developed computer system automates the process of evaluating wind conditions and recommending remedial actions for further improvement of wind environment.

1.4 THESIS OUTLINE

This thesis consists of eight chapters, a list of references and seven appendices. A concise section is provided at the end of each chapter to summarize the significant contents presented.

The literature information of pedestrian-level wind studies is briefly reviewed in Chapter 2 with concentration on the inter-relationships between buildings, wind and people. Detailed results are also cited in relevant sections whenever necessary for the knowledge expansion and confirmation. Experimental techniques developed and utilized in the current study are described in Chapter 3. Comparisons of these techniques are made with quantitative results of turbulent wind flows around buildings at ground level.

Chapter 4 displays experimental results of wind conditions around isolated building models. Detailed discussions are presented for wind speed variations and spatial impacts induced by the front vortex, corner stream, pass-through flow and wake turbulence. Chapter 5 presents wind speeds around more complex building models, including two buildings in different positions, building-enclosed courtyards, and tall buildings surrounded by street blocks.

These data are integrated with the literature information to derive a set of basic provisions for several building configurations. The knowledge regarding other aspects of the wind environment evaluation is organized and discussed in Chapter 6 focusing on the probability analysis of meteorological records, the estimation of terrain effects, the functioning of wind discomfort criteria and the decision making process for remedy selections.

Based on the information obtained, a knowledge-based computer system is developed for the assessment of wind environmental conditions around buildings. The system is described in Chapter 7 where its general architecture, primary components and application examples are presented.

As the conclusion of this study, Chapter 8 summarizes the contributions of this study to both wind engineering fundamentals and building applications. Recommendations for the future work are also provided in this chapter regarding such aspects as experimental techniques for wind measurements, the modelling of actual buildings, the refinement of the knowledge-based system, and the potential application in air pollutant dispersion and snow drifting.

CHAPTER 2

A BRIEF REVIEW OF EXISTING KNOWLEDGE

Wind flow around buildings has a multitude of effects, such as, increasing convective heat transfer, promoting rain penetration, diluting air pollutants, creating noise, flying dust and other debris, drifting snow, and damaging plants and trees. The most significant, however, is the mechanical and thermodynamic impacts on pedestrians. From time to time, buildings, especially tall buildings, are blamed for creating adverse wind conditions against pedestrian comfort and safety, that has to be considered during building design and city planning. Research attention has been drawn to investigate the inter-relationships between building, wind and man, see Fig. 2.0.1, that may be summarized in the following issues:

(1) How buildings induce adverse wind conditions at the pedestrian level;
(2) How the pedestrian-level wind affects human comfort and safety; and
(3) How designers and planners can build for better wind environmental conditions.

This chapter briefly reviews the state-of-the-art on the three issues. More specific data may also be cited in other relevant sections of the thesis. For general information about the pedestrian-level wind studies, see books by Aynsley, Melbourne and Vickery (1977), Lawson (1980) and Simiu and Scanlan (1986), and papers by Isyumov and Davenport (1975a), Lawson (1978), Durgin and Chock (1982) and Hosker Jr. (1985).

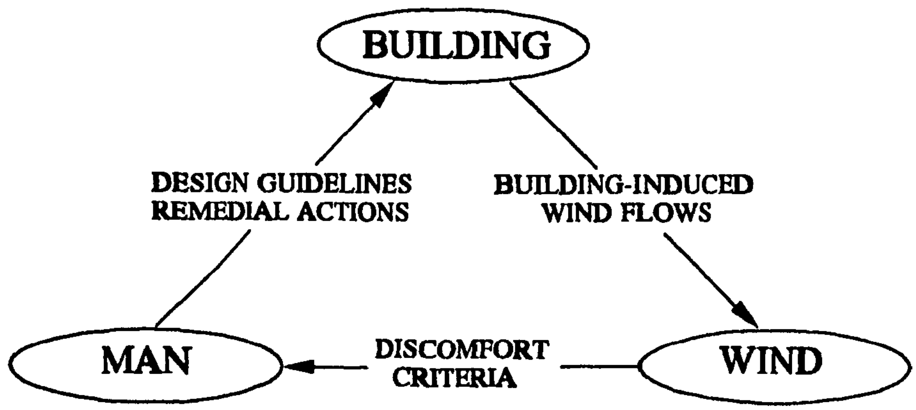

Fig. 2.0.1 Three elements and their relations in pedestrian wind studies.

2.1 BACKGROUND

Wind-tunnel tests, full-scale measurements and numerical computations can be employed for pedestrian-level wind studies. The full-scale measurement is a direct way but with several limitations; for example, it is time-consuming, expensive and impossible before the projected building is completed. Advancement of computational techniques, e.g. Paterson and Apelt (1986), Baskaran and Stathopoulos (1989) and Murakami (1990), provides another means to handle the problem, though more effort is still needed for the numerical simulation of wind characteristics, particularly the 3-D turbulence near ground. Comparatively speaking, the wind-tunnel testing is a convenient avenue to evaluate the wind conditions around buildings and to examine the efficiency of remedial actions. Natural winds over different terrains can be simulated and controlled as desired in an atmospheric boundary-layer wind tunnel with scaled models. Reliable predictions could be obtained after combining wind tunnel results with local meteorological records.

The variation of wind speeds induced by the presence of buildings may be described by the term of *Overspeed Ratio*:

$$K = \frac{V}{V_a} \tag{2.1.1}$$

in which the building-induced speed V is compared with the reference V_a taken at the same level, usually 2 meters above the ground, when the buildings of interest are absent.

These wind speeds can be the mean ($\bar{V}$) and rms (V_{rms}) values or the effective speeds (V_e) defined as:

$$V_e = \overline{V} + g\,V_{rms} \tag{2.1.2}$$

where the gust factor g may be in the range of 0-4 as suggested by several researchers, see Hunt et al (1976), Uematsu and Yamada (1991), Livesey et al (1992) and Letchford and Ginger (1993). However, the mean speed (when g=0 in Eq. 2.1.2) is more customarily utilized in the literature than others for calculating the wind speed amplification using the definition of Eq. 2.1.1.

The impact area of strong winds is another major concern in pedestrian-level wind studies. Beranek (1984) contributed a definition of the *Influence Area* through extensive sand erosion tests for isolated rectangular buildings. He studied the relation between building dimensions and the influence areas over which the overspeed ratio exceeds a certain level. Uematsu et al (1992) defined an overall indicator of wind environment, which is the integration of overspeed ratios over the windy areas around buildings. However, a functional geometric scale for estimating the spatial extent of pedestrian-level winds induced by buildings was not found.

2.2 WIND FLOW AROUND BUILDINGS

An isolated, rectangular building is the simplest model explored in pedestrian-level wind studies. Due to pressure differences around buildings, high speed winds may occur at regions of building's front, corners, wake area and any underneath passage, if applicable. The wind flow around the base of a building could be described through a set of *Flow Modules* (Morkovin, 1972). Fundamental investigation about these modules has been done by Baker (1977) and Hunt et al (1978), and reviewed by Hosker Jr. (1985) and Meroney (1988). One of these modules is the rolled-up horseshoe-shaped vortex, which is the major cause of speedy winds resulting in pedestrian discomfort around tall buildings.

More specifically, Melbourne and Joubert (1971) presented wind-tunnel measurements for buildings from 15 to 225 m high in terms of the velocity pressure ratios (mean speed ratios squared). Their data, converted to mean overspeed ratios, provided maximum values from 1.1 to 2.3 in an underneath passage of 7.5 meter high, and from 1.3 to 2.1 around the building upstream corner at 5 m above the ground. Kamei and Maruta (1979) studied effects of (1) the building height, (2) the aspect ratio of building cross section, (3) the wind direction, (4) the measurement height, (5) the geometrical scale of test, and (6) the wind profile. Some of their results were confirmed by Stathopoulos (1985) on a simulated suburban terrain in a boundary-layer wind tunnel.

Wind-tunnel studies on single buildings are essential for understanding the flow behaviour around buildings, but actual wind conditions are much more complicated. For the purpose of generalization, Gandemer (1975) investigated a large number of site plans, specified twelve typical aerodynamic effects (Fig. 2.2.1) likely to induce speedy winds

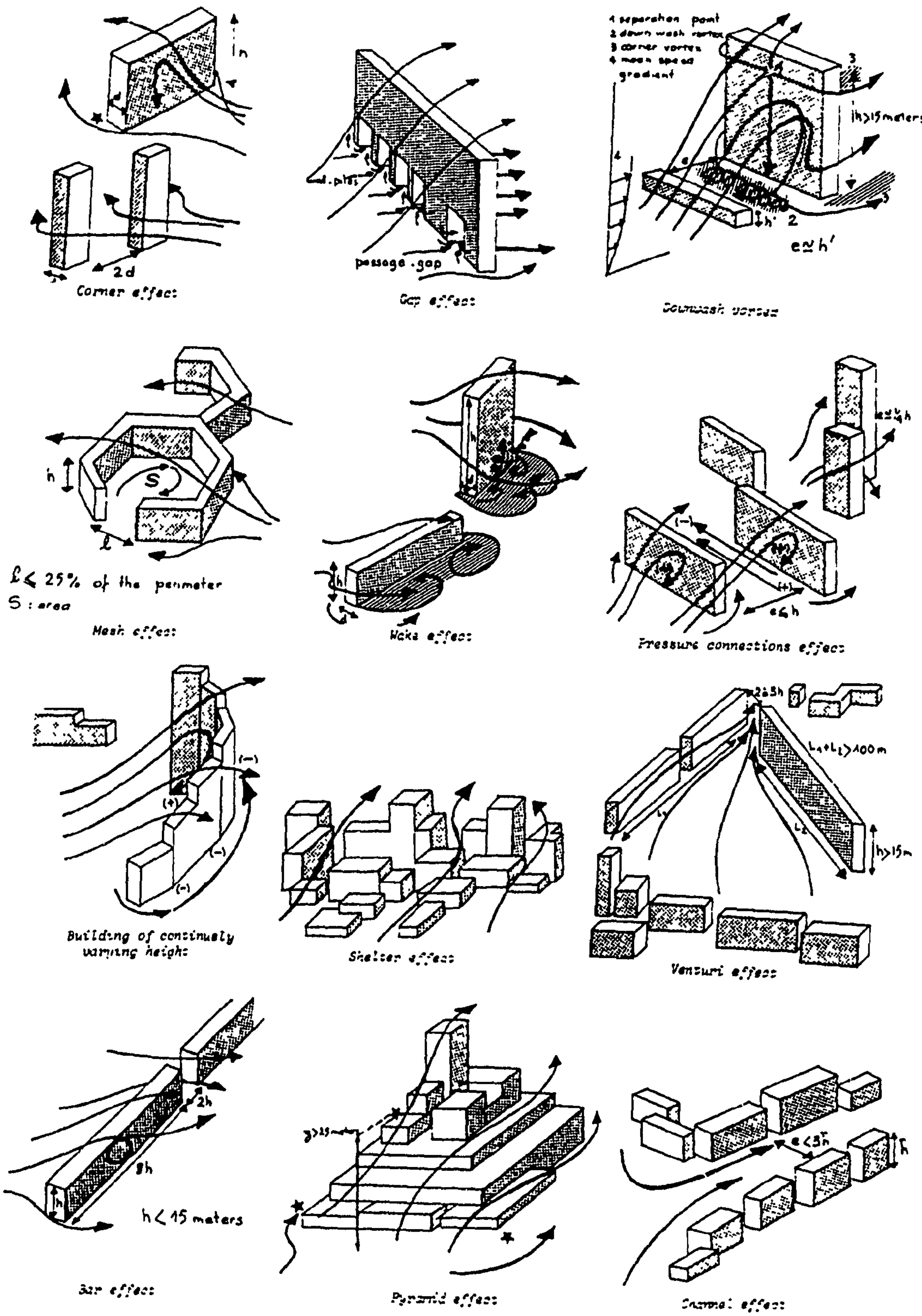

Fig. 2.2.1 Typical aerodynamic effects likely to induce high-speed winds, after Gandemer (1975).

and quantified the corresponding discomfort parameter defined by Eqs 2.1.1 and 2.1.2 with g=1. In addition, remedial actions were also recommended for preventing these model sites from unpleasant wind conditions.

Among those aerodynamic models, the combination of a tall building with a relatively low building upstream has been of particular interest to researchers. Tests have been carried out both in full scale field and wind tunnel environment by Wise, et al (1965), Melbourne and Joubert (1971), Isyumov and Davenport (1975a) and others. For example, Penwarden and Wise (1975) simulated suburban environment in their wind tunnel with a geometric scale of 1/120. The wind speeds were expressed in terms of ratio $\overline{V}/\overline{V}_H$, where $\overline{V}$ and $\overline{V}_H$ were mean wind speeds at pedestrian level (3 meters in their tests) and at building height H, respectively. Speed ratios at the front, corner and pass-through of the tall building were of the order of 0.5, 0.95 and 1.2 for a range of practical situations. Britter and Hunt (1979) even attempted to develop an analytical model for predicting the vortex flow between specific building combinations.

When the wind flow comes along the passage between two buildings, high speed flow may happen in the passage due to the so-called *Channelling Effect*. Wind speeds along the central line between two identical buildings were measured in a shear flow by Ishizaki and Sung (1971). Wiren's research (1975) for the passage flow between block-type buildings revealed that the relative wind speed increased with increasing height and width of buildings, and also with decreasing passage width, but his results were restricted by building heights (2-8 storeys). Stathopoulos and Storms (1986) measured the mean velocity and the turbulence intensity for different wind azimuths and for a number of dimensions including the building height from 20 to 60 m and the passage width from 6 to 10 m. Their results disclosed that the most critical wind velocity conditions occurred at a point near the passage entrance for a wind direction skewed by 30° from the passage central line. Beranek (1984) visualized the flow patterns around a group of high-rise buildings in both perpendicular and parallel arrangements. The concept of influence area for single buildings was applied to evaluate the flow interaction. One of his conclusions was that most phenomena which occurred around building complexes could be described as variations or modifications of the basic air flow patterns around single buildings or simple building configurations, but no quantitative relations were supplied in addition to this general statement.

Studies on more complex building configurations have also been reported. Wind speeds around the model of a high-rise building surrounded by relatively low blocks were measured by Murakami et al (1979), Isyumov et al (1985), Livesey (1991) and Jamieson (1992). Wind speeds on the streets between those blocks varied with street widths, building and surrounding heights and wind directions. The high-speed wind caused by a tall building might sweep into a few blocks downstream according to Livesey (1991).

Some special areas in cities, like play fields. courtyards and stadia, should be well sheltered so that calm wind conditions prevail. For these areas, Gandemer (1975) introduced a non-dimensional parameter $A_e/\bar{H}^2$, where A_e was the enclosed area and $\bar{H}$ the average height of the buildings forming the enclosure. The wind conditions in this area were found likely to be comfortable if $A_e/\bar{H}^2<30$ for closed surroundings, or <10 for openings not exceeding 25% of the perimeter. Ettouney (1977) studied the quadrangle-shaped house complexes and suggested that the internal courtyard with dimensions of the order of two to four times the height of the surrounding walls ($A_e/\bar{H}^2$=4 to 16) be optimum from the shelter viewpoint.

In addition to above model investigation, previous studies were also devoted to practical cases for evaluating the wind environment around specific building projects. Actual winds were simulated and building configurations were tested in wind tunnels. Comparisons of full-scale and wind-tunnel data implied a generally acceptable agreement as demonstrated by Apperley and Vickery (1974) for a high-rise building; Isyumov and Davenport (1975b) for a plaza surrounded by tall buildings; Lee and Hussain (1979) for a tower on a university campus; Dye (1980) for a relatively isolated tower, Williams and Wardlaw (1992) for the central area of the City of Ottawa and Letchford and Ginger (1993) for the Brisbane CBD. These data from specific cases are very informative for verifying model-study results and expanding the existing knowledge.

2.3 CRITERIA FOR WIND CONDITIONS

The most serious problem wind flow can create to a pedestrian is to blow him/her over. Wind can also cause difficulty for walking, strolling, shopping etc. For the assessment of wind effects, both the mechanical and thermal effects of wind have been evaluated and compared with observed data by means of basic mechanical and thermodynamic principles. An attempt to assess the effect of building-induced winds on people may become extremely complex due to the interaction of so many factors, such as the wind speed, temperature, warmth of clothing, humidity, human activity, precipitation and others. When safety is concerned, the mechanical force on human bodies plays a dominant role comparing with thermal effects. For details of thermal effects, see Fanger

(1972) and Penwarden (1973).

By a field observation, Wise (1971) noted that at 5 m/s, there was unpleasant disturbance to clothing and hair. Melbourne and Joubert (1971) referred to the danger of persons being blown over at a gust speed of about 23 m/s. These two wind speeds are usually cited as the onset of discomfort and the limit for safety, respectively. Penwarden et al (1978) measured wind drags on 331 people standing in a wind tunnel with steady, uniform speeds. Experiments carried out by Hunt et al (1978) showed how the performance of simple everyday tasks were affected by wind, with and without turbulence. Both the subjective verbal assessment and force measurements indicated the importance of gust wind variations. Movie records of over 2000 pedestrians were analyzed by Murakami and Deguchi (1981) for the so-called *Footstep Irregularity* and *Body Balance*. Residents' diaries were also surveyed by Murakami et al (1986) for evaluating the wind environment by daily peak gust winds. An evaluation of subjective semantic assessment was submitted to the City of Montreal by Stathopoulos and Saathoff (1989) regarding the state of mind, ability to walk and appearance for different wind conditions as perceived by adults and children.

Wind effects on people under different wind speeds are presented in Appendix A, based on various sources of wind-tunnel tests and registered observations. They constitute the background for the establishment of discomfort criteria of wind environment.

The discomfort criteria are statements specifying acceptable wind speeds under certain occurrence frequencies for given human activities. Since 1970, a number of wind discomfort criteria have been developed, e.g. Davenport (1972), Penwarden (1973), Lawson and Penwarden (1975), Penwarden and Wise (1975), Hunt et al (1976), Cohen et al (1977), Melbourne (1978), Murakami and Deguchi (1981), Murakami et al (1986) and Soligo et al (1993). About these criteria, detailed specifications are summarized in Appendix B. An example is given in Fig. 2.3.1, which shows the criteria proposed by Melbourne (1978). For each activity type, there are two curves indicating the mean and peak speeds for various frequencies of occurrence, above which wind conditions may become objectionable to individuals engaged in that activity.

An explicit comparison between those criteria seems infeasible due to different implementations of wind speeds (Beaufort Scale, mean, peak and equivalent speeds over variable time durations), human activities, exceedance frequencies (number or frequency of occurrence for all hours or day hours in grouped seasons) and presentation formats. After a comparison of several criteria for daylight hours for a specific turbulence intensity of 15%, Melbourne (1978) stated that the degree of agreement between the criteria when presented in probabilistic terms was quite remarkable for a phenomenon which relied almost completely on subjective assessment. In contrast, a review by Ratcliff and Peterka (1989) commented on differences among the criteria, with those of Melbourne (1978) being more restrictive and those of Lawson and Penwarden (1975) being too lenient. It was suggested in the review that using several criteria, along with engineering judgement regarding the behaviour and limitations of the criteria, be the most acceptable procedure.

2.4 DESIGN GUIDELINES AND REMEDIAL ACTIONS

As mentioned before, in the process of building design and city planning decisions made at the preliminary design stage have the largest impact on the building performance.

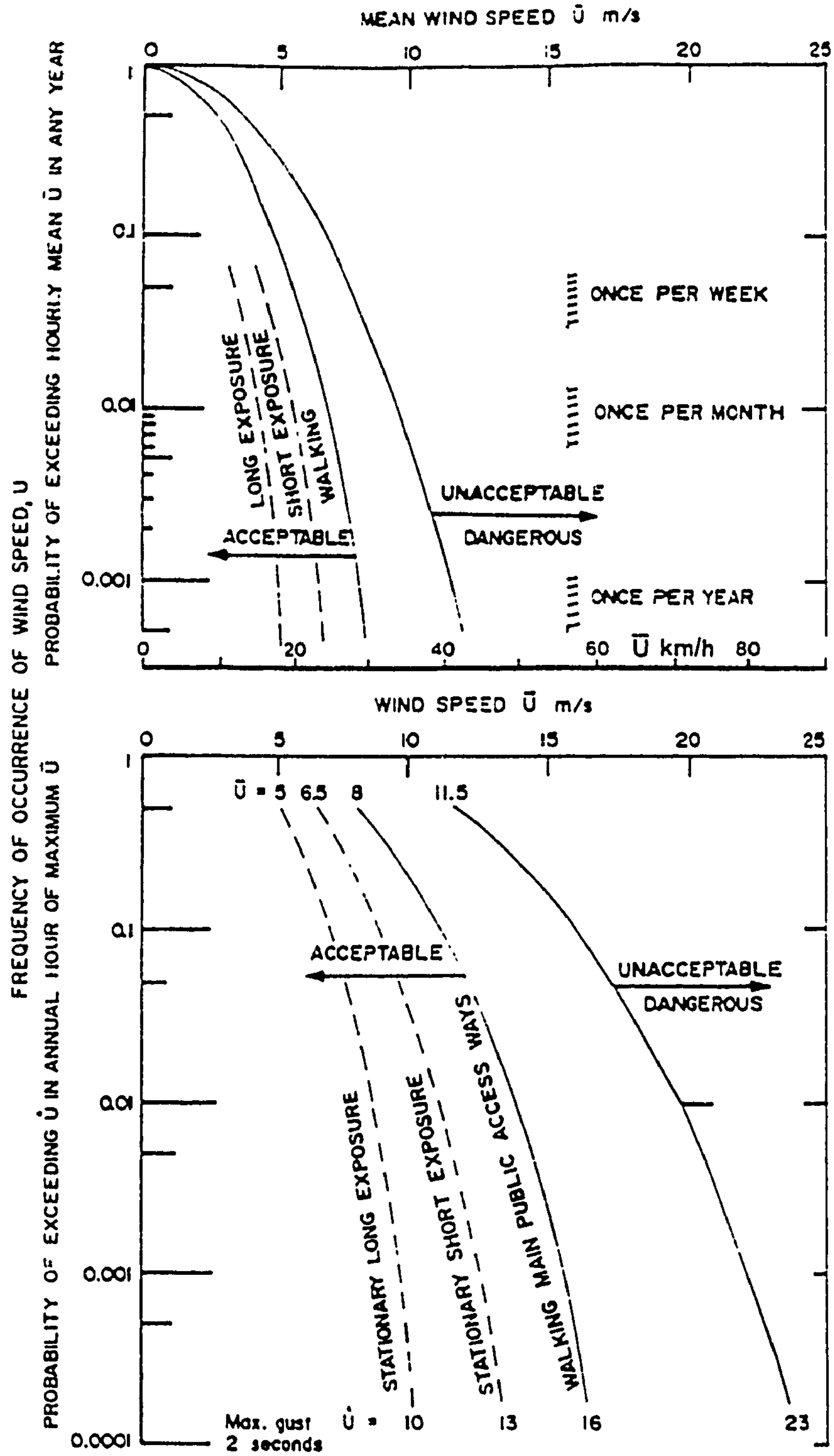

Fig. 2.3.1 Melbourne's criteria for daylight hours for a turbulence intensity of 30%, after Melbourne (1978).

Therefore, a number of cities have established by-laws and ordinances, as summarized in Appendix C, for purposes of guiding engineers and architects to achieve a better urban environment. If the wind conditions at a projected development are not acceptable, the design has to be modified.

In fact, the most substantial action for wind reduction is to reduce the building height. Numerous other measures, such as avoiding the direct exposure of a large building surface to prevailing winds, changing building geometry, placing building on a podium, designing building with setbacks, providing upstream shielding, and keeping pedestrian area away from tall buildings, have been suggested in practice. Murakami et al (1979) reported useful data such as shown in Fig. 2.4.1 for wind speeds around high-rise buildings of different cross sections. The wind-speed variation can be observed from the contours of speed ratios around main buildings. Stathopoulos (1985) pointed out that a chamfered building corner at 45 degree to the face of a tall square building might significantly reduce the strong wind area around the corner whereas maximum values of speeds are little affected. Jamieson et al (1992) carried out wind measurements for the effect of architectural details of a tall building surrounded by uniform street blocks.

For buildings after construction, however, the task of reduction of high wind speeds in their vicinity is much more complex and challenging. Remedial measures such as building a roof over pedestrian areas, installing screens and windbreaks, building canopies, providing handrails and using aerodynamic attachments can be used for improving existing wind conditions. For example, Merati et al (1979) found, by means of smoke visualization and speed measurements for a 20 cm high building model in a 60 cm deep simulated boundary layer, that the best position for attaching a canopy to lessen

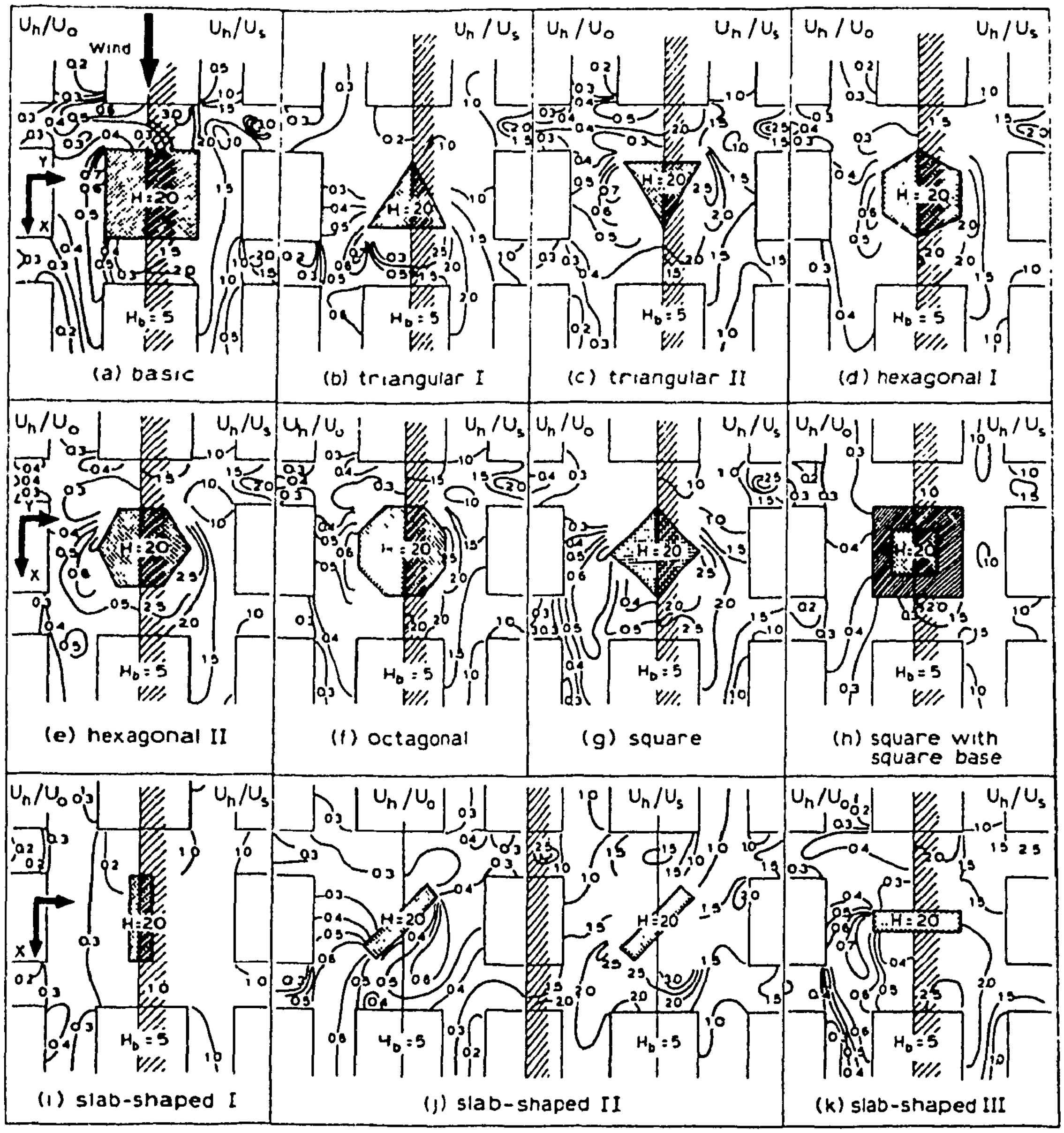

Fig. 2.4.1 Wind speed distributions around tall buildings of different cross sections, after Murakami et al (1979).

the pedestrian wind speed was at one quarter of building height. Other researchers recommended that the suitable canopy height be at the second or third floor (Lawson, 1980).

Various windbreaks were studied by Gandemer (1979) in open areas regarding the aerodynamic influence of their permeability, shapes and the sizes. Flow patterns and shelter effects in the lee of different fences were described and discussed in terms of their efficiency relating to pedestrian comfort. Similar results about the design of windbreaks are available in the book by Melarago (1982). Wake effects of obstacles like houses, trees and dikes were studied by Leene (1992). A set of graphs were proposed for determining the speed reduction as a function of the obstacle height and width, the wind direction, the end effect and the relative roughness. However, the efficiency of wind shelters has not been tested for urban environment, especially in the vicinity of tall buildings.

Besides, there are some apparent difficulties with the selection and evaluation of certain measures for a specific building site. An aerodynamically effective action might not be acceptable from the architectural, economic, or even political viewpoint.

2.5 SUMMARY

This chapter highlights some typical results in pedestrian-level wind studies in the last 30 years. Section 2.1 provides the background of research methods and describing parameters. Typical studies on the wind flow around buildings are discussed in Section 2.2. Wind effects on pedestrians along with several criteria for comfort and safety are explained in Section 2.3. Finally, Section 2.4 discusses remedial actions and their potentials for improving the wind environment.

Essential knowledge is, to a certain extent, available now for elucidating a variety of aspects of pedestrian-level winds. With the growth of experience in this field, more rules of thumb may be drawn out as design guidelines. However, this review indicates in general that some of model experiments are extremely idealized and dissociated from practical situations. On the other hand, data from most consulting case studies are somewhat disorganized so that universal trends cannot readily be obtained for other applications. In addition, a number of problems remain unsolved. These contain the criteria used to evaluate the data and the repeatability between results from different laboratories (Durgin, 1989), the latter depending upon wind climate analysis, atmospheric boundary-layer simulation, accuracy of station location, measurement technique and the accuracy of building and city models. Based on this review, it is determined to have the research project concentrating on the following topics:

(1) Development of better measurement techniques for assessing pedestrian-level winds;

(2) Investigation of wind mechanisms around typical building models to establish the relations between wind conditions and building configurations;

(3) Classification, generalization and integration of the information of pedestrian-level winds; and

(4) Representation of the knowledge in a user-friendly interface for building design and city planning applications.

These four topics are addressed in the thesis with Chapter 3 on Topic (1), Chapters 4 and 5 on Topic (2), Chapter 6 on Topic (3), and Chapter 7 on Topic (4).

CHAPTER 3

EXPERIMENTAL TECHNIQUES

3.1 WIND-TUNNEL FACILITIES

Experimental investigations for the wind environmental conditions around buildings have been carried out in a boundary-layer wind tunnel at the Building Aerodynamics Laboratory in the Centre for Building Studies, Concordia University. The wind tunnel (Stathopoulos, 1984), 12 m long and 1.8 m wide, has an adjustable ceiling height between 1.6 m and 2.0 m in order to ensure a zero pressure gradient along the flow direction under different simulated conditions. There is a turntable at the working section for studying the effect of wind directions. When a suburban exposure is simulated as in this study, the maximum wind speed at the gradient height is about 13 m/s. A typical profile of wind speeds can be fitted by the conventional power law with an exponent equal to 0.25 as shown in Fig. 3.1.1. The turbulence intensity is about 4% at the gradient height and increases to its maximum of 23% near the ground. A geometric scale of 1/400 to 1/500 is considered appropriate for the simulation of the most pertinent wind characteristics.

In addition, a small wind tunnel with a smoke generator has also been employed for the purpose of 3-D flow visualization (Stathopoulos and Wu, 1994). The tunnel is small in dimensions with a total length of 4 m and a square cross section of 0.25 m. Air flow in this suction, open-circuit tunnel is found uniform with controllable wind speeds

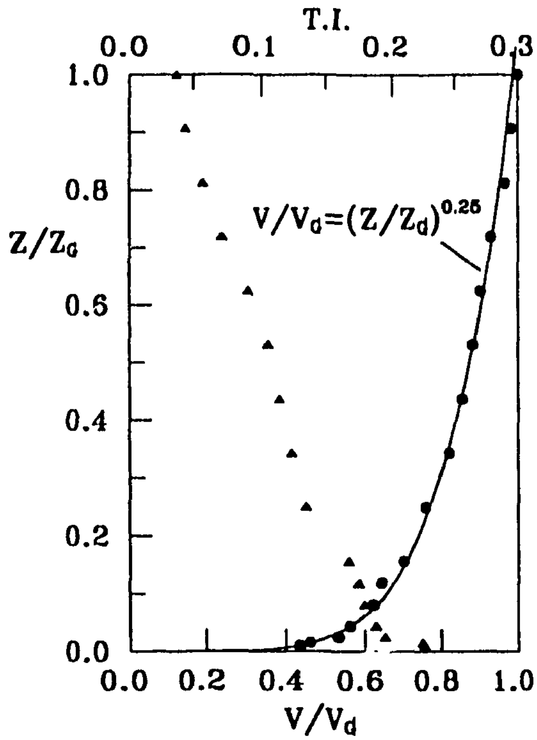

Fig. 3.1.1 Profiles of mean wind speed and turbulence intensity over a simulated suburban terrain.

from 0 to 9 m/s. Smoke is generated by feeding mineral oil through metering valves into heated stainless steel tubes. Two plexiglass viewing windows are set on the ceiling and the side wall of tunnel's working section to facilitate eye view as well as photography of flow patterns around buildings under adequate illumination.

The Laboratory is furnished with several updated equipments for wind measurements, including thermal anemometers, transducer-Scanivalve systems, a Laser Doppler anemometer, Data 6100 Universal Waveform Analyzer etc. Provided by other laboratories in the Centre, an infrared video camera, thermocouples, a colour laser printer and other facilities are also applied in the study in corporation with personal computers for data acquisition, processing and presentation.

3.2 REQUIREMENTS FOR PEDESTRIAN-LEVEL WIND MEASUREMENTS

Previous studies reveal that both mechanical and thermodynamic wind effects on pedestrians could be correlated with properties of wind flows. In addition to mean wind speeds, turbulent fluctuations as well as the variation in wind direction may affect human comfort and safety. The influence area of strong winds in the building vicinity is also of significance for the evaluation of overall wind impact on the environment.

In a typical boundary-layer wind tunnel test, the measurement of mean wind speeds at various locations near the ground is normally the minimum requirement for the evaluation of wind conditions. Gust speeds, probability distributions of wind speeds, wind directions and direction variations may also be necessary in some cases. These wind properties may vary with respect to both time and space to different degrees. Therefore, measurements have to be taken for considerably long periods at many locations or even over the entire field of interest.

The fact that only wind conditions near the ground have direct effects on pedestrians necessitates a low measurement height. A commonly used height is 2 meters above the ground in full scale, corresponding to about 5 mm in a simulated boundary-layer flow of 1/400 geometric scale. At such a low level, wind flow is expected with a low mean speed, a high turbulence intensity and a high shear stress. Limited to the sensitivity of human body response, only the turbulent flow within a low frequency range (e.g. 2 or 3-second gust in full scale) is substantial to pedestrian comfort and safety. By using this criterion, the frequency response required for instruments could be estimated from the geometric and speed scales of specific wind-tunnel environments, normally in the order of 100 Hz. Measurements in a consulting project must examine the influence of wind directionality and evaluate several design alternatives for the achievement of best wind environmental conditions. Appropriate experimental techniques for wind velocity measurements must be selected to fulfil these special requirements for pedestrian-level wind studies in addition to the general guidelines of low cost and disturbance, and high accuracy, sensitivity, stability and resolution.

Techniques for the wind assessment may be roughly categorized by *Point* and *Area* according to measurement approaches. Some typical methods are listed in Table 3.2.1 (Wu and Stathopoulos, 1993a). More details are given in the following sections dealing with the thermal anemometer (Section 3.3), the surface pressure sensor (3.4), the Laser Doppler anemometry (3.5), the flow visualization (3.6) and the infrared thermography (3.7). For other techniques, see the references by Ettouney and Fricke (1975), Isyumov and Davenport (1975a), Irwin (1982), Beranek (1984), Adrian, (1991) and Livesey (1991).

Table 3.2.1 Point and area techniques for assessing pedestrian-level winds.

Point Methods	Area Methods
Thermal Anemometry	Erosion Technique
Pitot Tube	Surface Flow Visualization
Surface Pressure Sensor	Particle Injection
Spherical Flow Indicator	Smoke Streaklines
Cylindric Force Indicator	Infrared Thermography
Optical Dynamometer	
Laser-Doppler Anemometry	
Particle-image Velocimetry	

3.3 THERMAL ANEMOMETER

Thermal anemometer is one of the most reliable and widely-used methodologies for flow measurements. Generally, a hot wire is small in size and high in frequency response (up to 100 kHz, temporally) within a wide velocity range, but it is far from ideal for pedestrian-level wind measurements because of its fragility, sensitivity to temperature change in the environment and undesired heat losses as well as calibration shift due to contamination. From this viewpoint, the hot film is superior, although it has a larger size and a lower frequency response (about 100 Hz) - which are, however, quite adequate for pedestrian-level wind measurements.

If the turbulence intensity to be measured is greater than 20%, thermal anemometers, especially the hot-wire type, may provide high mean and low rms velocities, mainly due to the non-linear calibration relation (Bradbury, 1976). For this reason, commercially-available linearizing units are not recommended for pedestrian-level wind measurements in high turbulence locations. This drawback, however, can be overcome by the so-called dynamic calibration, suggesting to *fly* the probe sinusoidally in a uniform flow for higher accuracy in calibration (Perry, 1982).

For the evaluation of pedestrian-level winds, a single-wire (or film) thermal anemometer is always positioned vertically in a wind tunnel. It measures the horizontal wind component and provides an average speed over the sensor length. From the recorded time history of instantaneous wind speeds, various flow attributes can be calculated, such as the probability distribution of wind speeds yielding the likely occurrence of specified wind speeds during a particular time period.

3.4 IRWIN'S SURFACE PRESSURE SENSOR

Irwin (1981) proposed a simple pressure sensor for pedestrian-level wind measurements. Figure 3.4.1 shows the sensor fabricated in the Building Aerodynamics Laboratory with slight differences from Irwin's original design.

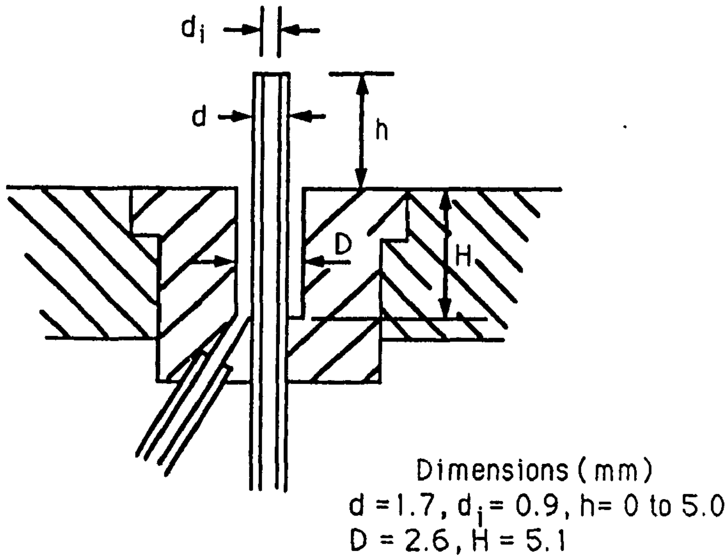

Fig. 3.4.1 Irwin's surface wind sensor reproduced and used in the present study.

The sensor consists of a mounting base and two brass tubes. One of the tubes protrudes out of the base as a probe, while the other is connected with a circular hole on the base around the probe. The pressure difference (ΔP) between the inlets of the two tubes is the output of the sensor. Pressure readings can be converted into instantaneous wind speeds (V) according to a pre-established relation:

$$V = \alpha + \beta \sqrt{\Delta P} \qquad (3.4.1)$$

where α and β are constants determined by calibration.

Unlike the thermal anemometer, the pressure sensor is sturdy, inexpensive and easy to fabricate. A large number of sensors can be installed on a model site provided they do not interfere with each other. Their outputs can be read by pressure transducers placed in a Scanivalve as in the case of pressure measurements. No alignment with wind direction is required due to the sensor's axisymmetric geometry, but this may become a disadvantage when information about wind directions is actually sought.

A comparison of mean and rms speeds measured by the hot film and the pressure sensor is shown in Fig. 3.4.2. The results are presented in terms of speed amplification factors (overspeed ratios) at the pedestrian level. In the wind tunnel of 1/400 geometric scale, wind speeds were measured by pressure sensors of 5 mm height and by a vertically-installed hot film with its centre at 5 mm above the tunnel floor at 37 and 42 selected points, respectively. Both measurements were taken in the same wind tunnel under the same simulated wind conditions by using the same building model. A generally good agreement between the data obtained by the hot film and the pressure sensor has been found for mean wind speeds and the fluctuating turbulent components as well.

Other findings on the sensor from the current study can be summarized in follows (Wu and Stathopoulos, 1994): (1) The sensor should be set at the same height as the measurement level of the wind speed for a reliable assessment; considerable errors have been found when a short sensor is used to measure the wind flow at a higher level above the ground; (2) In comparison with the thermal anemometer, the sensor may overestimate low-frequency fluctuations of wind flows at the measurement level; and (3) The spatial extent of the interference between sensors can be estimated as functions of the diameter of sensors. The longitudinal and lateral extents of disturbance are found to be twelve and

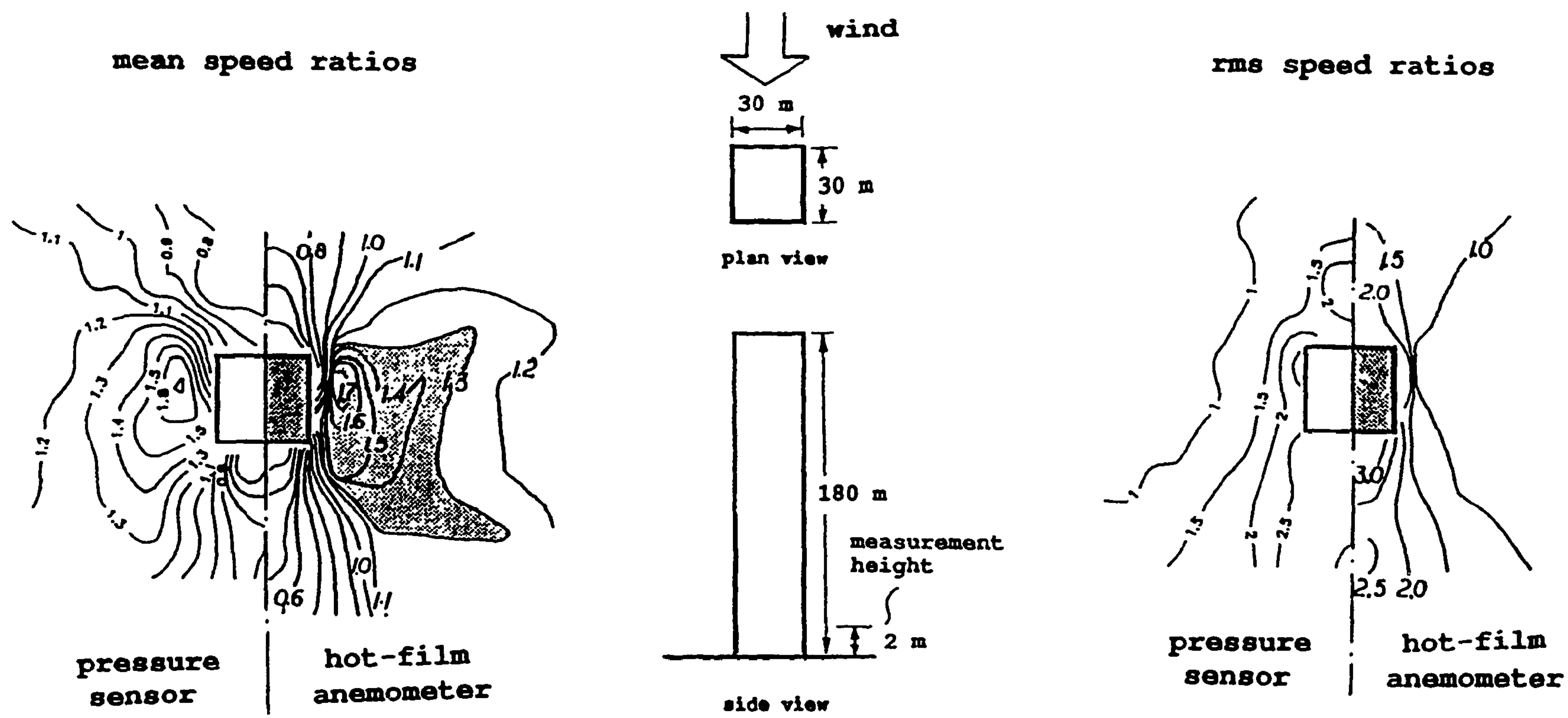

Fig. 3.4.2 Comparison of mean and rms overspeed ratios measured by a vertically-installed hot-film anemometer and surface wind sensors.

five times of the sensor diameter, respectively. For more detailed information about the sensor, see papers by Irwin (1981 and 1982) and Wu and Stathopoulos (1994).

3.5 LASER-DOPPLER ANEMOMETRY

The Laser-Doppler Anemometer (LDA) measures fluid velocities by detecting the Doppler frequency shift of laser light that has been scattered by small particles moving with the fluid. This non-intrusive measurement is independent of thermophysical properties of fluids. The relation between the wind velocity and the frequency shift is linear and needs no calibration. The LDA is capable of sensing one or more velocity components and flow reversals. It measures very low velocities adequately because it is not influenced by the *free convection* effects that affect thermal anemometer readings.

The LDA at the Centre for Building Studies is equipped with a long fibre cable and a 14 mm diameter probe with a 50 mm front lens, which focuses the laser beams and collects the scattered light. The probe, connected to the main LDA unit by the flexible cable, can freely move with the traverser in the wind tunnel and detect the wind speed at a distance of about 50 mm from the lens. The time required for installation and alignment has been greatly shortened with currently improved models of LDA systems. In addition, computer software is available for data acquisition, advanced statistical analysis and presentation.

A house-used humidifier is employed in the Laboratory for additional seeding which results in a typical particle rate about 400 per second. Figure 3.5.1 shows measurement results of 3-D wind speeds in front of a building (H=W=60 m, D=30 m) in

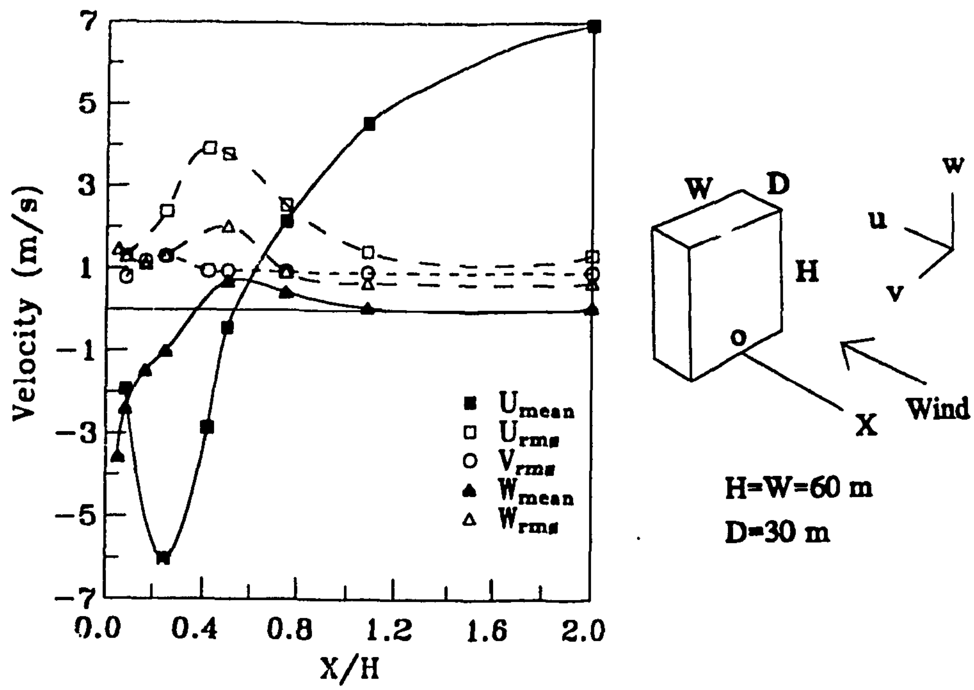

Fig. 3.5.1 3-D wind speeds in front of a tall building.

the wind tunnel. The vertical wind component is found high near the windward surface of the building and strong reversed flows are also detected (U_{mean}<0) against the upcoming wind direction. It provides a 3-D flow picture for the front vortex by mean and rms velocities.

However, the above-mentioned point techniques are only suitable for measurements at selected positions. For an overall assessment of the wind impact over a large influenced region, area methods have to be utilized.

3.6 FLOW VISUALIZATION

The pedestrian-level wind study focuses on the mainly viscous air flow near ground where the surface shear stress can be directly related to the wind speed near the surface. From this point of view, area methods based on the principles of surface shear stress measurements are particular informative.

Used in surface flow visualization are fluid mixtures like paraffin oil with kaolin powder. The test is conducted under a selected low wind speed for a considerably long period of time. The mixture is moved away from its original position by wind force and provides a somewhat qualitative indication of wind flow - low wind speeds occur in zones of accumulated visualization material, whereas high speed winds sweep the material away to other areas. Wind directions, in an average sense, may be read out directly from the visualized flow field. Moreover, the interaction of wind flows around a group of buildings can be investigated and understood with the help of visualized flow patterns.

Flow visualization is capable of providing the finest picture of flow traces, that may be very useful and impressive to architects and city planners. A typical surface flow pattern around a rectangular building is shown in Fig. 3.6.1. Note that in the picture there

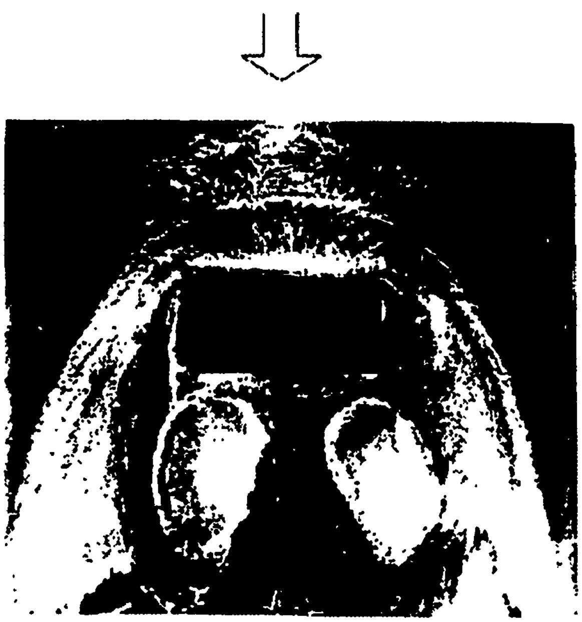

Fig. 3.6.1 Surface flow pattern around an isolated tall building.

is a distinct curve around the building base, about which details will be discussed in Section 4.2.

In order to understand the 3-D characteristics of wind flow around buildings, flow visualization tests are also performed in the smoke wind tunnel (Stathopoulos and Wu, 1994). Figure 3.6.2 displays flow patterns between two model buildings in tandem position with different distances.

For a small distance, the blockage effect of the front building is evident and no coherent vortex is formed between the two buildings. When the distance is increased, a

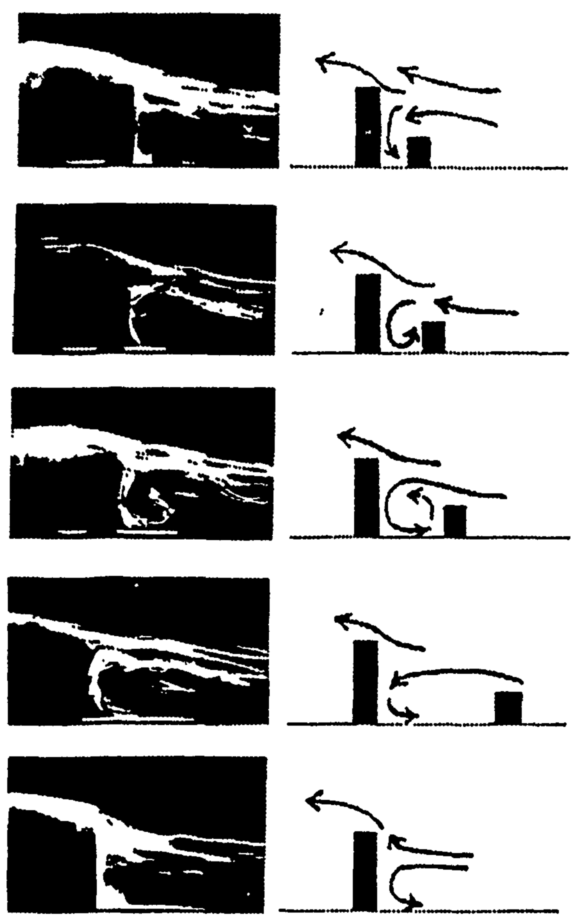

Fig. 3.6.2 Vortex flow between two buildings in tandem position.

large vortex, enhanced by the separated shear flow from the upstream building, brings the wind flow from a high level down to the ground. With an increasing distance, the stable, large vortex is replaced by the wake turbulence separated from the front building. A further increase of the distance reduces the influence of the front building and turns the two building combination to an isolated building model as the distance approaches infinity.

3.7 INFRARED THERMOGRAPHY

A technique using infrared thermography was proposed by Uematsu and Yamada (1991) for assessing pedestrian-level wind conditions. The methodology is based on the fact that the heat transfer from a heated body to the air is closely related to the flow conditions near the body surface. A simple experimental setup consists of a heated thick acrylic plate on which the building model is placed, and an infrared camera that detects the temperature distribution on the floor plate and registers it by colour pictures or video records. This technique is at its launching stage and no functional relationship between the temperature pattern and the flow conditions has yet been found.

The distribution of surface temperature was found fairly similar to that of the effective wind speed V_e with g=3 in Eq. 2.2.2, see Uematsu and Yamada (1991) and Wu and Stathopoulos (1993b). It appears extremely difficult to obtain such a functional relation due to the lack of a complete understanding of surface flow fluctuations (both in speed and direction), and the heat transfer inside the measurement plate as well as that from the plate to air flow. Efforts have been made to overcome these difficulties by improving the design of measurement system and applying numerical simulation techniques. A tentative approach towards the calibration of this technique has been proposed by Wu and Stathopoulos (1993b) based on specific features of heat and momentum transfer within the boundary shear layer near ground.

At the current stage, two indicators are defined for describing the temperature difference caused by the variation of wind speeds. The first is called *Reduced Temperature* [$\delta T(x,y)$] and refers to surface temperature changes due to the presence of new buildings. It is defined by

$$\delta T(x,y) = T_a(x,y) - T(x,y) \tag{3.7.1}$$

where $T_a(x,y)$ and $T(x,y)$ are surface temperatures when the buildings of interest are absent and present, respectively. The reduced temperature has been found generally increasing with the wind speed. Figure 3.7.1 displays three typical images of $\delta T(x,y)$ around isolated buildings. Values of $\delta T(x,y)$ are observed high in front and around corners of buildings. Temperature patterns around other building models will be shown later in this thesis.

The other indicator is called the *Overall Impact* of building-induced wind flow.

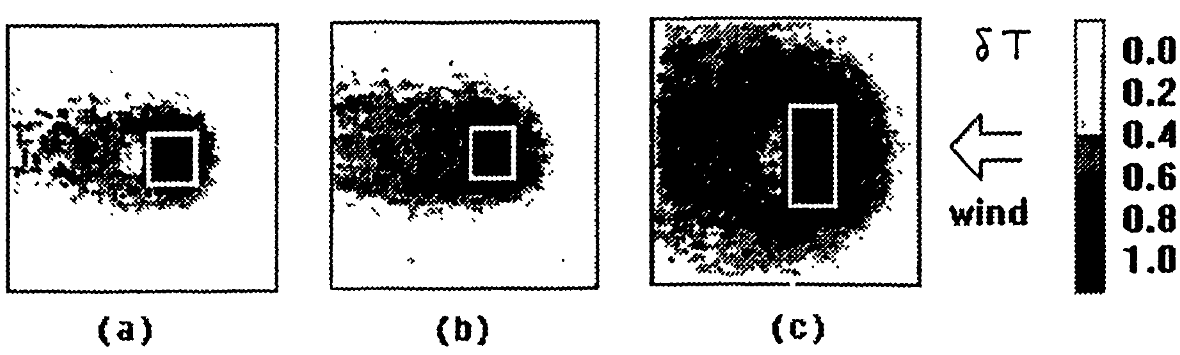

Fig. 3.7.1 Reduced temperatures around isolated tall buildings.

It is defined as an area integration of $\delta T(x,y)$ over influenced zones around buildings:

$$\Omega = \iint_{\delta T(x,y)>0} \delta T(x,y)\, dx\, dy \tag{3.7.2}$$

where the condition $\delta T(x,y)>0$ limits the integration only for the areas over which wind speeds are increased by the presence of new buildings, i.e. those of main interest in pedestrian wind studies Applications of the overall impact will be demonstrated in Section 5.4 and 5.5.

The advantage of this technique in comparison to the other area methods is that no extra materials are introduced in the measurement field. The methodology is potentially capable of providing a quantitative evaluation of wind flows through digital image processing techniques. Only one wind speed, instead of a number of speeds as in the erosion test, could provide a high resolution of wind speed distributions. The temperature difference between the measurement plate and the air flow can be set at a relatively low value - say 10 °C - so that interference to wind flow from the heated plate becomes negligible. Although still under development, the infrared thermography technique for the evaluation of pedestrian-level winds has shown great potential. More efforts are currently made to establish this technique for routine measurements.

Nevertheless, the infrared system, at the current stage, is capable of visualizing surface flow fields through colour images; quantifying windy zones in terms of the reduced temperature; and evaluating the overall impact of pedestrian-level winds by additional calculations.

3.8 SUMMARY

A number of techniques applied for the assessment of pedestrian-level wind conditions have been discussed in this chapter. They are summarized in Table 3.8.1. The table may be used as a quick reference for selecting the proper instrumentation for pedestrian-level wind measurement in addition to any specific requirements of the particular experimental environment. Note that details about two widely used methods, namely Force Indicators and Erosion Technique can be found in papers by Ettouney and Fricke (1975), Irwin (1982), Beranek (1984) and Wu and Stathopoulos (1993a).

Generally, point measurement systems are capable of providing quantitative information about the turbulent wind flow locally at several points. For a better spatial coverage, these systems may be supplemented by area methods which, however, have their own limitations in supplying quantitative evaluations. A logical approach adopted in the current study is to use area methods first for assessing the wind behaviour and identifying windy zones in a wide area, then to perform point measurements for detailed information at selected positions.

Table 3.8.1 Comparison of wind-tunnel methods for the assessment of pedestrian-level winds.

Methods		Advantages	Disadvantages
POINT	Thermal Anemometry	small size sensor; high frequency response; possible for wind directions; well developed and widely used	fragile; response shift caused by temperature change and contaminants; alignment required; non-linear calibration relation
	Surface Pressure Sensor	no alignment required; suitable for automatic Scanivalve system; easy to make and operate	unsuitable for low wind speed and high turbulence flow; horizontal wind component only
	Force Indicators	measuring average forces on human body; force direction and fluctuation possible	large size; low frequency response; data difficult to process and interpret
	Laser Doppler Anemometry	non-intrusive; no calibration needed; independent of flow's thermophysical properties; capable for sensing flow reversal and direction	expensive; alignment required; tracing particles needed
AREA	Erosion Technique	quantitative evaluations possible for both wind speed and influence area if several speed stages used	fundamental relation with wind speed uncertain; suitable only for horizontal surfaces
	Surface Flow Visualization	easy to conduct; good indication of wind direction and flow interaction	no clear indication of speeds; suitable only for horizontal surfaces
	Infrared Thermo-graphy	quantitative results possible; only one wind speed needed; non-intrusive and small interference from heated base	expensive; under develop-ment; heat convection along wind flow inevitable

CHAPTER 4

WIND FLOW AROUND ISOLATED BUILDING MODELS

In a built-up site, wind environmental conditions are affected by a large number of elements. Among them, nearby large buildings play an important role. According to their configurations and combinations with surroundings, buildings can be classified into several categories. The simplest model is an isolated building without any surrounding objects. This chapter is devoted to the illustration of wind mechanisms around the isolated, rectangular buildings. More complex building models will be discussed in the next chapter.

4.1 FLOW MECHANISM OF ISOLATED BUILDINGS

For a given wind direction, high-speed winds may occur in regions of building's front, corners, wake and ground-level passages as shown in Fig. 4.1.1. The root cause for air movements is the spatial difference in wind pressure, though it may have different appearances in respective regions.

Within an atmospheric boundary layer, the increase of wind speeds with the elevation from ground is usually described by the so-called power law or logarithmic law. Such a wind speed gradient may result in two pressure differences in front of a building. One is a vertical pressure difference between the stagnation zone and the bottom part of the front surface of the building - it drives the fast-moving air from high levels down-

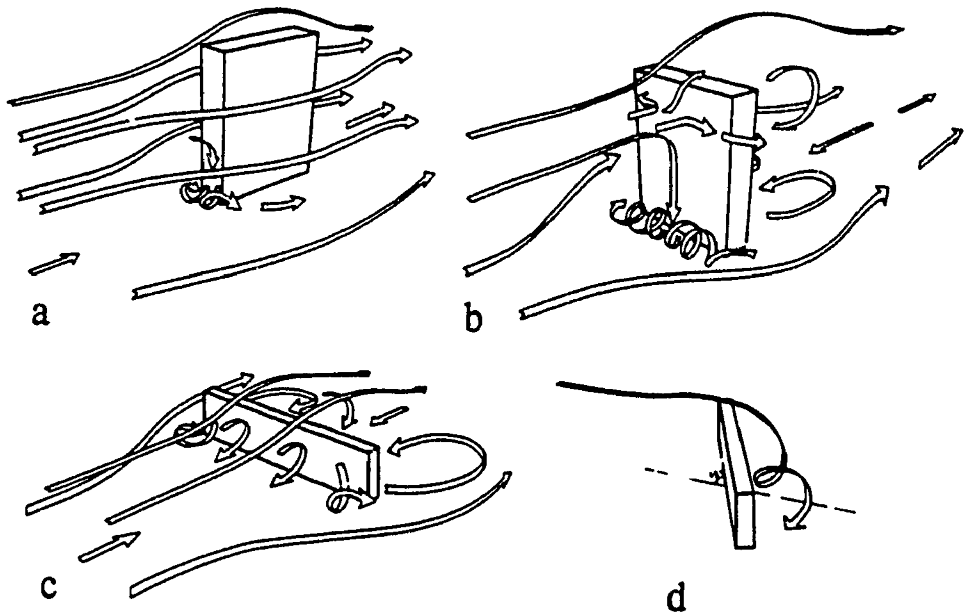

Fig. 4.1.1 Windy regions around isolated buildings, after Beranek (1984).

washing to the ground. The other is a horizontal difference between air pressures at the foot of the building and that in the oncoming wind. Wind flow is retarded by the horizontal pressure difference in addition to surface frictions, and eventually separates from the ground in front of the building. The down-washing flow and the separated flow interact with each other and compose a stationary vortex in front of the building. At the bottom of this *Front Vortex*, flow reversal can be observed with high speeds.

For an isolated building, high air pressures take place near the windward surface of the building and relatively low pressures near the leeward surface. The front vortex may be stretched transversally from the centre to the sides of the building. It initiates a vortex system wrapping around the building base - that is the well-known *Horseshoe Vortex*. This vortex system entrains speedy air flow from higher levels and creates *Corner*

Streams around building sides, especially near windward corners. Due to the same pressure difference, air flow, including the low-level oncoming wind and the down-washing flow, may be channelled through a ground-level passage into the wake area. Such a speedy current inside the passage underneath a building is called *Pass-through Flow.*

In the wake area of a building, mean wind speeds are usually low compared to those at other regions. However, *Wake Turbulence* is found significant under all directions and this may also develop uncomfortable environmental conditions. For some specific building configurations such as low, wide buildings oblique to incident winds, high-speed gusts may occur in the wake area because of the flow reattachment on ground after jumping over building roofs.

These flow phenomena are summarized in Table 4.1.1 for isolated, rectangular buildings with hot spots and major contributing parameters highlighted. Windward dimensions, building heights in particular, are the key parameters in most situations, whereas the along-wind depth has a little impact on wind-speed amplifications with exceptions for certain circumstances of the wake turbulence and the pass-through flow. Wind direction is by all means an influential parameter and so are the characteristics of approach flows, namely, the wind profile and the turbulence intensity. In the following sections, these parameters will be examined in detail regarding their impacts on respective flow mechanisms. Coordinate systems, measured positions (axes for the front vortex, corner streams and wake turbulence) and directions of three velocity components are also shown in Table 4.1.1. Unless otherwise indicated, most measurements are made by Irwin's pressure sensors (Section 3.4) in the present study for horizontal wind speeds with the mean and rms values denoted as $\bar{V}$ and V_{rms}, respectively. Variations of wind speeds

Table 4.1.1 Flow mechanisms around isolated, rectangular buildings.

Section	Flow Mechanism	Hot Spot	Contributing Parameter	Coordinate System
4.3	Front vortex	In front of windward face	Building height & width Wind direction	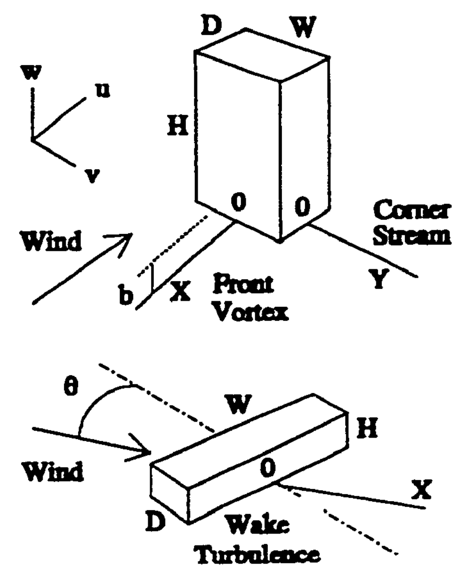
4.4	Corner stream	Building corners & sides	Building height & width Wind direction	
4.5	Pass-through flow	Passages underneath building	Building height & width Wind direction Building depth Passage width & location	
4.6	Wake turbulence	Lee of building	Wind direction, building width, height & depth	

are presented by overspeed ratios defined similarly to Eq. 2.1.1 for wind speeds at the measurement height b=2 meters (full scale) above the ground:

$$K = \frac{\overline{V}}{\overline{V}_a} \qquad and \qquad k = \frac{V_{rms}}{(V_{rms})_a}$$

where the subscript a refers to the *absence* of building models. When LDA results are presented, wind velocities in three directions are shown by symbols in Table 4.1.1.

4.2 INFLUENCE SCALE FOR AN ISOLATED RECTANGULAR BUILDING

In addition to the magnitude of wind speeds, the spatial extent of amplified wind speeds is the other parameter which should be examined in pedestrian-level wind studies. Wilson (1989) defined a length scale for estimating dimensions of the flow recirculation region on building roofs:

$$S = (B_L B_S^2)^{1/3} \tag{4.2.1}$$

where B_L and B_S are the larger and smaller dimensions of the building's windward surface. When B_L is larger than $8B_S$, B_L=$8B_S$ is to be used. In the current study, the potential of this definition for the wind flow around building bases has been investigated through surface flow visualization and speed measurements.

Around a building base, the horseshoe-shaped vortex is the main flow system in determining the pedestrian-level wind conditions. In every picture obtained from the flow visualization for isolated, rectangular buildings, Fig. 3.6.1 for example, there is a clear thick curve around the building base with similar patterns. The curve is sketched in Fig. 4.2.1(a). In front of the building, the curve is parallel to the building face and it marks the switch line of wind direction near the ground (also see Fig. 3.5.1 for velocity measurements); then it turns around building corners and separates the primary horseshoe vortex from a secondary vortex. The curve is created through the accumulation of visualization materials driven by wind flows in different directions, more precisely, the different rotating directions of vortices. Regions enclosed by the curve mark the zone of interest to pedestrian-level wind studies, over which high speed winds are likely to occur.

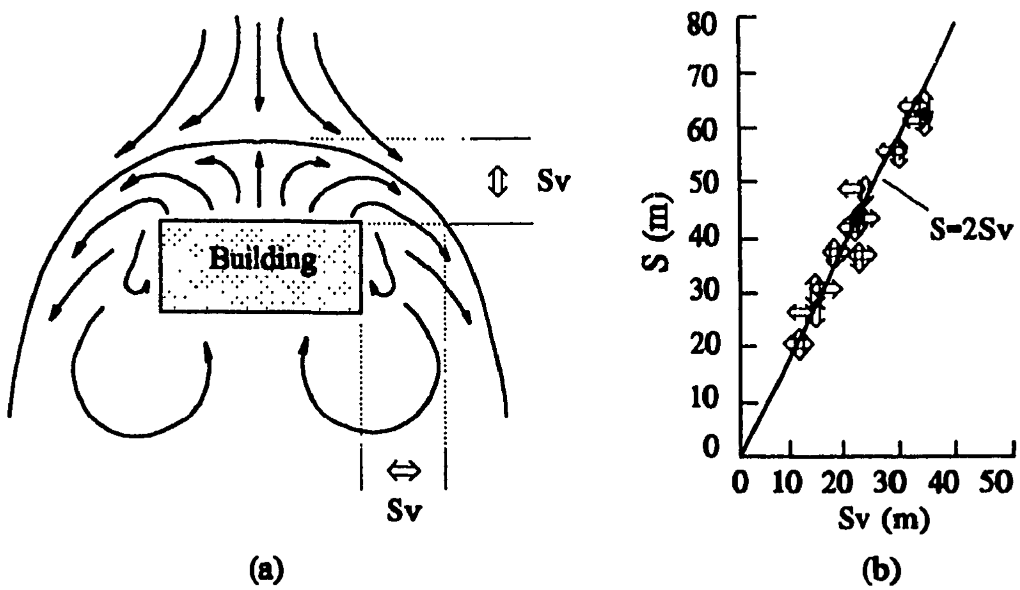

Fig. 4.2.1 (a) Sketch of the flow pattern around a building base; and (b) Relation between the vortex size and the influence scale.

The influence scale S can be employed as a representative length scale for the flow pattern. For wind flows around a number of isolated buildings with windward heights and widths from 20 to 120 m, two interesting features are recapitulated in Fig. 4.2.1(b). First, to such an identified curve, the longitudinal distance (⇕) from the middle of the building front surface is comparable to the lateral distance (⇔) from the windward corner of the building. Both distances are designated as S_v in the figure; and second, the value of S_v can be estimated by taking one half of the influence scale S of the building. Evidently, there is an inherent correlation between the vortex size and the influence scale as shown in the figure. Defined by the windward dimensions of buildings, the influence scale S can be applied for estimating the influence area of strong wind conditions around buildings. The maximum overspeed ratios caused by the front vortex and the corner stream are found to occur inside the curve at (0.3 to 0.4)S from building surfaces for the tested building dimensions. The influence scale can also be used to evaluate the intensity of the potential flow interaction around two or multiple buildings. For example, the flow interference between two side-by-side buildings may simply be described by a modification function of the ratio of the distance between buildings to their influence scales.

It should be noted that the empirical relations between the influence scale, building dimensions, vortex sizes and windy locations are also dependent to a certain extent upon the wind profile and the turbulence characteristics of the oncoming wind. These have to be taken into account for a more accurate estimation, though the resulted differences might be insignificant for actual building cases. Building geometry and wind direction, on the other hand, are critical for the influence scale of the buildings. An effective influence scale is proposed and explained in Appendix D.

4.3 FRONT VORTEX

Vortex systems in front of buildings have been studied in several laboratories as reviewed in Section 2.2. However, there are no generally acceptable rules for estimating the speed of the reversed wind flows. The ground pressure distribution around buildings, which is the most direct indicator of the wind acceleration at the pedestrian level, has not been investigated yet. In this study, pedestrian-level wind speeds and ground pressure distributions have been measured in front of buildings in order to establish an empirical relation between the maximum wind speed of front vortices and building dimensions.

4.3.1 Wind Speed in Front of Buildings

Figure 4.3.1 shows mean overspeed ratios along the central axis X when wind flow is normal to one of building faces. The value of overspeed ratio varies with the building size by a similar tendency when the distance from the building is normalized by the respective influence scale S as defined by Eq. 4.2.1. From a minimum value near the building face, the overspeed ratio increases to its maximum at $X/S \approx 0.35$; then it drops to the second minimum before returning to the unity in the regions out of the influence of buildings. Although they are only sensed at discrete locations, results of wind speeds provide a general picture of the variation of overspeed ratios with building dimensions. While the along-wind depth has little influence on the front vortex, the height and width of the building determine the maximum overspeed ratios. Figures 4.3.1 (a) and (b) indicate that, to the maximum speed of front vortices, the building width has at least as much contribution as the building height.

Note that the horizontal wind speeds supplied by surface pressure sensors are non-directional. A direction shift between the reversed flow and the oncoming wind occurs

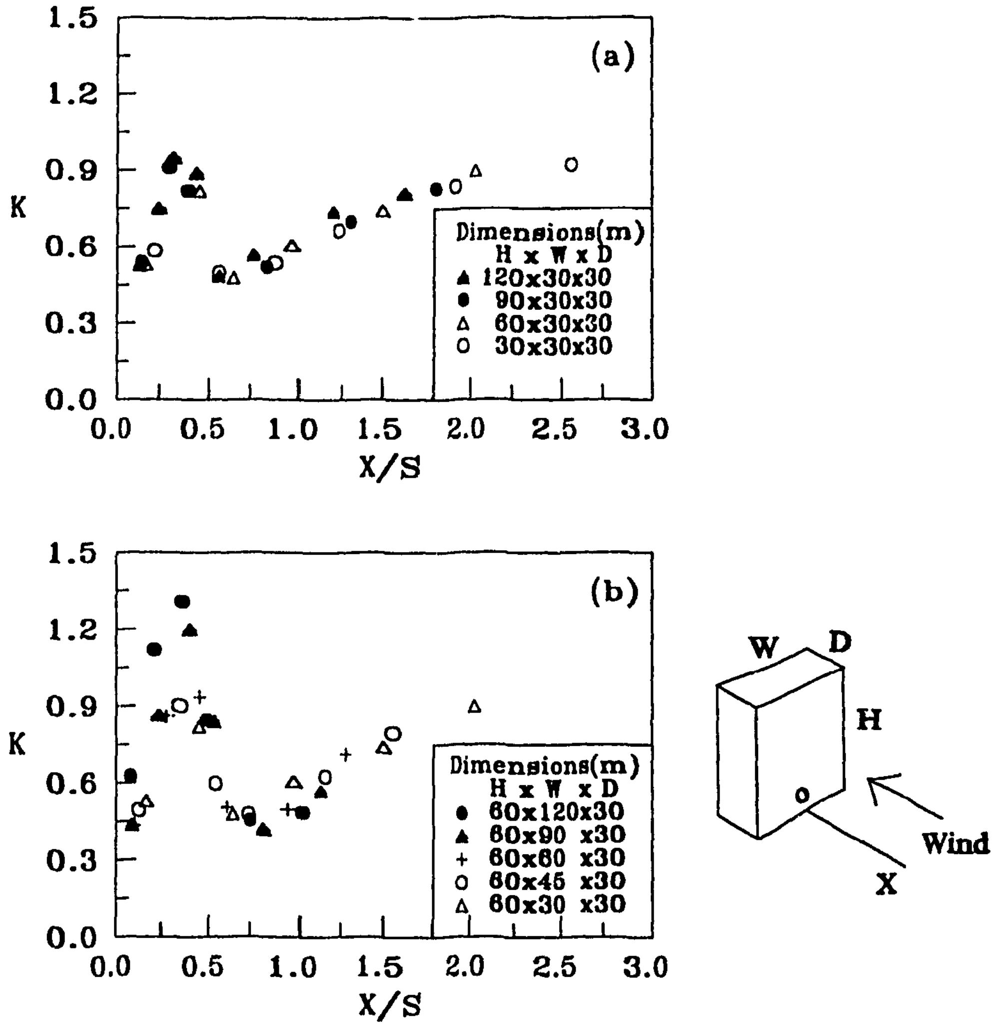

Fig. 4.3.1 Mean overspeed ratios in front of buildings.

at around X/S=0.5, which corresponds to the size of the horse-shoe vortex in front of the building, see Figs. 3.5.1, 3.6.1 and 4.2.1.

4.3.2 Ground Pressure Distribution

Since the flow field of interest to the pedestrian-level wind studies is very close to the ground, it is reasonable to presume that there is a direct dependence of wind speeds on ground pressure distributions. In defining a pressure coefficient C_p, the reference pressure P_a is the wind pressure at the same position when building model is absent and the reference pressure is calculated from the mean wind speed of the approach flow at the height of $S/2$, which is assumed to be the approximate height of the horse-shoe vortex:

$$C_p = \frac{P - P_a}{\frac{1}{2}\rho \overline{V}_{S/2}^{2}} \tag{4.3.1}$$

Figure 4.3.2 shows the variations of ground pressure coefficients with (a) the height; (b) the width; and (c) the size of buildings. Regardless of building dimensions, the pressure coefficient, from its maximum at positions close to the building, decreases linearly to a levelling point at X/S=0.3 to 0.4. For buildings with different dimensions, the C_p value at the levelling point decreases with increasing influence scale S of the building, which is more evident in Figs. 4.3.2 (b) and (c). After the levelling point, the pressure coefficient keeps decreasing, but with a much slower rate. In general, the variation of C_p complies with the same inclination, similar to the conclusion given by Baker (1978) who measured the pressure distribution in front of circular cylinders in turbulence shear flows. These findings make it possible to estimate the wind speeds from building dimensions.

4.3.3 Relation between Wind Speeds and Building Dimensions

The front vortex system, the horizontal speed variation and the surface pressure distribution are sketched in Fig. 4.3.3. The flow pattern is drawn from observations of

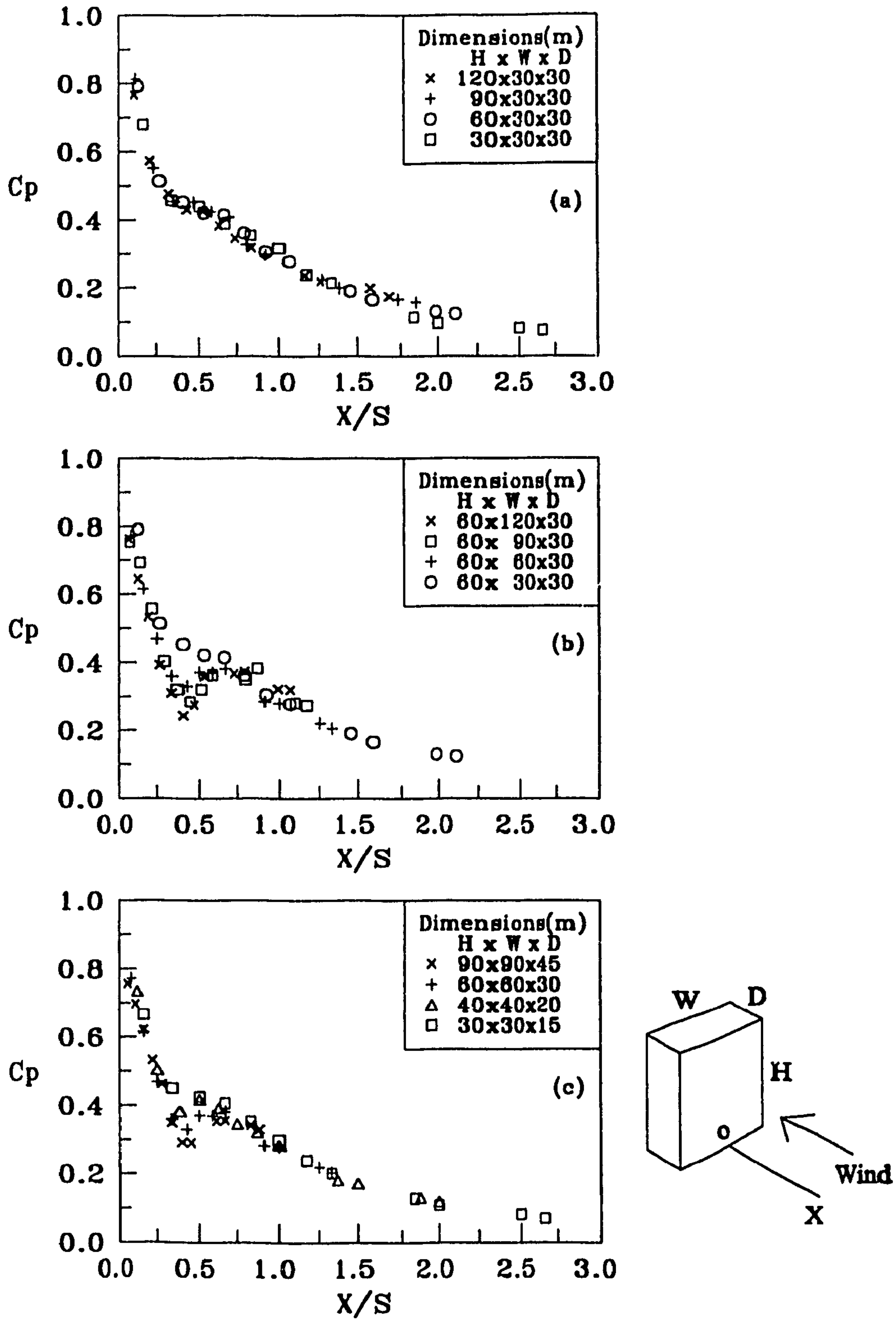

Fig. 4.3.2 Distributions of ground pressure coefficients in front of buildings with different (a) heights; (b) widths and (c) sizes.

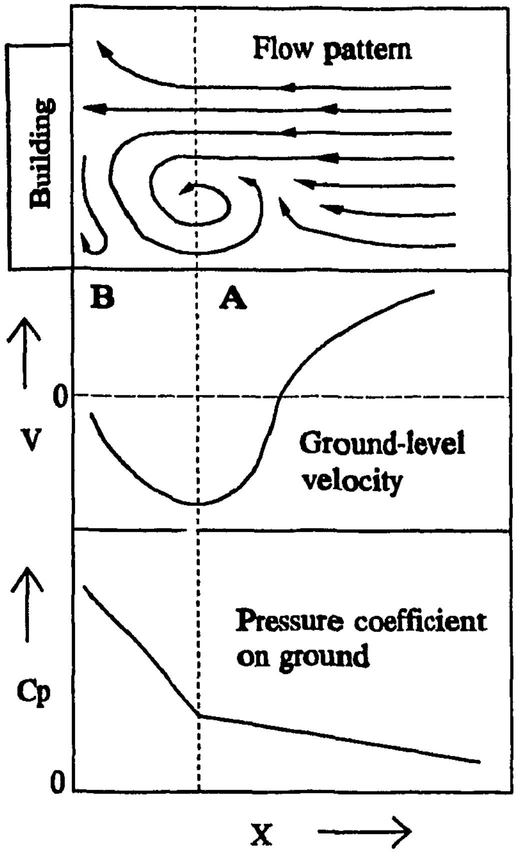

Fig. 4.3.3 Schemes of the front vortex system, pedestrian-level velocities and ground pressure distributions in front of a building.

flow visualization such as Figs. 3.6.1 and 3.6.2. Beneath the centre of the primary front vortex (position **A**), the negative wind speed reaches a peak while the ground pressure has the value of C_{PA} at the levelling point. If the linear relation could be extended to position **B**, the pressure coefficient would have its maximum C_{PB} when both the distance X and the wind speed V approach to zero. The difference of pressure coefficients between location **B** and **A** is found increasing with the influence scale S by following the relation:

$$C_{PB} - C_{PA} \propto \sqrt{S} \tag{4.3.2}$$

The maximum mean wind speed $\bar{V}_A$ varies with the measurement height b and the square of $\bar{V}_A$ should be proportional to the pressure difference P_B-P_A by assuming $\bar{V}_B$=0.

$$\bar{V}_A^2 \propto (P_B - P_A) f(b) \propto \bar{V}_{S/2}^2 (C_{PB} - C_{PA}) f(b) \tag{4.3.3}$$

Therefore,

$$\bar{V}_A^2 / \bar{V}_{S/2}^2 \propto \sqrt{S} f(b) \propto \sqrt{S/b} \tag{4.3.4}$$

The last proportional sign in Eq. 4.3.4 is based on the dimension consideration. If the speed at the height b is $\bar{V}_a$ with the absence of building models, the maximum value of mean overspeed ratios is defined as:

$$K_{FV} = \frac{\bar{V}_A}{\bar{V}_a} \propto \frac{\bar{V}_{S/2}}{\bar{V}_a}\left(\frac{S}{b}\right)^{1/4} \tag{4.3.5}$$

This indicates the maximum overspeed ratio of front vortices K_{FV} can be estimated by the influence scale S, the measurement height b, and the oncoming wind speeds at heights of $S/2$ and b as well. If the power law is applied for the oncoming wind profile, the speed ratio on the right-hand side of Eq. 4.3.5 can be replaced by a power function of the height ratio. The overspeed ratio then becomes:

$$K_{FV} = C_1 (S/2b)^{\alpha} (S/b)^{1/4} = 2^{1/4} C_1 (S/2b)^{\alpha + 1/4} \tag{4.3.6}$$

where α is the exponent of the power law and C_1 is a constant. The latter is determined by the linear regression with C_1=0.25 or $2^{1/4}C_1$=0.3, based on the data in Fig. 4.3.1 and the literature information. Figure 4.3.4 displays the comparison of measured and predicted maximum overspeed ratios for different buildings. Note that conversions for data from other studies to the overspeed ratio at respective measurement heights were based on the

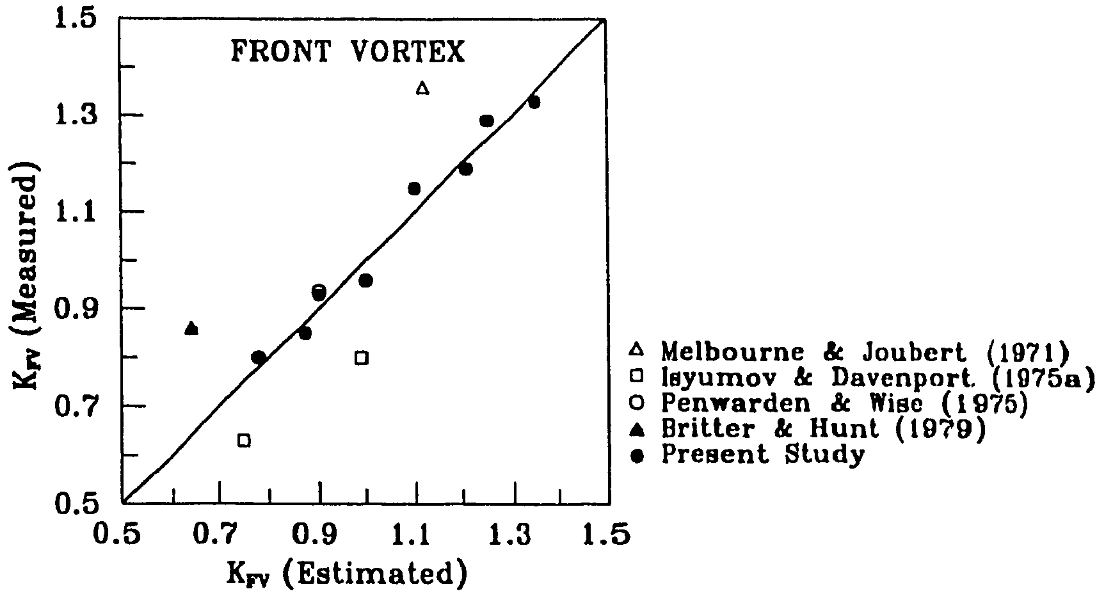

Fig. 4.3.4 Comparison of front-vortex speeds derived from wind-tunnel experiments and empirical estimations.

information provided for two tandem buildings when the distance between two buildings is infinite or the height of upstream building is zero.

Deviations of data from some laboratories may be caused by differences in measurement techniques and locations. The general trend in the figure indicates that the maximum overspeed ratio of the vortex flow in front of isolated, rectangular buildings can be estimated by the simple formula of Eq. 4.3.6. The magnitude of wind-speed amplification depends not only on the building height, but also on the building width as well as the profile of the oncoming wind and the measurement height. If other buildings are present in the vicinity of the building, especially in the upstream sector of the building, Eq. 4.3.6 has to be modified, as will be discussed in the next chapter for two buildings in tandem position.

4.4 CORNER STREAM

4.4.1 Flow Pattern and Speed Distribution

Corner streams around the windward corners of a tall building are developed mainly by the air from well above ground down the windward face of the building. Flow separation from a sharp windward corner is the other reason for speedy winds around buildings. Figure 4.4.1 shows the overspeed ratios K measured along the axis Y, starting from the middle of a building side surface. The figure shows that maximum speed ratios of corner streams increase (a) significantly with building heights and (b) slightly with building widths. The maximum value of K for different buildings seems to occur at the position Y/S=0.35, that is the same as the result for front vortices. As illustrated in Figs. 3.6.1 and 4.2.1, the cross-wind distance from a windward building corner to the boundary of the horse-shoe vortex is 0.5S and the boundary is farther apart from the building side along the wind stream. Therefore, the position of Y/S=0.35 from the middle of a building side is right at the bottom of the primary vortex system, where corner streams have the maximum horizontal wind speeds.

The effect of the along-wind depth of a building is insignificant on the intensity of corner streams which occur around windward corners of the building, but the speed variation along the Y axis specified in this section is typical for corner streams only if buildings have relatively short depths. For buildings with long depths, the Y axis may be located far away from building corners and wind speeds along this axis may be much lower than the maximum speeds of wind streams around windward corners.

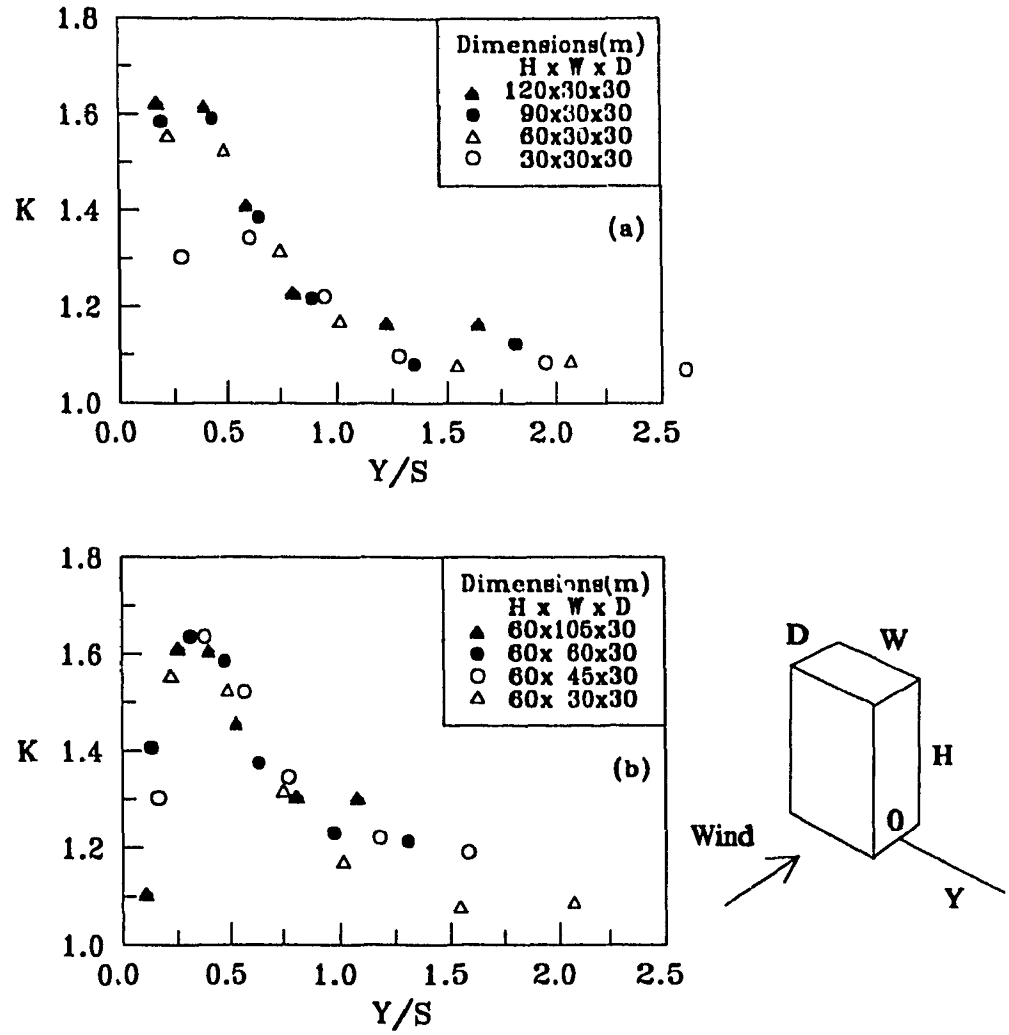

Fig. 4.4.1 Mean overspeed ratios of corner streams.

4.4.2 Wind Speed Variation

An approximate estimation of the maximum speed of corner streams may be based on the consideration that the fluid kinetic energy of corner streams results from a combination of the energy of the oncoming wind ($\bar{V}_a$) and that of the down-washing flow ($\bar{V}_d$). The latter is dependent upon the building geometry (shape, size etc.). Assume these two contributing components are integrated by a weighted summation of kinetic energies:

$$\overline{V}_{CS}^2 = C_2\overline{V}_a^2 + C_3\overline{V}_d^2 = C_2\overline{V}_a^2 + \varphi(bldg)\overline{V}_a^2 \qquad (4.4.1)$$

where C_2 and C_3 are constants, and $\varphi(bldg)$ a building-related function to be determined by experimental results. In the absence of any buildings, the maximum value of mean wind speeds of corner streams $\overline{V}_{CS}$ is equal to the oncoming wind speed $\overline{V}_a$ at the same level. Therefore, C_2=1 and the maximum overspeed ratio K_{CS} for corner streams becomes:

$$K_{CS} = \frac{\overline{V}_{CS}}{\overline{V}_a} = \sqrt{1+\varphi(bldg)} \qquad (4.4.2)$$

When the approach wind is perpendicular to one of building faces, the maximum overspeed ratio of corner streams increases with the building height H. Less significantly, the ratio also increases with the building width W and the power-law index α as well. On the other hand, lower overspeed ratios have been found for higher measurement level b (Kamei and Maruta, 1979). These facts lead to a definition of a single parameter $H_{CS}=H(W/b)^{\alpha}$ for the building function and

$$K_{CS} = \sqrt{1+\varphi(H_{CS})} \qquad (4.4.3)$$

A power function is obtained for the building parameter H_{CS} by best fitting the experimental results:

$$K_{CS} = \sqrt{1+0.02H_{CS}^{3/4}} \qquad (4.4.4)$$

Figure 4.4.2 shows the maximum overspeed ratios for a variety of rectangular

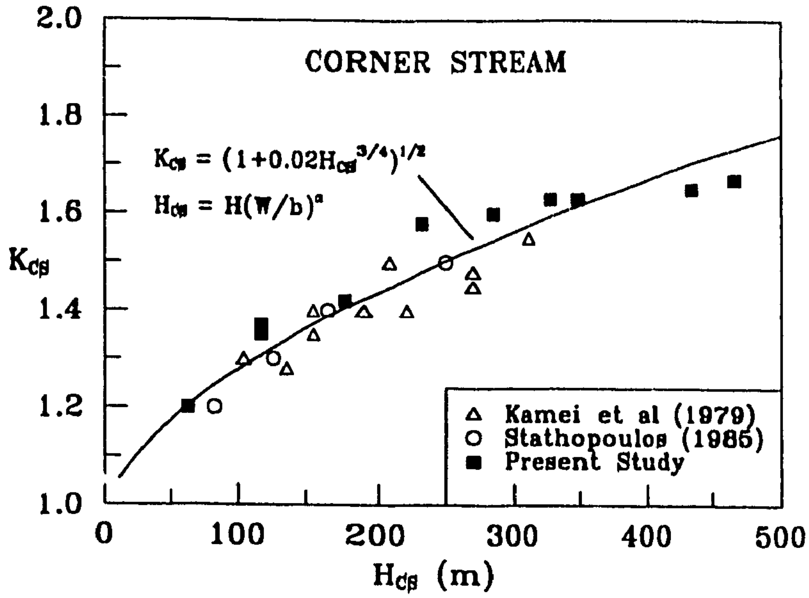

Fig. 4.4.2 Maximum mean overspeed ratios of corner streams.

buildings from both the literature and the current measurements.

4.5 PASS-THROUGH FLOW

Inside a passage underneath a tall building, there is usually very strong wind due to the pressure difference across the opening. Considering the opening as a long *orifice*, the average wind speed over the passage ($\overline{V}$) can be calculated by

$$\overline{V} = C_4\sqrt{(P_f - P_b)/\frac{1}{2}\rho} = C_4\overline{V}_H\sqrt{C_{Pf} - C_{Pb}} \tag{4.5.1}$$

where $\overline{V}_H$ is the mean wind speed at the building height H, C_4 the orifice coefficient, ρ the air density. P_f and P_b are pressures at the front and the back end of opening, respectively. C_{Pf} and C_{Pb} are the corresponding pressure coefficients referenced to the velocity pressures at the roof height. BRE experiments (Penwarden and Wise, 1975) suggested that the value C_{Pf} - C_{Pb} be a constant of 0.88 and C_4=0.75 for high-rise buildings. Therefore, $\overline{V}=0.7\overline{V}_H$ is obtained. Obviously, the time-average speeds are not uniformly distributed over the passage. Their spatially maximum values should be higher than $\overline{V}$, say $\overline{V}_{PT}=C_5\overline{V}$, in which C_5 is another constant greater than one. The maximum overspeed ratio of pass-through flow K_{PT} in the passage is then given by

$$K_{PT} = \frac{\overline{V}_{PT}}{\overline{V}_a} = C_5\frac{\overline{V}}{\overline{V}_a} = 0.7\,C_5\frac{\overline{V}_H}{\overline{V}_a} = 0.7\,C_5(\frac{H}{b})^{\alpha} \qquad (4.5.2)$$

where K_{PT} is evaluated at the height of b above the ground, V_a is the oncoming wind speed and α is the exponent of a given power-law wind profile.

Figure 4.5.1 shows K_{PT} values derived from experimental data collected from the literature with b=2 to 3 m and α=0.20 to 0.28. A simpler relation, regardless of the measurement height and the wind profile, is derived in the figure by the best-fitting technique. It relates the maximum overspeed ratio inside a passage to the building height only.

It is worth noting that for those building models tested by Penwarden and Wise (1975) on the pass-through flow, windward heights and widths were comparable to each other so that building widths had not been taken as an independent parameter which, however, might have a significant impact on pressures in both windward and leeward regions. For a slender building, the overspeed ratio inside an underneath passage is expected slightly lower than that shown in the figure; the opposite is expected for a wide building. Furthermore, a long passage may reduce the wind speed in the passage due to

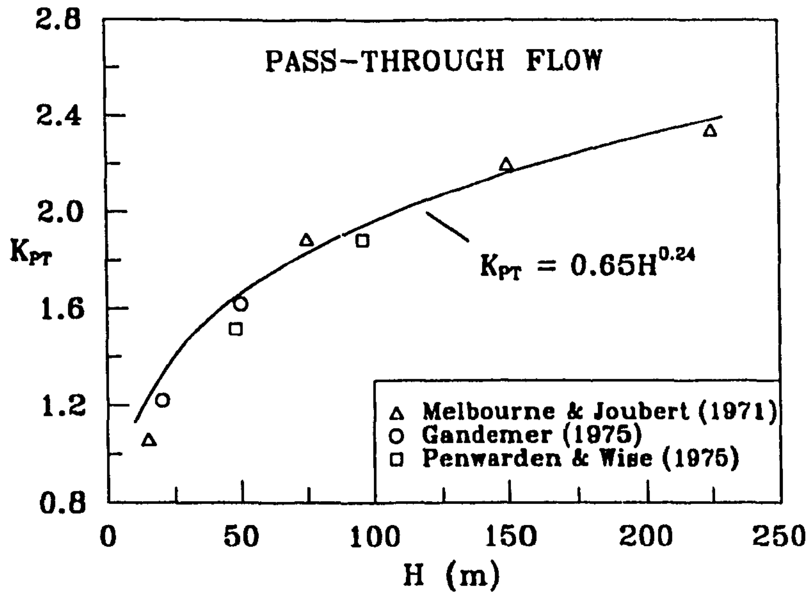

Fig. 4.5.1 Variation of maximum mean overspeed ratio of pass-through flow with building height.

changes in air pressures at the leeward end and the pressure gradient over the passage. The size and location of the passage also affect wind speeds of pass-through flows (Wiren, 1975 and Isyumov et al, 1985).

4.6 WAKE TURBULENCE

Owing to the so-called sheltering effect, low-speed winds may prevail in wake regions behind a building. The wake flow bears some common features such as strong turbulence, low mean speeds and high unsteadiness. In such a 3-D turbulent flow field, flow entrainment and energy dissipation may take place with eddies in various scales. The influence region over which air flow has a noticeable reduction in mean speeds and a growth in turbulent fluctuations may vary from two to twenty times of the building height, depending upon the building's width and the turbulence characteristics of upcoming flows (Peterka et al, 1985). Observations in the present study suggest that the wake size be about (4 to 6)S for high-rise buildings, where S is the influence scale defined by Eq. 4.2.1 for the windward dimensions of buildings. At the near wake zone immediately behind a building, the mean speed is about a half of that in the upcoming flow at the ground level, and gradually recovers to the unity at the far end of the wake area. The wind conditions may be different for buildings with a long depth, when the separated flow from windward edges reattaches on building roofs and sides. Nevertheless, the wake region behind a building is always considered as a safe zone from the viewpoint of pedestrian-level wind comfort.

Wind speeds behind a number of wide buildings were detected by surface pressure sensors along the centre line X up to 100 m away from buildings. Figure 4.6.1 shows mean overspeed ratios K defined by Eq. 4.1.1 behind buildings with the same width (W=120 m) and depth (D=20 m), but a different height (H from 8 to 60 m). For a low building (H/D=0.4), wind speeds increase consistently with the distance from building. For higher buildings, wind speeds increase much faster with the distance, from the same lowest point immediately behind buildings. After the increase, however, there is a modest drop of wind speeds before a full recovery over farther distances. This phenomenon may be created by the flow separation from building roof, forming a large, unstable vortex behind the building. The size and intensity of this vortex are dependent upon the building height as shown in Fig. 4.6.1.

The along-wind depth of buildings is the other geometric factor affecting the wake turbulence. In this case, buildings have a fixed height (H=20 m) and width (W=120 m).

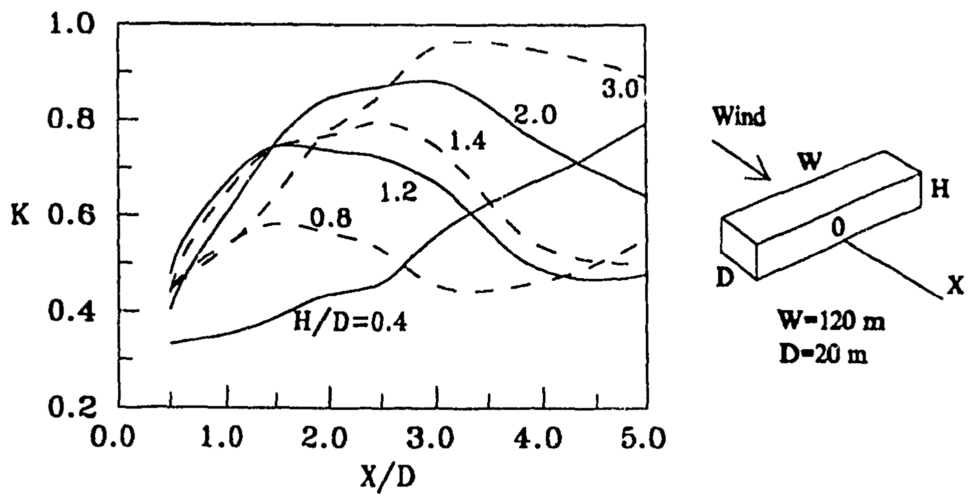

Fig. 4.6.1 Effect of building height on the mean speeds behind buildings.

The along-wind depth (*D*) varies from 8 m to 60 m. As shown in Fig. 4.6.2, the shorter the building depth, the higher the wind speed behind the building. This might also relate to the flow separation from building roofs since a long depth may weaken the flow separation from the front edge or even cause a flow reattachment on the roof. It consequently reduces the intensity of wake vortices.

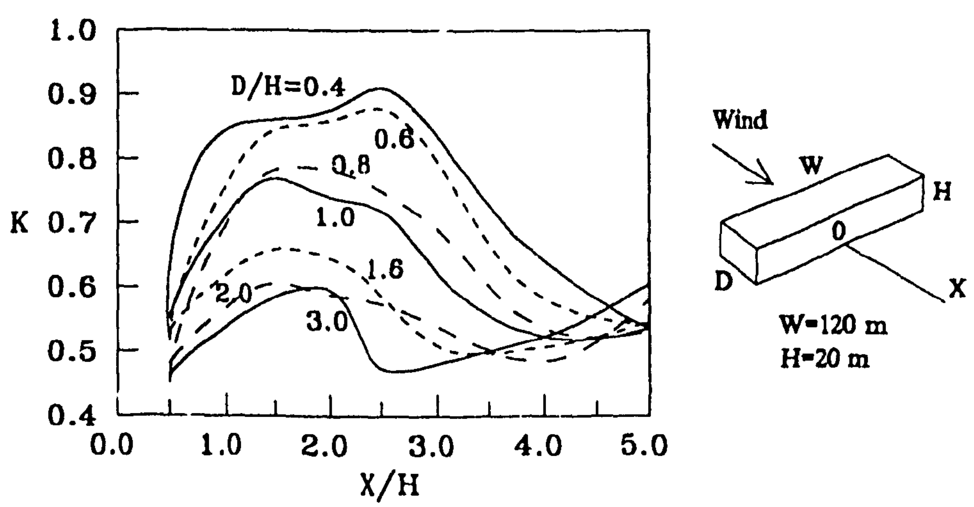

Fig. 4.6.2 Effect of along-wind depth on mean speeds behind buildings.

In the two sets of data shown in Figs. 4.6.1 and 4.6.2, all mean overspeed ratios are found lower than one, i.e. buildings generally provide some protection in the wake regions.

4.7 FLUCTUATION OF 3-D TURBULENT FLOW

Previous research has revealed that human bodies are sensitive to gusty winds of short durations such as a few seconds. It is, therefore, of importance to study wind fluctuations. Unfortunately, some technical limitations impede accurate measurements of 3-D turbulence in both laboratory and full scales. Information of mean and fluctuating speeds in all directions can be obtained only when more sophisticate instruments are employed, as for instance, the Laser Doppler Anemometry (LDA), which has been utilized in the present study. As shown in Fig. 3.5.1, the mean wind speed of reversed flow in front of an isolated building (H=W=60 m and D=30 m) is nearly as high as that in the oncoming flow at X/H=0.3 - note that building height H is equal to the influence scale S in this case since W=H. The surface flow changes its direction at X/S≈0.5, that is consistent with the observation from flow visualization. The down-washing flow near the building face may reach a half speed of the impinging wind. Mean wind speeds in the lateral direction are not plotted in the figure since they are close to zero along the central line. Rms wind speeds in three directions should be emphasized in the figure. Both longitudinal and vertical rms speeds reach their maxima at about X/S=0.5, where the direction shift of longitudinal flow occurs and they could be as high as 60% and 25% of the mean speed of the upcoming wind, respectively. At all other locations, rms speeds are relatively low.

Figure 4.7.1 shows the LDA measurements of corner streams around a tall building (*H*=60 m and *W*=*D*=30 m). Wind velocities in three directions were measured along the *Y* axis. The longitudinal wind flow dominates the wind field with a mean speed much higher than other components. It reaches the maximum at about *Y/S*=0.3. The lateral and vertical speeds, however, have their maxima at different spots, depending upon the location and rotation of the horse-shoe vortex. All rms speeds are consistently low along the *Y* axis, with relatively high values near the building side face.

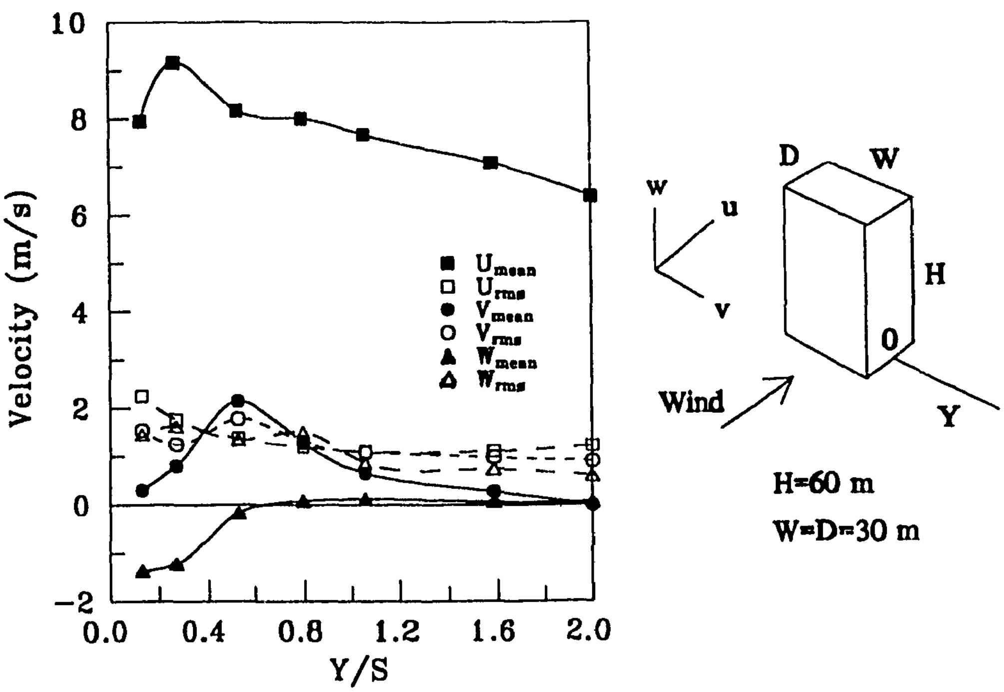

Fig. 4.7.1 Mean and rms overspeed ratios near the side of a tall building.

For the wake turbulence, rms speeds were measured by Irwin's sensors for the same building models used for Figs. 4.6.1 and 4.6.2. Results are shown in Figs. 4.7.2 and 4.7.3 by the rms overspeed ratio *k* defined by Eq. 4.1.1. Despite the complexity of rms speed ratios, some common features can be observed in these two figures: (1) Turbulent

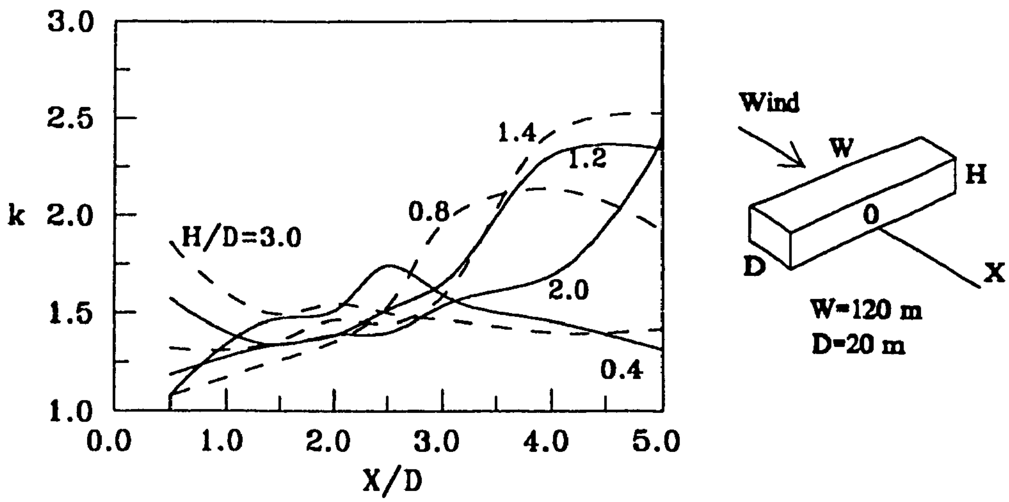

Fig. 4.7.2 Effect of building height on rms overspeed ratios behind buildings.

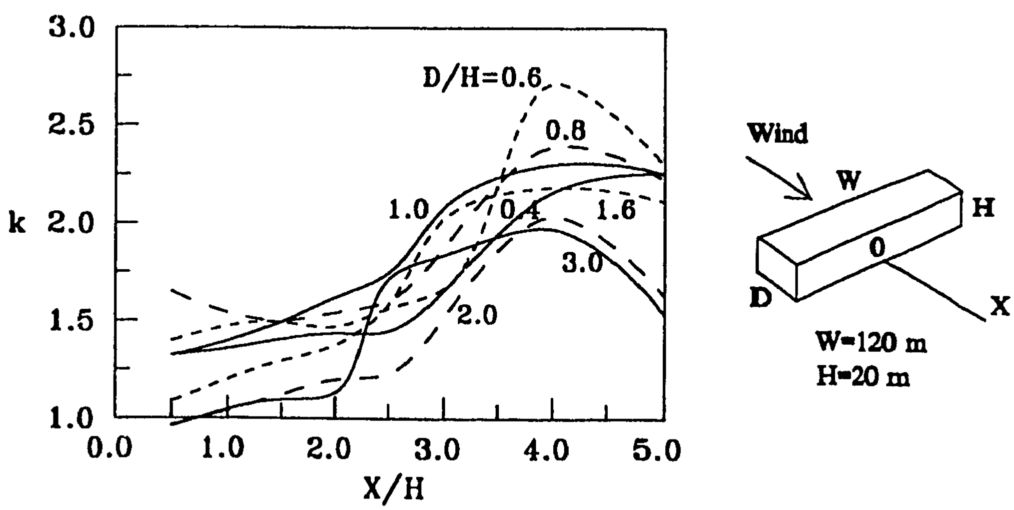

Fig. 4.7.3 Effect of along-wind depth on rms overspeed ratios behind buildings.

fluctuations are generally higher than those of the oncoming wind (k>1); (2) Relatively low values of rms overspeed ratios take place immediately behind the building with X/D<2.5 in Fig. 4.7.2 and X/H<2.5 in Fig. 4.7.3; and (3) The k values have their maxima when H/D=1.2 and 1.4 in Fig. 4.7.2, and D/H=0.6 and 0.8 in Fig.4.7.3, i.e. when the building height is a little larger than the along-wind depth. Unfortunately, no other trends can be figured out from these two groups of wind results. Considering the complex pattern of the trends shown in Figs. 4.7.1 to 4.7.3, no quantitative relations have been established for the estimation of wind fluctuations.

4.8 EFFECT OF WIND DIRECTION

Wind speed variations have been discussed so far only for cases with flow normal to one of the building surfaces (θ=0°). Actual wind flows may come from any direction, although the wind from one or several directions may prevail over a built-up site. A systematic approach to handle the directionality issue is to take all possible wind directions into consideration and combine them in a probability format. A detailed procedure developed in association with the meteorological statistics for estimating the overall effect of wind directions will be presented in Chapter 6. In this section, the directionality effect on wind flow pattern is illustrated for isolated building models.

When wind flow approaches a building at an angle, wind speeds measured along X and Y axes in previous figures may no longer be representative for the flow in respective regions. Critical wind speeds and hot spots may move with the wind direction and measurements over the entire field around a building model may become necessary.

Wind speeds were detected by a large number of surface pressure sensors installed around isolated buildings in this study. Contours of overspeed ratios K are shown in Fig. 4.8.1 for a building with H=60 m and W=D=30 m for five wind angles between 0° and 45°. For corner streams around buildings with θ=0° and 45°, only a half of the contours

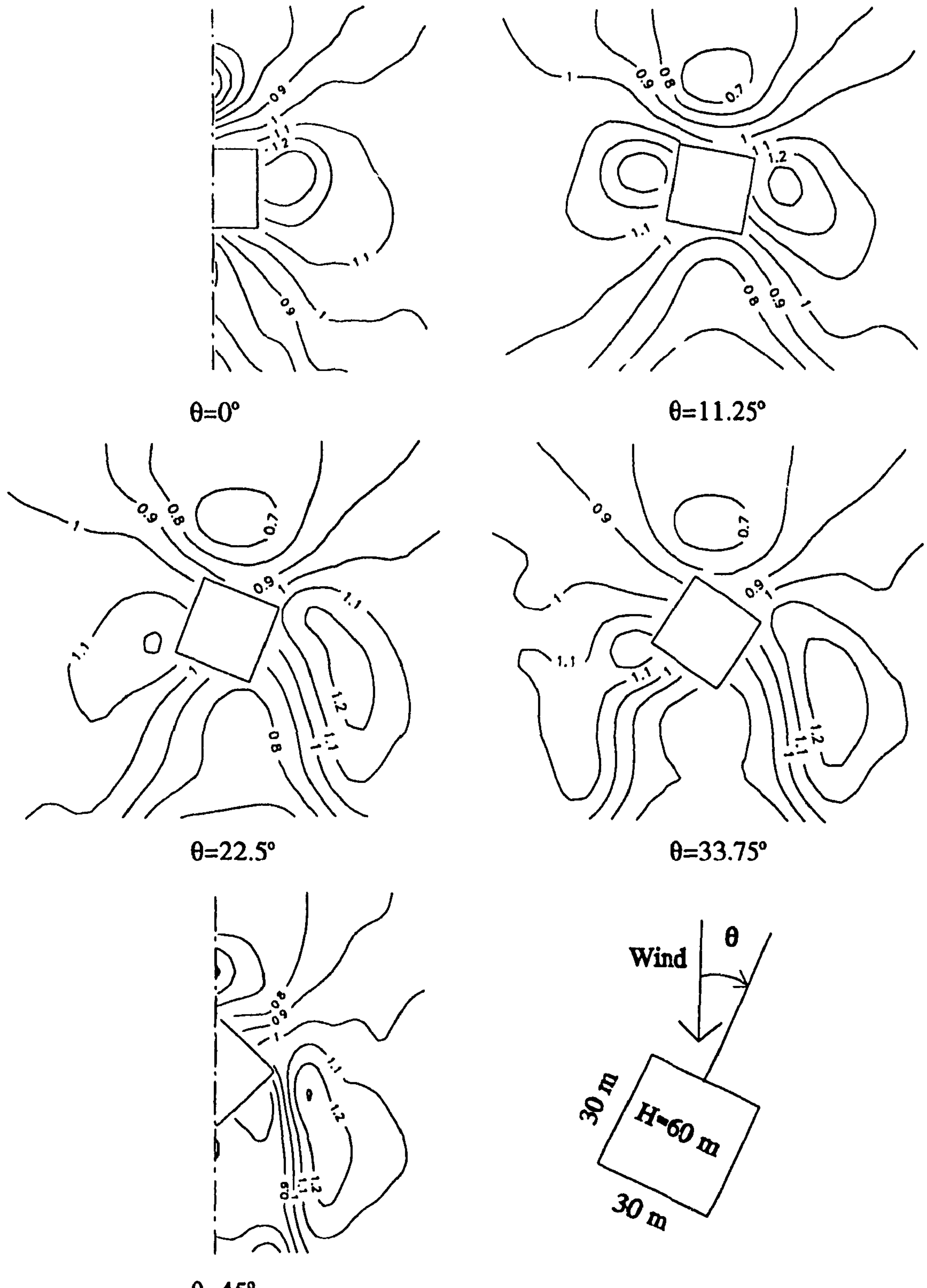

Fig. 4.8.1 Overspeed ratios around a slender building with different wind incidence.

is shown due to the symmetry. On the other hand, for two of three asymmetrical flow patterns (θ=22.5° and 33.75°), the total influenced areas with K>1.1 and 1.2 are obviously higher on one side than those on the other. They are also somewhat higher than those in the symmetrical situation (θ=0° and 45°).

A better example of the direction effect is shown in Fig. 4.8.2 for a tall building with a long width and a short depth (H=W=60 m and D=30 m). When the wind direction varies from 0° to 90°, the windward area of the building decreases, causing a reduction in corner-stream speeds in general. There are slightly higher wind speeds on one side for θ=22.5° and 45°. For a larger angle, θ=67.5°, the flow separation from one corner overshadows the whole wind field. Due to the reduction in windward area, the width of the wake region also drops for a larger angle.

Practically, more attention should be paid to locations very close to buildings, where streets or public-access ways are usually planned. By examining Figs. 4.8.1 and 4.8.2, one can find that a region next to a building face may be subject to the front vortex, corner stream and wake turbulence under different wind directions. The speed variation caused by the wind direction may be more dramatic in such a case, depending on the specific situation under consideration.

For the wake turbulence, an incident angle between 30° and 60° may induce critical wind conditions behind a long building of 15 to 35 meters high (Gandemer, 1975). For the same building models used in obtaining the data of Fig. 4.6.1 (W=120 m, D=20 m and H=8 to 60 m), wind speeds were measured along the wind direction behind buildings from the middle of the leeward face to the far wake region. Figure 4.8.3 shows mean and rms overspeed ratios for θ=30°. High K values are observed for medium height

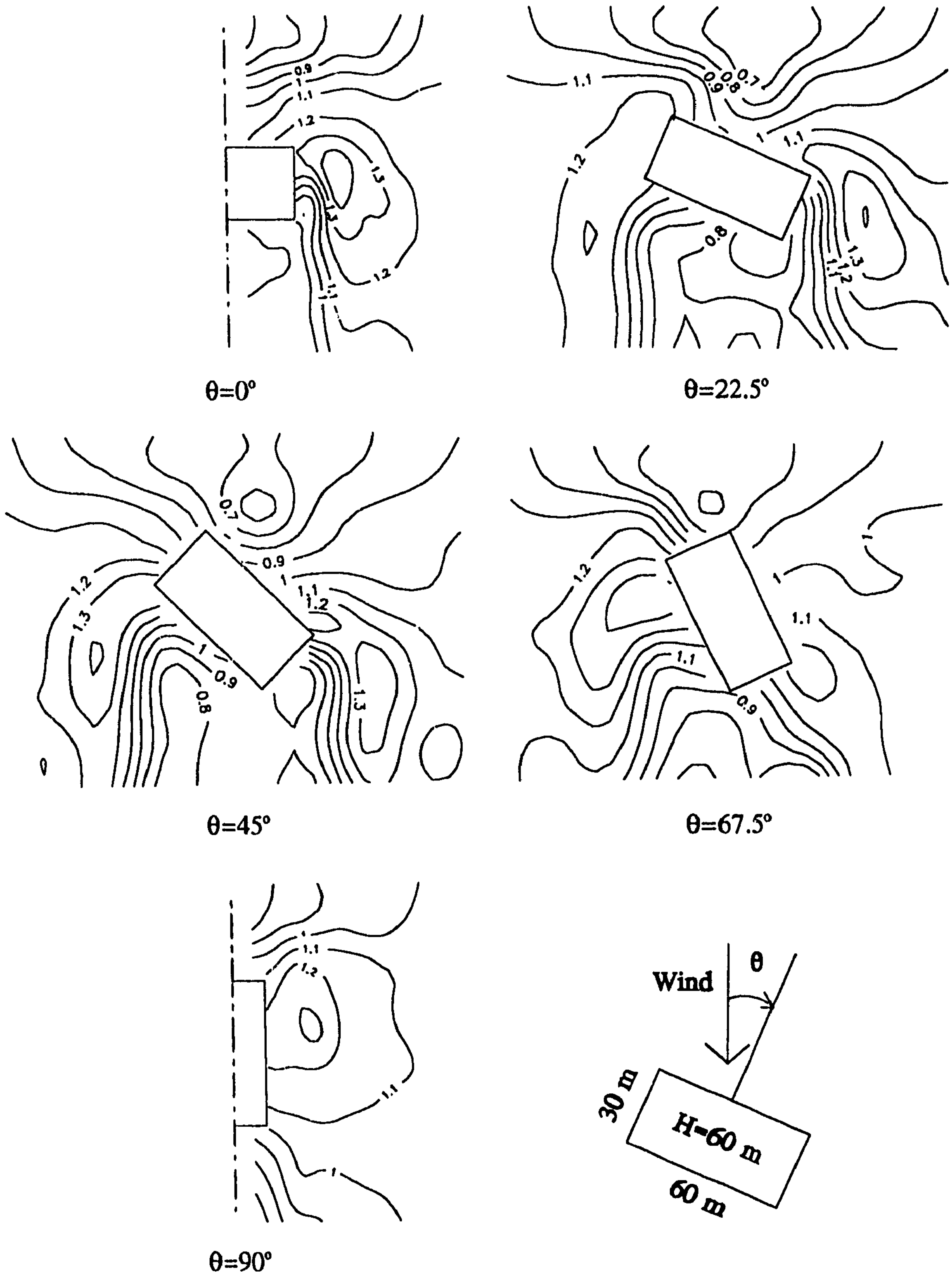

Fig. 4.8.2 Overspeed ratios around a large building with different wind incidence.

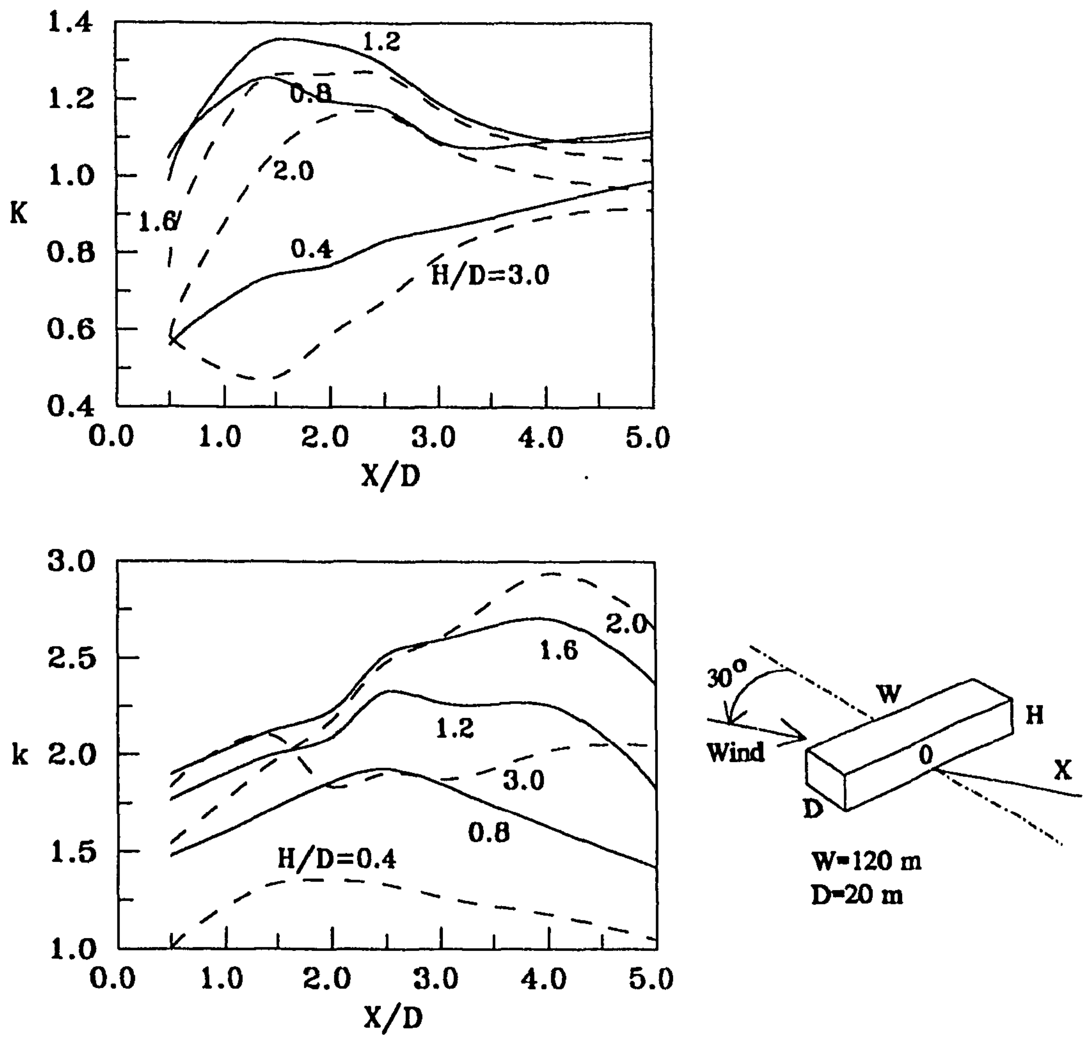

Fig. 4.8.3 Mean and rms overspeed ratios behind buildings oblique to incident wind with θ=30°.

buildings (*H/D*=0.8 to 1.6) with the maximum of 1.34 for *H/D*=1.2. On the other hand, wind speeds behind low or high buildings (*H/D*=0.4 or 3) are generally low. All overspeed ratios converge to the unity at *X/D*=5 where the disturbance caused by the building becomes negligible with respect to mean wind speeds. The values of rms overspeed ratios, however, vary in a wider range from 1 to 3. The distance with a noticeable disturbance is also much longer than that for mean speeds.

Within the measured region (up to 100 m from the building leeward surface), the maximum mean and rms overspeed ratios are collected and presented in Fig. 4.8.4 for buildings with W=120 m and D=20 m under two wind directions of $\theta=0°$ and 30°. The building height is in the range of 8 to 60 m. It shows the general variation of mean and rms overspeed ratios with building dimensions and wind directions.

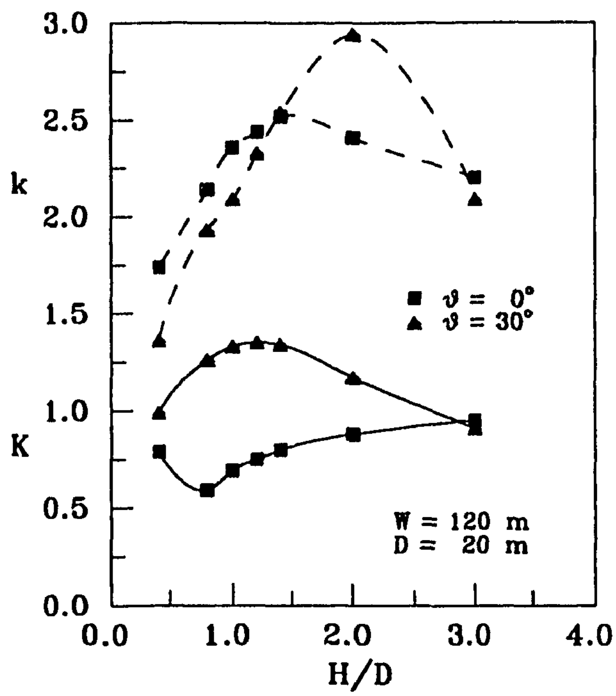

Fig. 4.8.4 Variation of wind speeds over wake areas within 100 m from buildings with building height and wind direction.

In Sections 4.6 to 4.8, typical results of the wake turbulence, 3-D flow fluctuations and the effect of wind directions on pedestrian-level winds have been presented. When 3-D turbulent flows are investigated under different wind directions, there are many wind and building parameters involved in determining the wind speeds and their spatial impact around buildings. Consequently, it becomes extremely difficult to develop simple, empirical relations for the prediction of building-induced wind conditions as in the previous sections. Based on experimental observation and literature information, some rules of thumb have been generated and presented in Appendix D for the effect of wind direction, although their applicability requires further verification.

4.9 SUMMARY

In this chapter, wind flow around isolated, rectangular building models have been studied for different wind directions.

Flow mechanisms have been investigated for the front vortex, corner stream, pass-through flow and wake turbulence around isolated, rectangular buildings. The root cause for wind speed variations is the spatial differences of air pressures, which occur at several regions around buildings. In front of a building, the down-washing flow creates a flow reversal at ground level. The front vortex extends to building sides and induces the so-called horse-shoe vortex around the building base. Due to the difference of pressures in the windward and the leeward regions of a building, air flow may be channelled through any passage underneath the building with a considerably high speed. In the wake area, where speeds are usually low because of the sheltering effect, the jumping over flow may induce a windy zone behind a long, low building oblique to incident winds.

Extensive wind-tunnel measurements have been carried out for a range of buildings with various dimensions. Major contributing parameters have been identified and examined with respect to both buildings and upcoming winds. The variations of wind speeds are described by the so-called overspeed ratios. Empirical relations between overspeed ratios and building dimensions have been derived from experimental findings and the literature information.

In addition to mean speeds, wind fluctuations around buildings have also been investigated here. Speed components in three directions are captured by the LDA around buildings. The impact caused by the wind direction is demonstrated by point measurements around several isolated buildings.

As mentioned earlier, the isolated, rectangular building is a bench-mark model in this study. The wind flow around two- and multiple-building combinations will be treated as the interaction of flows around respective isolated buildings. The intensity of such an interaction will be quantified by the modification functions in Chapter 5 with respect to the basic flow modules presented in this chapter. The effect of the building geometry, or shapes, other than rectangular, will be discussed in Chapter 6 where several influence factors are incorporated into the evaluation of wind flows around actual building configurations.

CHAPTER 5

WIND FLOW AROUND TWO- AND MULTI-BUILDING MODELS

The isolated building models discussed in the previous chapter are fundamental for understanding the flow mechanisms around building groups, but they are too idealized from practical viewpoints. Actual buildings are always accompanied by other objects, that may create various aerodynamic effects. Examples include twin towers, a tall building with low buildings across streets, a courtyard enclosed by buildings, uniformly distributed residential developments and tall buildings surrounded by low street blocks. Some simplified building models subject to the wind environmental problems are identified in Table 5.0.1 with associated hot spots, flow mechanisms and influencing parameters. Flow patterns around these models are expected to be complex due to the interaction of flows around individual buildings. Depending upon the building dimensions, distance and wind incidence, the flow interaction may be of diverse intensities that in turn may bring different wind conditions to pedestrians. Regarding these building models, this chapter presents details about wind flows and their interactions at the pedestrian level.

5.1 TWO BUILDINGS IN TANDEM POSITION

The model of two *Tandem* buildings refers to a tall building and a relatively low, long building, shown in Fig. 5.1.1. When wind flow approaches the low and then the tall building, the region between the two buildings is subject to an adverse flow reversal,

Table 5.0.1 Flow mechanism around two and multiple building models.

	Hot Spot	Flow Mechanism	Contributing Parameter	Section
Two Buildings				
TANDEM	Front of downstream tall building	Front vortex, Separated shear flow	Building height & width, Wind direction, distance	5.1
SIDE-BY-SIDE	Gap between buildings	Corner stream, Channelling effect		5.2
STAGGERED	Corners around downstream building	Corner stream, Channelling effect	Building height, width & depth, Wind direction Relative position	5.3
OTHERS	Regions between buildings	Venturi effect, Corner stream, Channelling effect		5.4
Multi Buildings				
COURTYARD	Space enclosed,	Jumping-over vortex	Building height, plan size	5.5
	Opening if any	Channelling effect	Opening width, wind direction	
STREET BLOCK	Streets adjacent to tall buildings	Corner stream Front vortex Channelling effect	Block height and width, Tall building height, Street width, wind direction	5.6

induced by the interaction of the down-washing flow in front of the tall building and the separated shear flow from the upstream building. By using Irwin's surface sensor, mean and rms wind speeds at 2 m above ground have been measured along the central line between the two buildings, as shown by the dashed line in Fig. 5.1.1. It has been found that the speeds of wind flow in this region are dependent on the distance and windward dimensions of buildings when the approach wind is normal to both buildings.

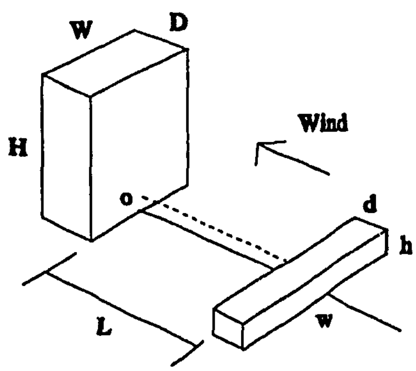

Fig. 5.1.1 Two buildings in tandem position.

5.1.1 Effect of Building Height and Distance

In order to understand the flow pattern around tandem buildings, a series of flow visualization tests have been performed in the smoke wind tunnel. Effects of the distance between buildings and the height of the upstream building on the vortex flow have been investigated, e.g. Fig. 3.6.2. These are further quantified by the wind-speed measurements discussed in this section.

The maxima of mean and rms overspeed ratios (K and k) for various building configurations are displayed in Fig. 5.1.2 versus h/S and L/S.

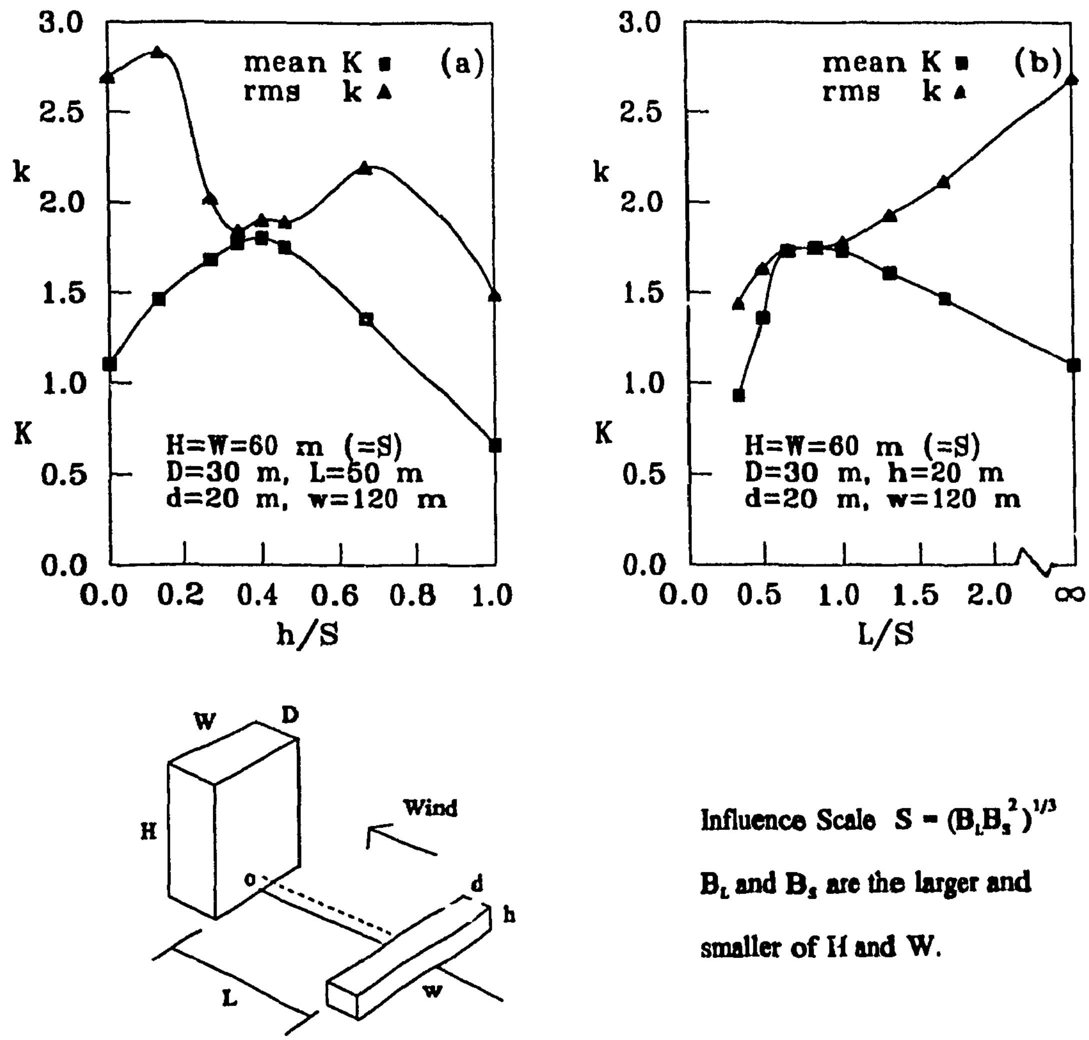

Fig. 5.1.2 Maximum overspeed ratios of the mean and rms speeds between two tandem buildings.

(a) For a given distance, L/S=5/6, the maximum mean overspeed ratio increases with the relative height (h/S) to a critical value (K=1.78 at h/S=0.4 in this example). The front vortex is reinforced by the separated shear flow from the front edge of upstream building. With a further increase of h/S, the sheltering effect of the upstream building becomes prevailing. A tall upstream building may force the separated flow to reattach on, or even to jump over the downstream building so a low-speed region is created between buildings.

(b) For an upstream building with a fixed height, say $h/S=1/3$, the sheltering effect creates a low-speed area when two buildings are very close to each other. No coherent vortex is formed between buildings. With an increasing distance, the shear layer after the separation from the upstream building entrains wind flow from a high level down to the ground and enhances the stationary vortex in front of the downstream building ($K=1.73$ at $L/S=0.8$). When the distance gets larger and larger, the separated flow will reattach on the ground and the flow behaviour in front of the tall building tends to be the same as that in front of an isolated building.

In most cases, the maximum rms overspeed ratios for tandem buildings are lower than those for isolated buildings; the latter are shown in Fig. 5.1.2(a) at $h/S=0$ and (b) at $L/S=\infty$. Hence, only mean wind speeds are considered in the following discussion for tandem buildings.

5.1.2 Ground Pressure Distributions

For the same building models used in Fig. 5.1.2, ground pressure distributions were also measured along the central line between two buildings. Typical pressure coefficients are shown in Fig. 5.1.3 using the same notations as in the previous chapter.

For a given distance, Fig. 5.1.3(a), air pressures between two buildings generally decrease with the increasing height of the upstream building due to the entrainment of wake turbulence. When $h/S=1$, ground pressures become the lowest with a flat distribution

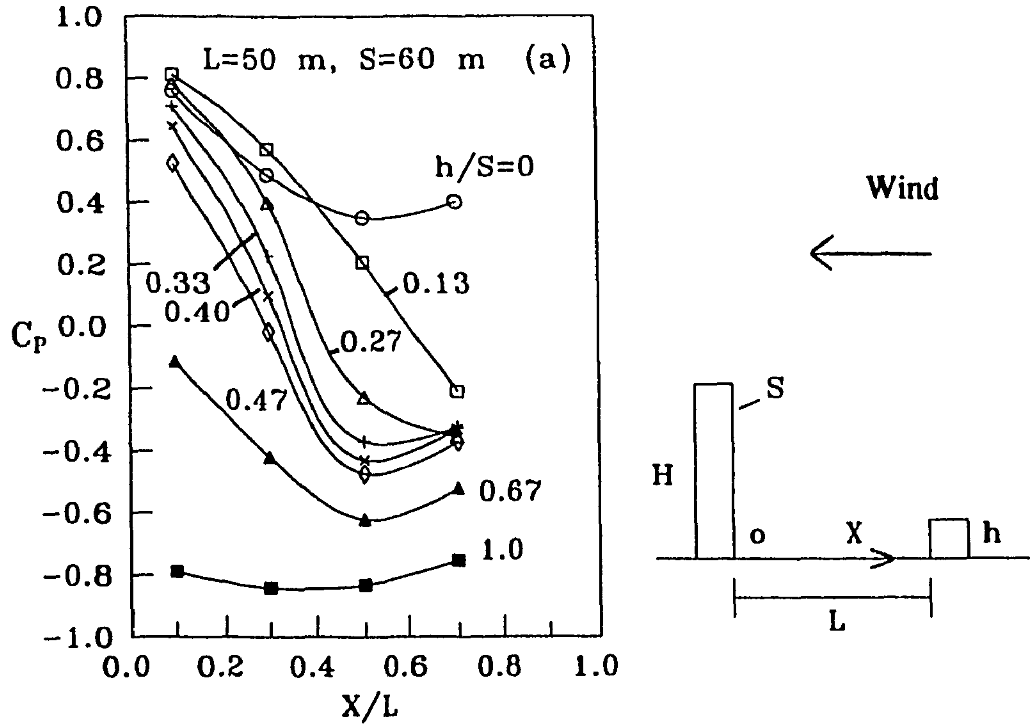

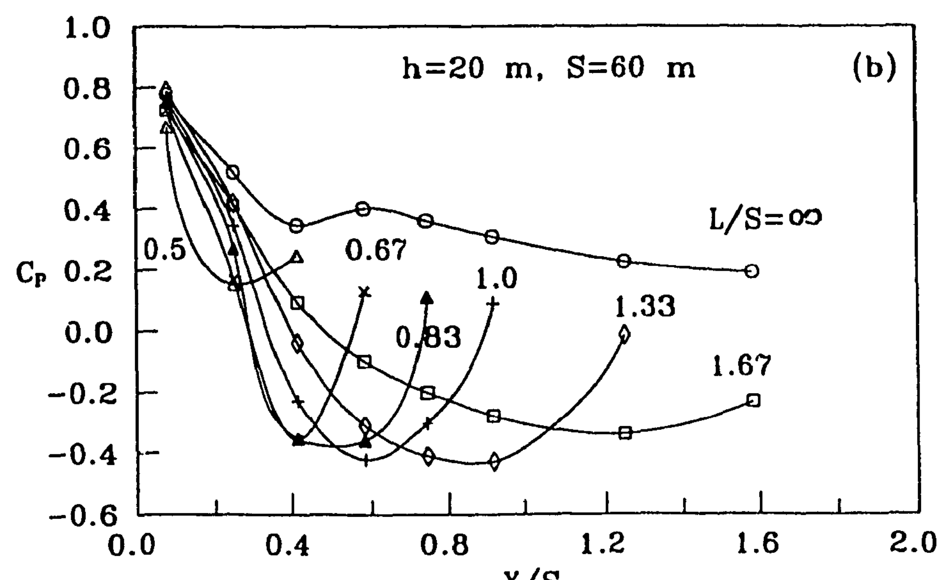

Fig. 5.1.3 Ground pressure distributions between two tandem buildings with various (a) heights of the front building and (b) distances between buildings.

throughout the gap. In contrast, dramatic pressure drops can be observed in front of the tall building for h/S=0.13-0.47. For most combinations, the lowest pressure coefficient in front of the tall building is detected at about X/L=0.5 where the maximum wind speeds take place. It is also observed that building combinations with the highest rate of pressure drop (h/S=0.33 and 0.40, for example) correspond to the models with the maximum wind-speed amplification, see Fig. 5.1.2(a).

Similar conclusions can also be drawn from Fig. 5.1.3(b) where the upstream building is located at various distances from the tall building. With the variation of distance L/S, wind pressures fluctuate slightly at the point adjacent to the downstream building, but substantially elsewhere.

The above results indicate once again that the ground pressure distribution is an informative measure of wind-speed amplifications. It certainly deserves more effort to relate the gradient of ground pressures to the amplification of pedestrian wind speeds, that may furnish another avenue to the estimation of wind speeds at the pedestrian level.

5.1.3 Prediction of Wind Speed

As reviewed in Chapter 2, the wind flow around tandem buildings has been investigated at several laboratories. However, difficulties were encountered during the comparison of these results (Britter and Hunt, 1979). Besides some obvious dissimilarities from laboratory to laboratory, the selection of appropriate scales for a dimensionless presentation is another key factor for an explicit comparison.

The literature data of overspeed ratios between two tandem buildings are plotted in Fig. 5.1.4(a) along with the results of the current study. The average values of wind speeds on two different terrains are used for the data of Isyumov and Davenport (1975a) for H=36 m. The maximum overspeed ratios for tandem buildings, K_{TD}, vary with h/H and L/H as expected. The discrepancy among those results may be explained by differences in the relative building height, the simulation of wind environment, building dimensions and the measurement equipment, height and position(s).

However, these results may be represented by the relative height h/S and the relative distance L/S, because of the important role played by the vortex in front of the downstream building. The maximum overspeed ratio between two tandem buildings (K_{TD})

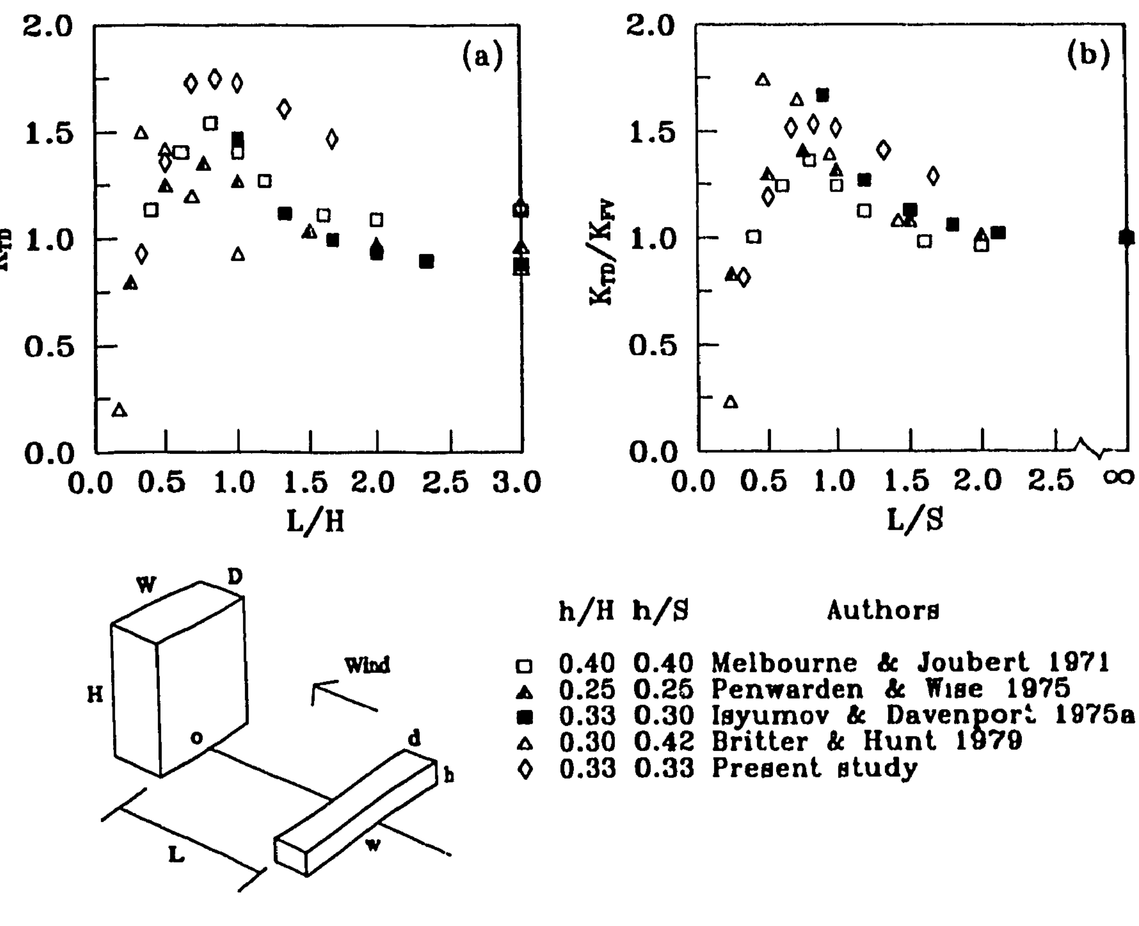

Fig. 5.1.4 (a) Overspeed ratios and (b) modification functions for tandem buildings (data from several sources).

can be related to that in front of the isolated downstream building (K_{FV}) modified by a function of h/S and L/S:

$$K_{TD} = K_{FV} \times M_{TD}(L/S, h/S) \tag{5.1.1}$$

In this presentation form, the previously scattered data can be reorganized in Fig. 5.1.4(b). Despite the difference in relative height (h/S), all data apparently acknowledge a similar trend - having a low value of the modification function for a small L/S, reaching maxima when L/S=0.5 to 0.8 and returning to unity for any further increase in distance. These data, together with other available results, are presented by the modification function in a contour form in Fig. 5.1.5 for the relative height h/S and distance L/S

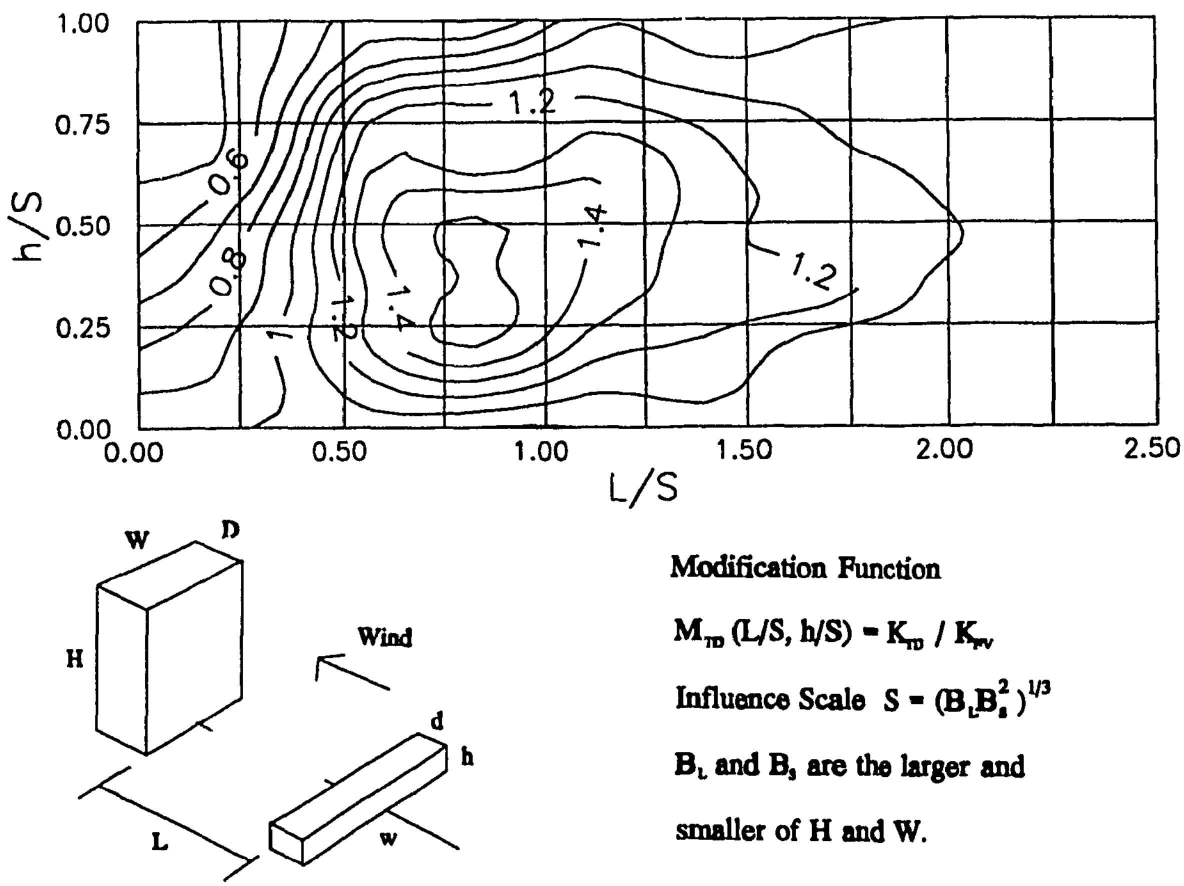

Fig. 5.1.5 Contours of modification function for tandem building models, derived from literature information and the current study.

between buildings. The value of modification function can be found in the figure for h/S<1 and L/S<2.5 and it can then be combined with the overspeed ratio of vortex flow in front of the isolated, downstream building (K_{FV}) using Eq. 4.3.6 to obtain the maximum mean overspeed ratio between two tandem buildings, as formulated in Eq. 5.1.1.

It has been found that the modification function shown in Fig. 5.1.5 can be approximated by an analytic expression, which simplifies the estimation of wind speeds between two tandem buildings. Details are discussed in Appendix E.

In the above process, the two parameters, h/S and L/S, are considered most significant for the flow interaction around the simplified tandem buildings, while some limitations exist for other building dimensions. For the upstream building, the width (w) is assumed to be wide enough to ensure a quasi-two-dimensional flow separation from the central part and the depth (d) is relatively short to avoid any reattachment of the separated flow on the roof. The impact of the depth of downstream building (D) is insignificant on the vortex flow. Further more, these contours only apply for the normal wind incidence with the upstream building lower than the downstream building.

5.2 TWO SIDE-BY-SIDE BUILDINGS

When wind flow passes through a gap between two tall buildings, it may be accelerated due to the so-called *channelling effect*. Two adjacent buildings with the incident wind generally parallel to the gap are called *Side-by-Side* buildings. The channelled flow in the gap could be considered as an interaction of corner streams around individual buildings. The intensity of such an interaction may be strong, weak or even non-existent depending upon the dimensions and distance of buildings.

Results of wind speeds measured along the central line between two tall buildings are discussed first and then expanded for general building dimensions. Wind speed distributions over the gaps between buildings of different dimensions are also discussed for an overall view of the flow pattern around side-by-side buildings.

5.2.1 Wind Speed along Central Line

As mentioned previously, the difference of air pressures is a direct cause of speed variations. When two buildings stand side by side against the oncoming wind flow, they block a larger amount of air flow than does a single building. A strong disturbance to the wind flow creates high pressures in front of buildings and high suctions behind buildings. Due to the increase in pressure difference, wind speeds in the gap between buildings are usually higher than the corner streams around an isolated building. In addition, the channelling effect induced by the side-by-side buildings may restrict lateral movements of air flows and consequently increase the longitudinal wind speeds inside the gap.

Figure 5.2.1 presents mean overspeed ratios along the central line between two identical rectangular buildings (H=W=60 m and D=30 m). The distance between buildings, or the gap width L, varies from 5 to 120 m. As shown in the figure, the overspeed ratios are clearly higher than unity throughout the gap. For a large distance of L/H=2.0, the central line is far from both buildings and a weak interference is observed with the maximum K value around 1.25, which is even lower than the speed of corner streams around an isolated building. When buildings get closer, the maximum K may

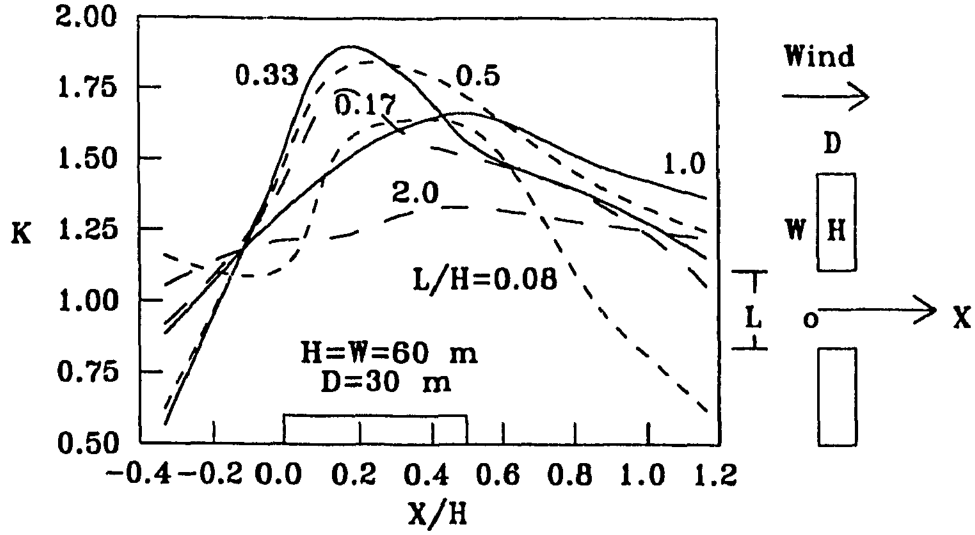

Fig. 5.2.1 Overspeed ratios in the gap between two identical buildings.

reach a value as high as 1.88 for *L/H*=0.33. The wind flow is channelled from the building front of high pressures to the wake of low pressures. For an even narrow channel (*L/H*=0.17 or 0.08), wind speeds inside the gap decrease from the peak. This has not been reported in previous studies - see Wiren (1975) and Stathopoulos and Storms (1986). It appears that for a narrow channel, the wind flow is more likely to fly around the roofs and far corners of buildings, rather than to squeeze into the channel bounded by two parallel building surfaces. This is also manifested in the figure by lower wind speeds in the wake area and higher speeds in front of buildings when *L/H*=0.08, i.e. two buildings act seemingly as one against the oncoming wind.

5.2.2 Effect of Building Dimensions and Distances

By using surface flow visualization, the interaction of horse-shoe vortices is observed around side-by-side buildings with different distances and dimensions. When two buildings are far from each other, two undisturbed horse-shoe vortices are patterned around each building base while the central line is not in the influence zone of either building. For a smaller distance, on the other hand, two vortices overlap and air flow jams into the gap, inducing a channelling flow with high speeds. If buildings get even closer, the two vortices are found to integrate into a single vortex wrapping around a building with a doubled width. The influenced area increases at regions around the outside corners of buildings whereas a little air passes through the channel.

A modification function for two side-by-side buildings may be defined by the ratio of maximum overspeed ratio in the gap over that of corner streams around an isolated building. If the two buildings are identical, the modification function is found only dependent upon the relative distance L/S:

$$K_{GP} = K_{CS} \times M_{GP}(L/S) \tag{5.2.1}$$

where the influence scale S is utilized again because of the vortex interaction around buildings. For four different pairs of buildings measured in the study, the modification function seems to vary with L/S by obeying the same trend as shown in Fig. 5.2.2. If the relative distance is large, $L/S>1.25$ for example, there will be no interaction for the high-speed areas of the two buildings. Wind speeds along the central line are even lower than those around the corner of an isolated building. If $L/S<0.1$, air flow will mainly go around outside corners of buildings and the modification function has a value around one. For an intermediate distance, however, the modification function $M_{GP}(L/S)$ varies with the relative distance and reaches its maximum at around $L/S=0.45$ when the wind speed at the

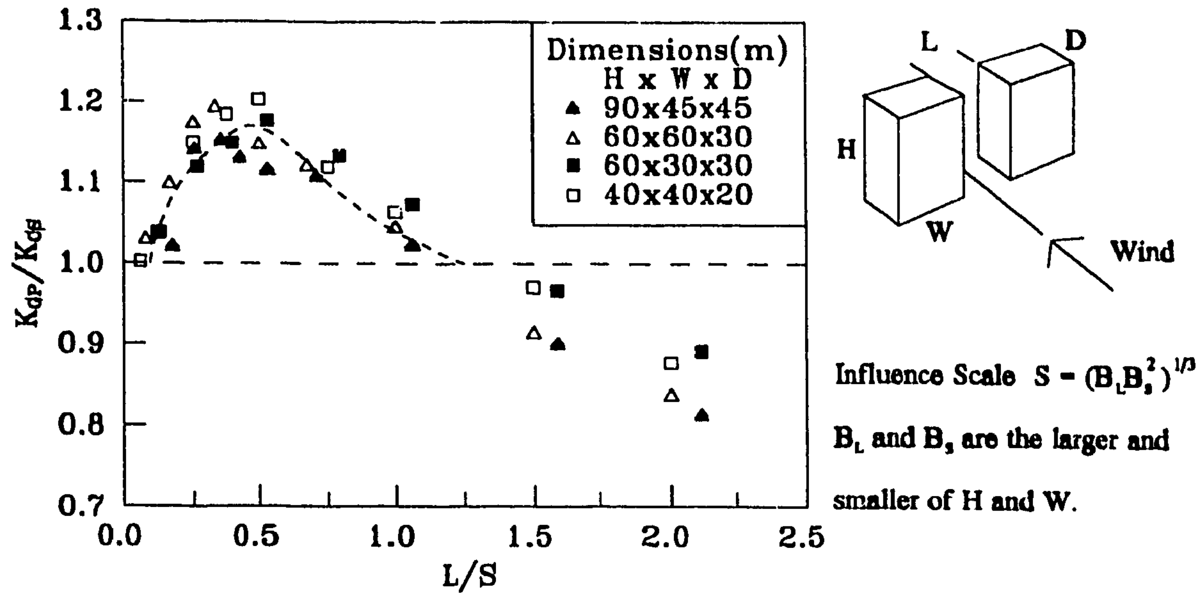

Fig. 5.2.2 Modification functions for the gap flow between two identical side-by-side buildings.

centre of gap may be 20% higher than that of corner streams. For the gap flow between two identical buildings, the value of $M_{GP}(L/S)$ can be estimated by the curve shown in the figure, which is derived by fitting the experimental data.

Note that this approach has to be expanded for the flow between two different buildings. Possibly, the function will remain valid if K_{CS} and $M_{GP}(L/S)$ are considered as some kind of averages with respect to the dimensions of both buildings.

5.2.3 Speed Distribution over Gap

Another issue for the side-by-side model is whether wind speeds along the central line best estimate the wind intensity over the gap. Figure 5.2.3 shows distributions of overspeed ratios for three pairs of buildings. For two ident' :al buildings at the centre of

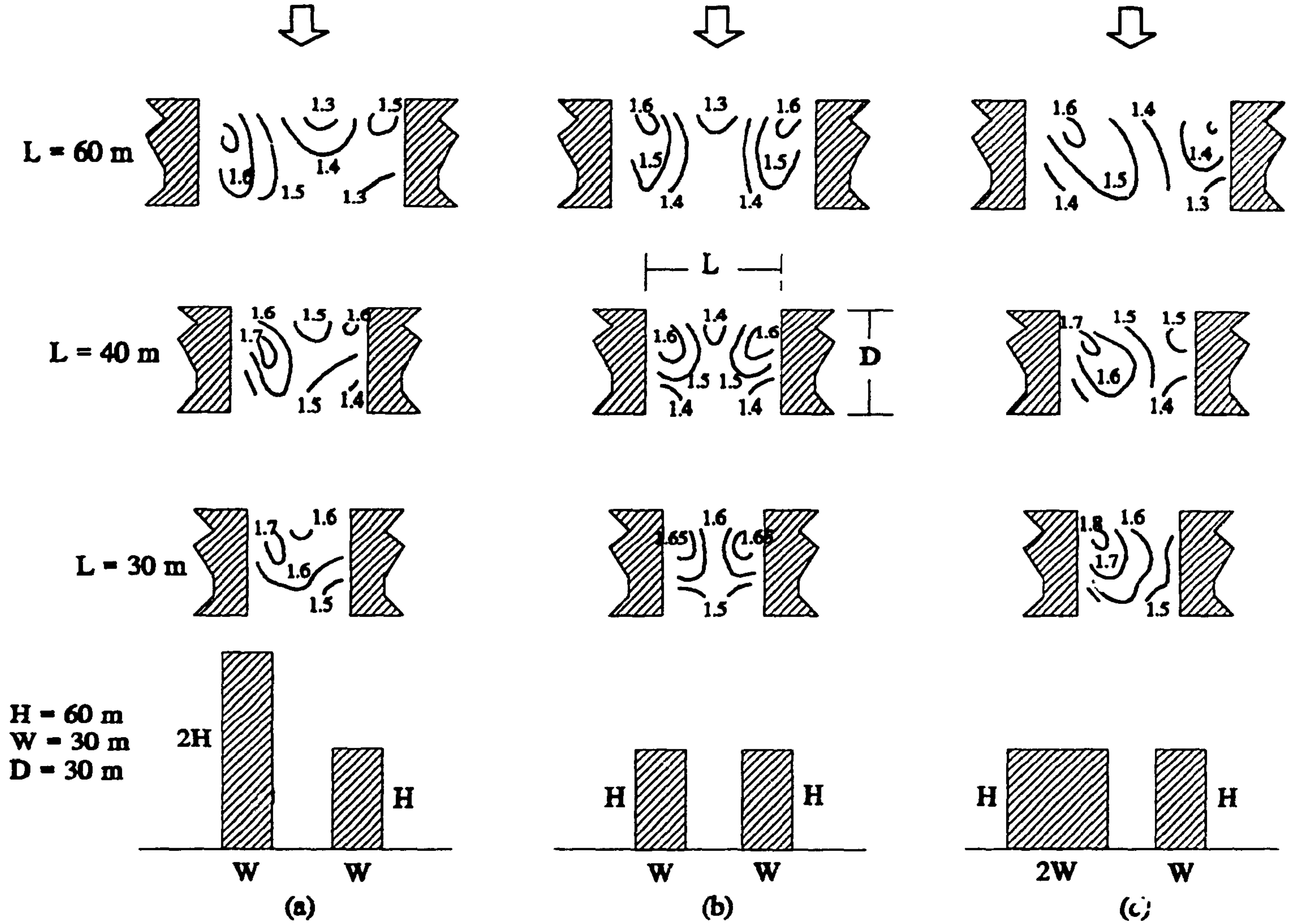

Fig. 5.2.3 Distributions of mean overspeed ratios over gaps between buildings.

the figure, Model (b), wind speeds are found symmetrically distributed over the gap. Wind speeds increase with the decreasing distance from 60 to 30 m. However, speeds along the central line do not represent the maximum speeds over the gaps in general. This is especially true for the model with L=60 m when central-line speeds are much lower than those around building corners.

Also shown in the figure are two combinations with one building either (a) higher or (c) wider than the other. Basically, corner streams around the larger buildings dominate flow fields for all distances, although wind speeds tend to be uniform as the distance decreases. Similar to that for two identical buildings, the smaller the distance down to L=30 m, the higher the wind speeds over the gap. These speed contours suggest that speeds along the central line between buildings underestimate the speeds over the gaps.

Practically, it is the sidewalk around building bases, rather than central portions of streets, that draws attention in pedestrian-level wind studies. The modification function defined for the central line requires some adjustments to represent the variation of wind speeds over the entire passage. Given two buildings with the influence scales $S=S_1$ and S_2, the maximum overspeed ratios of corner streams $K_{CS}=K_1$ and K_2, and the distance L, two overspeed ratios are needed for describing the regions close to respective windward corners around two buildings. When $L/S_i>1.25$ for i=1 and 2, K_i can directly be used for two corner streams with a weak or no interaction. For a narrow street with $L/S_i<0.1$, the speed of uniform gap flow can be estimated by the maximum value of K_1 and K_2; For the intermediate distances, the modification function squared may be more appropriate for the maximum wind speeds of two corner streams channelled by buildings. These observations can be expressed by a single function:

$$
(K_{GP})_{i=1,2} = \begin{cases} K_i & \text{if } L/S_i > 1.25 \\ \max(K_1, K_2) & \text{if } L/S_i < 0.1 \\ K_i \times [M_{GP}(L/S_i)]^2 & \text{else} \end{cases} \tag{5.2.2}
$$

5.3 TWO STAGGERED TALL BUILDINGS

If one of the buildings in the side-by-side model is moved along the wind direction, it will have a longitudinal distance (L_X) in addition to the lateral distance (L_Y) from the other. Buildings become *Staggered* relative to the incident wind. The staggered building model, including the side-by-side model when L_X=0 and the tandem model when L_Y=0, has not been studied as systematically as the other models. For two staggered buildings, the main concern is about the effect of upstream building on the corner streams around the downstream building. Although the existence of downstream building also affects the wind flow around the upstream building, the extent of such an influence is expected to be much less consequential.

A typical model tested in the current study consists of two identical buildings with H=60 m and W=D=30 m. Around the test building, totally 12 wind sensors are installed along the Y axis at both sides of the building in Fig. 5.3.1. The other building is moved around as an influence object. Figure 5.3.1 shows the selected results of mean overspeed ratios along the Y axis for various distances (L_X and L_Y) between the two buildings.

(a) When L_Y/W=3, the two buildings are kept with the same cross-wind distance. Wind speeds around the outside corner of the test building is hardly affected by the location of the influencing building. Corner streams between two buildings, however, do

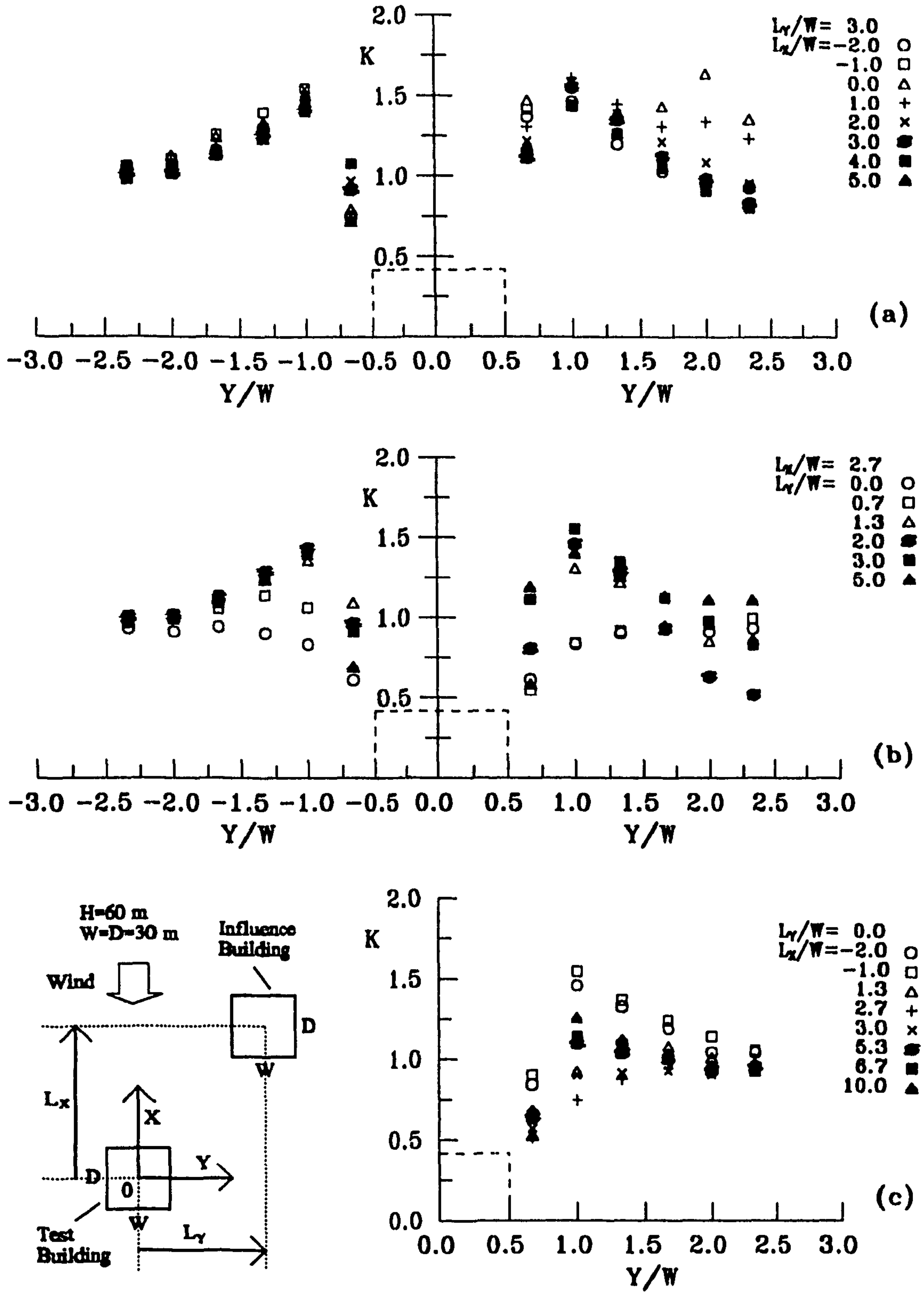

Fig. 5.3.1 Overspeed ratios around corners of a slender building staggered to the other.

vary significantly with the relative locations. When two buildings stand side by side, i.e. L_X/W=0, two peaks are detected between the buildings.

(b) When L_X/W=2.7, the influence building is placed upstream of the test building. At L_Y/W=0, all measured points on both sides of the building are trapped into the wake of upstream building, resulting in low magnitudes of the wind speeds. While the influence building moves to right, wind speeds around the left corner of the test building start to recover. In the mean time, the speeds at right remain at a low level when L_Y/W=0.7 and increase to the maxima at L_Y/W=3 caused by the separated shear layer from the upstream building. For L_Y/W>1.3, wind speed distributions at left appear little differing from that around an isolated building.

(c) L_Y/W=0 indicates two buildings are in tandem position, but flow patterns around two slender buildings are different from what observed for the tandem buildings in Section 5.1. Because of the geometrical symmetry, only right-side wind speeds around the test building are displayed. When the influence building is located downstream of the test building (L_X/W=-2 or -1), the wind speeds are similar to those around an isolated building. If the influence building is moved upstream, the test building falls in the wake area subject to low wind speeds. Such an effect remains evident up to L_X/W=10 for the current building configuration.

An attempt to generalize these experimental results starts with the selection of the representative point for wind speed variations. For most combinations, the maximum wind speed takes place at the second point, i.e. 15 m in full scale from the walls of the test building. For the measurements on this point, contours of overspeed ratios are plotted in Fig. 5.3.2. The contour value at position (L_X, L_Y) shows the wind speed at 15 m from the

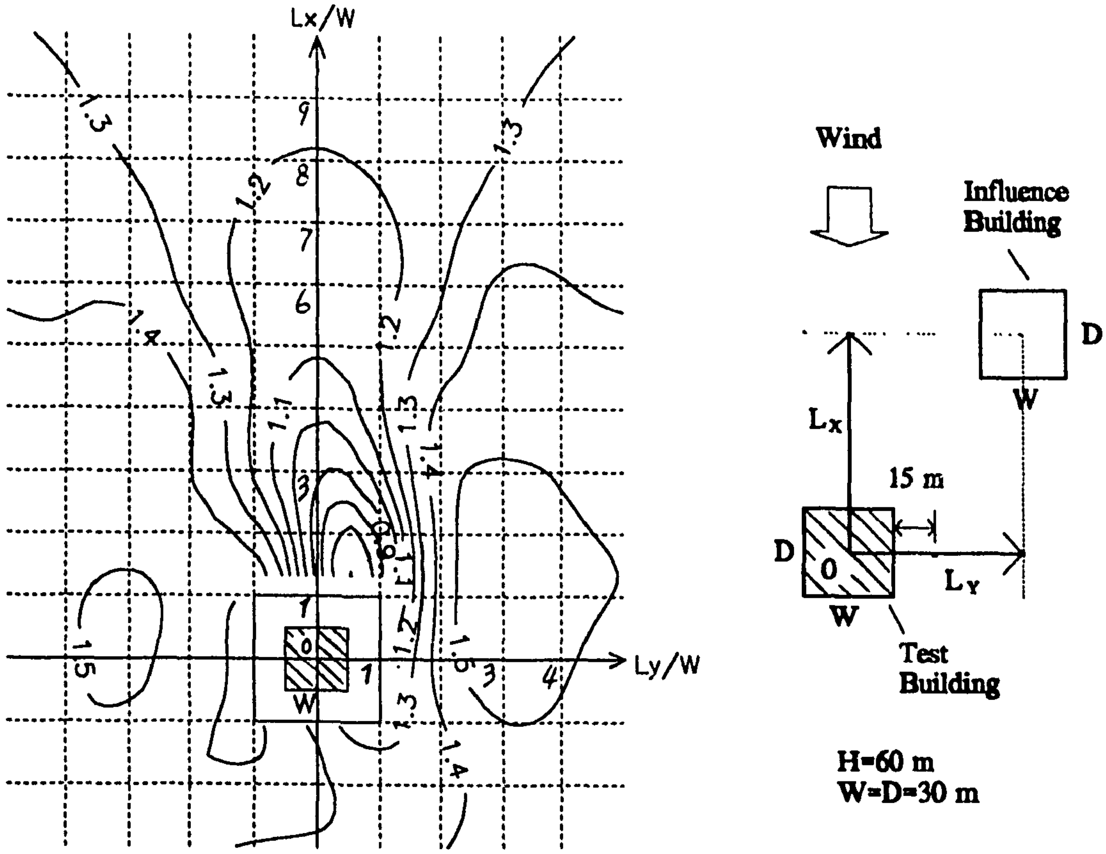

Fig. 5.3.2 Contours of overspeed ratios of corner streams around staggered buildings.

right wall of the test building when the influence building is (L_X, L_Y) apart from centre to centre. Contours are distributed asymmetrically around the building. It is more likely for the speed ratio higher than 1.5 when the influence building is on the right side, compared to that on the left side. It is caused by the channelling effect between two buildings.

Note that, for slab-type buildings, the flow interaction may have different patterns due to the so-called circuit short-cutting of wind pressures (Lawson, 1980, Benarek, 1984 and Bottema, 1993). As illustrated in Fig. 5.3.3, the separated flow attaches on the downwind building and induces a high-pressure zone marked by "+", from which wind flow is driven transversally to the low-pressure zone behind the upstream building. The wind-speed amplification is determined by the overlap portion and the distance between buildings as well as the wind incidence. More experiments are needed for a generally valid modification function for the staggered building models.

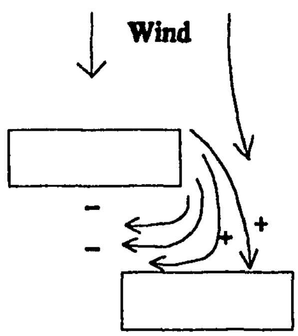

Fig. 5.3.3 Transversal wind drift caused by circuit short-cutting of pressure field around two slab-type buildings.

5.4 OTHER BUILDING COMBINATIONS

5.4.1 Two Buildings

Besides the tandem, side-by-side and staggered combinations, encountered in building design could be other building arrangements, which may induce different wind conditions. Several examples are displayed in Fig. 5.4.1 for two identical tall buildings with the same minimum distance. Wind speeds were measured along the central line of the gap in wind direction. The maximum overspeed ratios of mean speeds and rms values (in parentheses) are given at locations where they actually occur. For Models (a)-(d), both mean and rms

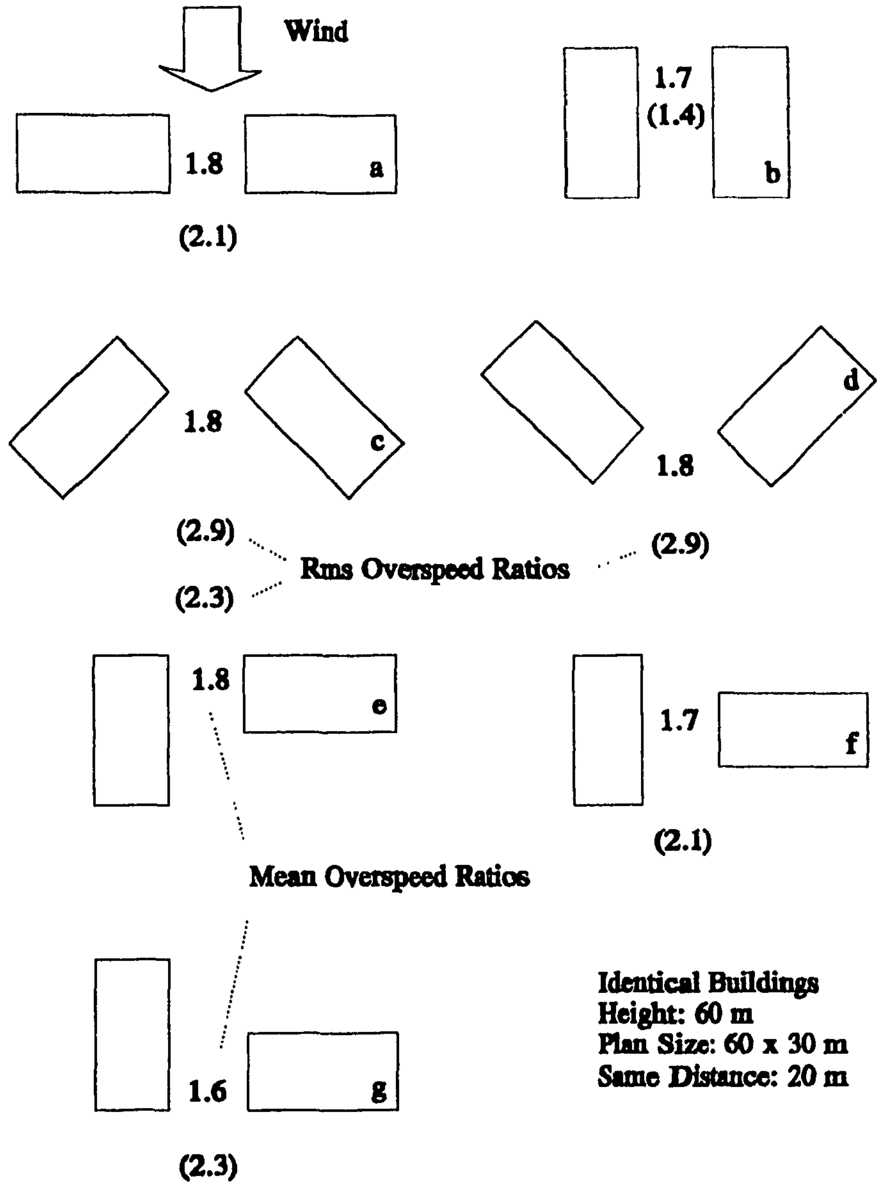

Fig. 5.4.1 Maximum overspeed ratios of the mean and rms wind speeds at their occurring positions in gaps between two tall buildings.

wind speeds in the gap of Model (b) are the lowest due to the smallest windward surface area of the model. High rms overspeed ratios are observed in the wake of Models (c) and (d). For Models (e)-(g), the maximum wind speeds are found decreasing when the right-side building is dragged downwind along the wind direction. It appears that only the building area directly exposed to the approach wind makes contribution to the variation of wind speeds in the gaps between buildings.

Different wind conditions may be created by low buildings. For two identical buildings (15 m in both height and depth, and 60 m in width), infrared thermal images are displayed in Fig. 5.4.2 for a number of building arrangements. For the model with a wide gap, 15 m in (a), the wind impact in wake area is partially alleviated by the gap jet. The flow pattern in (b) with a narrowed gap (10 m) is similar to that around a single long building. Models (c) and (d) create less wind disturbance because of the smaller blockages to the oncoming wind compared with other cases. Behind buildings (e) and (f), the jumping-over flow can be observed with relatively high temperature reductions. More specifically, combination (e) is more critical than (f) in the wind environmental aspect, although buildings in the latter case form a funnel open to the oncoming wind. This is no

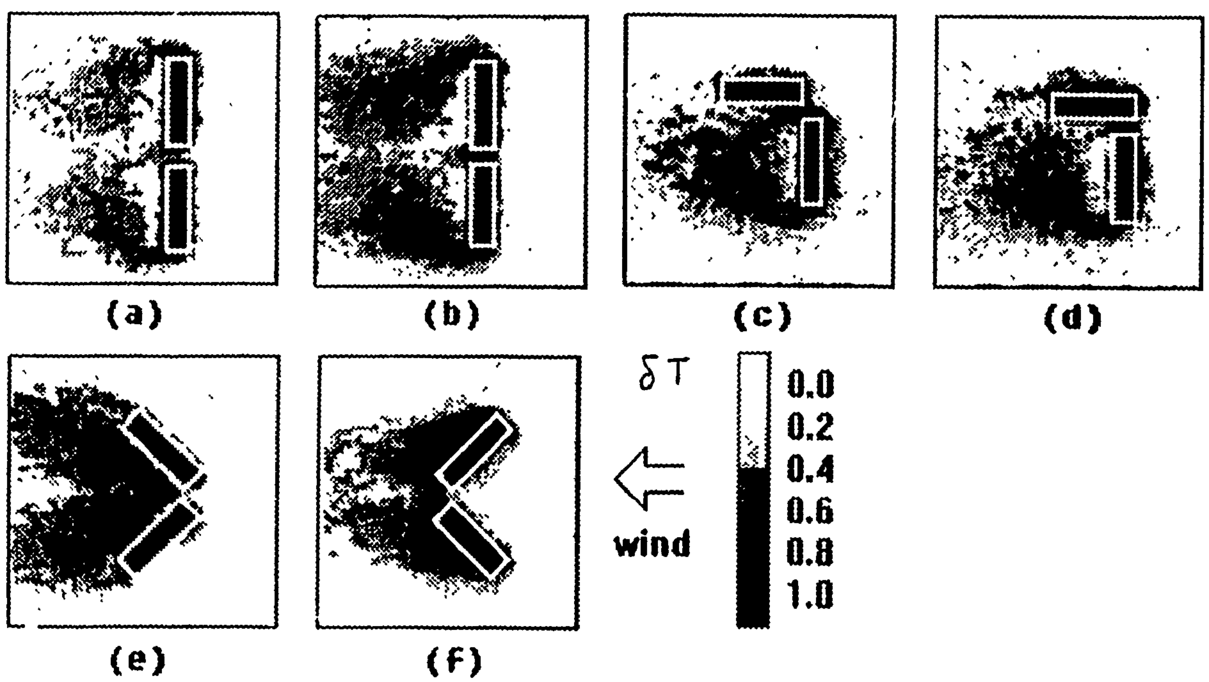

Fig. 5.4.2 Thermal images of reduced temperatures around two-building models.

surprise for low buildings due to the reattachment of jumping-over flows and it agrees with wind speed measurements reported by Wiren (1975). For all six models in Fig. 5.4.2, the overall impact values, defined by Eq. 3.6.2, are listed in Table 5.4.1, which conforms above observations.

Table 5.4.1 Overall impact values of the building models in Figure 5.4.2.

Model	a	b	c	d	e	f
Ω (°Cm^2×1000)	11.3	13.3	9.4	9.7	11.7	11.1

5.4.2 Multiple Buildings

Two-building models have been investigated in this chapter by evaluating the interaction of flows around isolated buildings. For multiple buildings, the flow interaction remains as the key word in interpreting the resulted wind patterns. In other words, the dimensions, relative locations and orientations of buildings have the same importance for multiple buildings as they do for two-building models.

Around four or more buildings mutually parallel or perpendicular to each other, wind speeds were measured by Shoda et al (1979), Wiren (1991) and To, et al (1993), visualized by Beranek (1984) and calculated by Bottema (1993) and others. For a large portion of building groups, high-speed winds only occur around windward corners of buildings with spatially limited flow interactions, that can be assessed in principle by one or two adjacent buildings. For these cases, a superposition of flow patterns around isolated and two-building models is applicable (Beranek, 1984).

For other buildings, integrated wind effects created by multiple buildings have to be considered. Reliable estimations of wind conditions may be obtained by wind-tunnel experiments and numerical calculations. Two common flow phenomena are worthy to be emphasized here for multiple buildings. One is the sheltering effect provided by upstream buildings, which works beneficially for pedestrian winds. Most buildings create shelter in their wake areas with relatively low wind speeds. The other is the circuit short-cutting of pressure fields as explained in Section 5.3. Designers may confront such an effect more frequently when dealing with multiple buildings.

In the following sections, typical multi-building models such as building-enclosed courtyards and tall buildings surrounded by uniform street blocks are discussed in detail.

5.5 COURTYARDS ENCLOSED BY LOW BUILDINGS

A group of buildings may construct a courtyard, inside which a calm wind atmosphere is required for daily activities such as recreation and rest. In this study, building models are designed of 15 m in both height and depth, based on a recent residential development at the Old Montreal. Building lengths and thus courtyard dimensions are variable, and so is the wind direction. The infrared-thermography technique (Wu and Stathopoulos, 1993b) was applied to study the flow patterns inside courtyards and around openings. The thermal images have been analyzed and compared with some reported measurements.

5.5.1 Courtyard without Opening

For a courtyard with a rectangular plan, the approach wind flow hits the windward building first and separates from the roof. The separated shear flow induces a wake vortex whose size and intensity are dependent upon the dimensions of front building and the space between buildings as well.

Figure 5.5.1 shows the distribution of reduced temperatures in seven courtyards with different internal dimensions of (a) 30 m × 30 m, (b) 45 m × 45 m, (c) and (g) 60 m × 60 m, (d) 75 m × 75 m and (e) and (f) 60 m × 30 m. For a small yard in Model (a) or (e), the separated flow from the windward building entrains the air, hence the heat, from the entire yard. Wind flow circulates with a high turbulence intensity. When the along-wind distance between buildings increases as in Models (c), (d) and (f), a well-

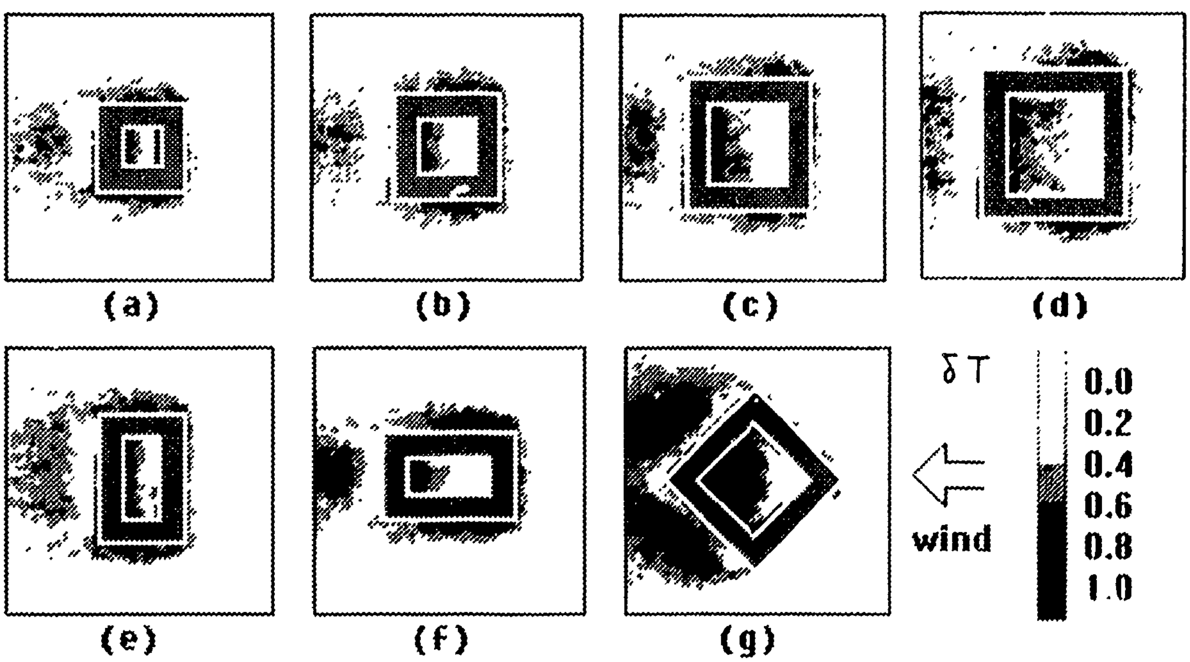

Fig. 5.5.1 Thermal images of reduced temperatures around courtyards enclosed by low buildings without openings.

protected region emerges right behind the windward building while other regions are affected by the possible reattachment of the separated flows. Different temperature distributions are observed for Models (e) and (f) with the same dimensions but different wind directions. For Model (g) with an oblique wind incidence, the wind conditions inside and outside the yard become more unfavourable compared to the Model (c) with the same size. This is the result of the reattachment of jumping-over flow behind low buildings oblique to the incident wind, as discussed before.

The overall impact is calculated only for the inside area of these models and normalized by the corresponding courtyard area A_e, as listed in Table 5.5.1. The normalized value is of the unit of temperature and shows the average temperature reduction inside each courtyard. The highest value is detected for models (g) and (a).

Table 5.5.1 Normalized overall impact values of the courtyard models in Figure 5.5.1.

Model	a	b	c	d	e	f	g
Ω/A_e (°C)	0.66	0.61	0.59	0.54	0.64	0.50	0.70

The thermal images visualize flow patterns inside courtyards enclosed by low buildings. The along-wind length of the courtyard relative to the front building height is the most important parameter in determining the wind conditions inside the yard. Other parameters consist of the along-wind width of the windward building and the wind direction. According to the measurements made by Ettouney (1977), the mean wind speeds inside courtyards increase with the internal dimensions. However, contradictory results are indicated by the thermal images. The reason is simply that the temperature reduction may be induced not only by the mean horizontal wind speeds, but also by the vertical wind flow as well as turbulence fluctuations. All these factors have to be taken into account when the overall impact of wind flow is evaluated for courtyards enclosed by buildings.

5.5.2 Courtyard with Opening

In practice, a courtyard is usually designed with one or more openings connecting the internal yard to external space. High-speed winds may take place at openings depending upon the orientation. In addition, the existence of openings may change the entire flow pattern inside the courtyard.

In Fig. 5.5.2, all openings have the same width of 10 m except in (a) and (c), whose widths are 5 m and 15 m, respectively. The courtyard areas are 60 m × 60 m for Models (a)-(g), 45 m × 45 m for (h) and (i), and 30 m × 30 m for (j). In general, an opening to courtyard increases the ventilation inside the yard and lessens the down-washing wind in front of the downstream building to certain extent. Temperature patterns are similar to each other for Models (a)-(c) regardless of the opening width, although the wind speed over the opening increases with a decreasing opening width. Models (b) and (d)-(g) have the same dimensions but different wind incidence. Surprisingly, Model (b) with its gap facing the wind induces the lowest wind impact inside the courtyard. This is observed again with Models (h) and (j) with smaller size courtyards. The wind effect in Models (e), (f) and (g) with openings not direct to wind is much more severe than

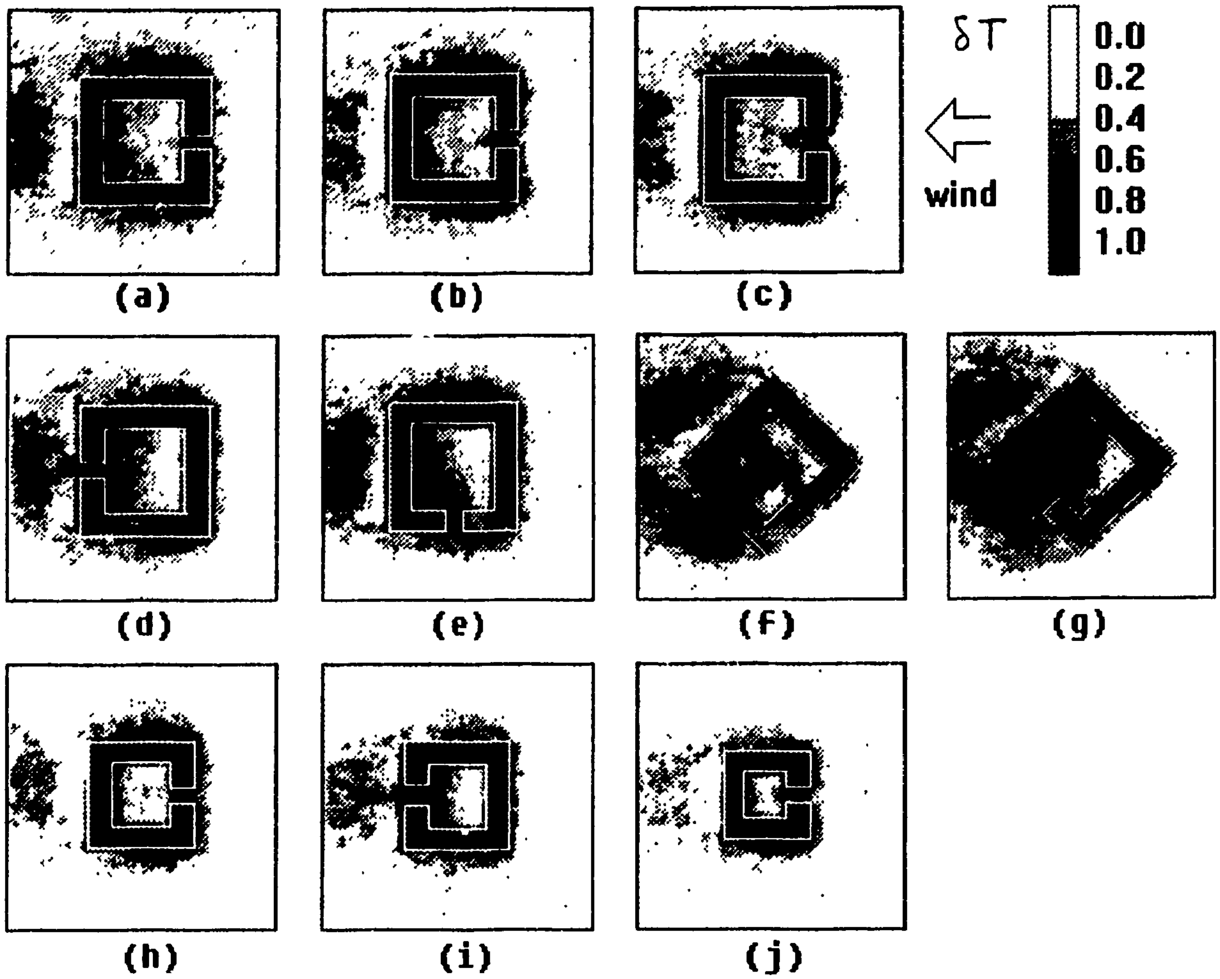

Fig. 5.5.2 Thermal images of reduced temperatures around courtyards enclosed by low buildings with openings.

others. An explanation for such a phenomenon may be that the wind flow through openings into the courtyard raises the air pressure inside the yard and eases the reattachment of the jumping-over flow separated from the windward buildings.

The normalized overall impacts are also calculated for the inside courtyard areas and listed in Table 5.5.2. Once again, these values conform the above descriptions in general. The highest values are observed for Models (g), (e) and (f).

Table 5.5.2 Normalized overall impact values of the courtyard models in Figure 5.5.2.

Model	a	b	c	d	e	f	g	h	i	j
Ω/A_e (°C)	0.50	0.50	0.51	0.57	0.62	0.62	0.68	0.46	0.55	0.56

Information can be found from the literature for wind speeds inside the courtyard (Ettouney, 1977) and for the gaps between two low buildings with various combinations (Wiren, 1975). More studies are required to explore the wind environmental conditions around building-enclosed courtyards. By combining the literature information and the current findings, rules of thumb are attempted in this study for the estimation of wind conditions inside courtyards and at openings. See Appendix F for details.

5.6 STREET BLOCKS

Discussed so far are simplified building models approached by simulated wind profiles over uniform upstream roughness. However, effects of surrounded street blocks and other parameters have to be properly taken into consideration.

5.6.1 Models and Instrumentations

In modelling street blocks, models were made of wood pieces with the same dimensions of 19 × 100 × 200 mm, corresponding to full-scale street blocks 9.5 m high and 50 × 100 m in plan size under a geometric scale of 1:500. The block height could be increased easily by piling up wood pieces, as shown in Fig. 5.6.1. In a typical model arrangement, there were usually five rows of blocks upstream of the main building which was located at the centre of the turntable of wind tunnel. Both the block height h and the main building height H were multiples of 9.5 m,the plan dimensions W and D were either 100 m or 50 m depending on the wind direction, the width of along-wind street (L_A) was 25 m or 15 m whereas that of cross-wind street (L_C) was kept constant at 25 m.

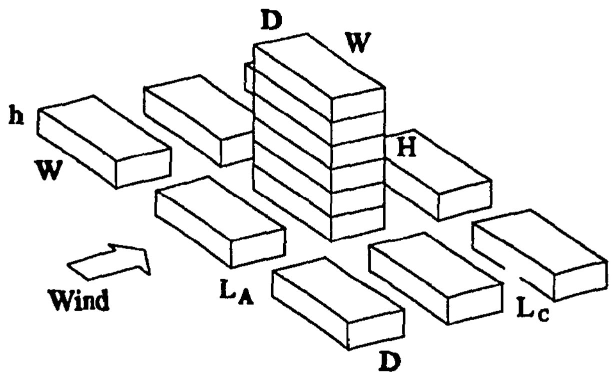

Fig. 5.6.1 A typical model arrangement with a tall building surrounded by uniform street blocks.

Irwin's surface pressure sensors were utilized considering their advantages in measuring a large number of horizontal wind speeds. With the height of 4 mm (2 m in full scale) above the ground, 37 sensors were distributed as shown in Fig. 5.6.2 for street widths of 25 m. The least distance between sensors was 20 mm in order to avoid any possible interference. The sensors were installed in the centre of streets and at distances of 5 mm (2.5 m in full scale) from buildings, mainly on sidewalks and crosswalks of streets where both high-speed winds and pedestrian activities take place. While most attention was paid to the along-wind street, the wind speeds on cross streets were also

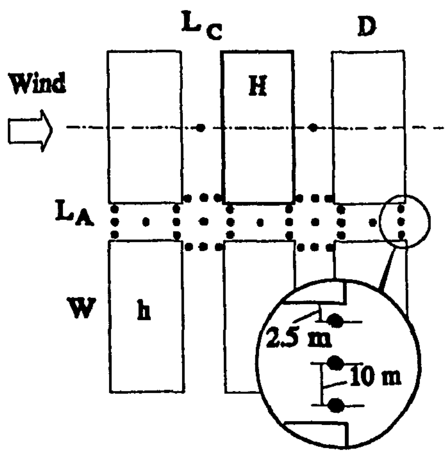

Fig. 5.6.2 Measurement points on streets 25 m wide.

measured on crosswalks, as well as in front of and behind the main building. Such a sensor arrangement also applied for the street models with the short side (50 m) facing the approach wind. When a narrow street (L_A=15 m) was tested, six points of measurement were covered by building models.

Mean wind speeds (V) are normalized by two reference speeds, namely, V_O, the mean wind speed at each measured point when no building models are present, and V_S, the wind speed on streets between uniform blocks when all street blocks are of the same height ($h=H$). By definition, V/V_S=1 at all measured points when H/h=1. For the same building configuration, values of V/V_O are usually lower than one due to the sheltering effect caused by buildings.

5.6.2 Uniform Street Blocks

For uniform street blocks, the wind speeds along streets are mainly dependent upon the distribution and density of blocks. If buildings on a street block can be typified by a single cuboid as shown in Fig. 5.6.3, the following two area ratios can be defined according to Oke (1988): (1) the plan density, A_R/A_L, which is the ratio of the roof area of building over that of the building lot; and (2) the roughness density, A_S/A_L, based on the front area of the building. These ratios can be expressed as follows:

$$\frac{A_R}{A_L} = \frac{W \times D}{(W+L_A)\times(D+L_C)} \quad , \quad \frac{A_S}{A_L} = \frac{W \times h}{(W+L_A)\times(D+L_C)} \qquad (5.6.1)$$

where W and D are cross- and along-wind lengths of a block, L_C and L_A are widths of cross- and along-wind streets around the block, and h is the block height. The two ratios have the same value if the street block is a cube, i.e. W=D=h. The roughness density is related not only to the plan dimensions, but also to the building height; it may be more indicative than the plan density from the viewpoint of wind conditions on streets.

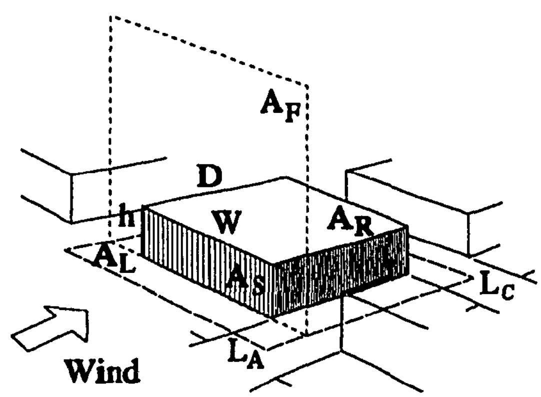

Fig. 5.6.3 A sketch of simplified street blocks: dimensions and areas.

However, both ratios are based on the lot area, that, sometimes, may not be quite suitable for the representation of street densities and wind intensities. For non-cubic blocks, an increase in the along-wind length (D) will, by definition, reduce the roughness density, but may increase the plan density in certain cases. On the other hand, it is well known that the effect of along-wind length is insignificant on the wind speeds around building corners and between two side-by-side buildings. It is the windward building surfaces that affect the oncoming wind flow and influence the wind conditions at street level. Based on these considerations, a new area ratio using only windward areas of buildings and streets is proposed here:

$$R_B = \frac{A_S}{A_F} = \frac{W \times h}{(W + L_A)^2} \tag{5.6.2}$$

in which R_B is called the blockage ratio, describing the percentage of approaching air flow *seen* by the building block. The value of R_B increases with an increasing block height h and a decreasing street width L_A (simplified as L in the following sections), while the windward length of blocks W has a complex effect on the blockage.

An average wind speed $\overline{V}_S$ is taken over all measured points on an along-wind street, excluding 14 points on cross-wind streets as sketched in Fig. 5.6.4. The value of $\overline{V}_S$ is found decreasing with an increasing block height, which is the primary influence parameter. On the other hand, the street width and the plan size of blocks show their impact on the average wind speed in more complex patterns. The integrated impact, however, is found directly related to blockage ratio R_B instead of any single parameter. An empirical relation, obtained by the regression technique, can be expressed by:

$$\overline{V}_S / V_O = 1 - 0.9 R_B^{0.4} \tag{5.6.3}$$

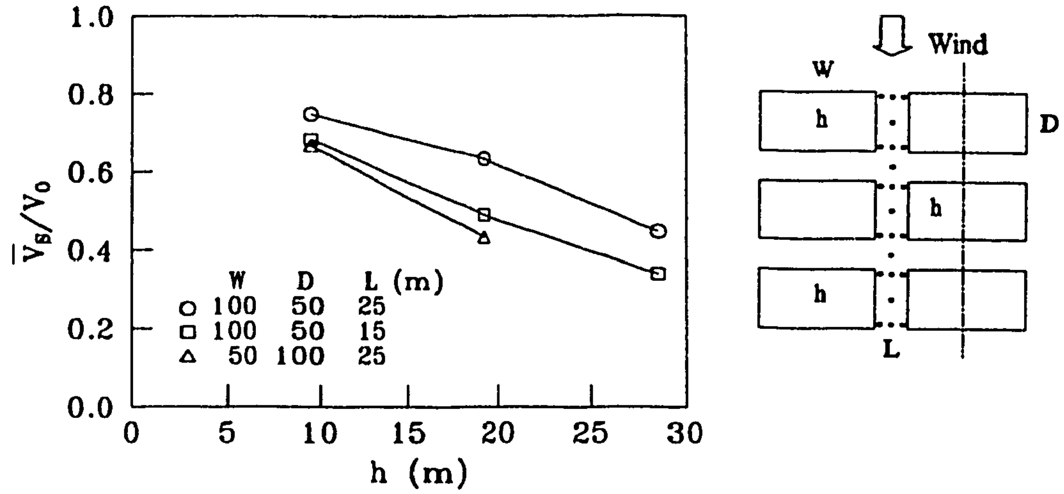

Fig. 5.6.4 Averaged wind speeds over the along-wind streets between uniform blocks.

The agreement of such a relation with the wind-tunnel results is demonstrated in Fig. 5.6.5 containing data from the literature and the present study. According to this relation, wind speeds along streets decrease with an increasing blockage ratio. For

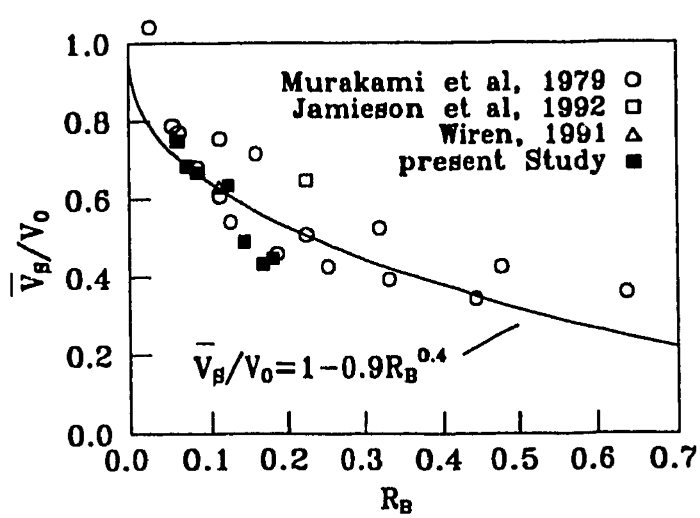

Fig. 5.6.5 Empirical relation between the average wind speed and the blockage ratio.

example, suburban terrains with low R_B values cannot provide shelter for street winds, whereas wind flows may skim over downtown cores of large cities with high R_B values without disturbing pedestrians on streets. However, this is true only for blocks with the same, or comparable heights. If a building is much taller than its surroundings, wind patterns on streets around the building may change significantly.

5.6.3 Tall Buildings above Uniform Surroundings

The street-level wind patterns become different when the height of the main building increases, as indicated in Fig. 5.6.6 - note that the building models in Fig. 5.6.6(b)-(d) are not plotted to scale. The maximum values of V/V_O are 0.74, 1.3 and 1.7, and those of V/V_S are 1.0, 5.0 and 5.7 for H/h=1, 2 and 4, respectively.

The speed variation may be attributed to several geometric factors such as H, h, W and L, but the most direct cause is the height difference (H-h). For a tall building in a built-up region, only the building surface above surroundings obstructs and deflects air flow down to the street level. For a number of building configurations, the ratio of maximum mean speed over that in the oncoming wind at the ground level (V_M/V_O) is plotted in Fig. 5.6.7 and it increases with the height difference. Although the same measurement height (2 m) was used in the present study, it is well known that the higher the measurement level, the lower the mean wind speed ratios such as V_M/V_O. Further analysis indicates that such speeds also increase with a decreasing blockage ratio of surroundings, or an increasing average speed over the along-wind street. In other words, the increase of kinetic energy of wind flow at street level stems from the approach wind

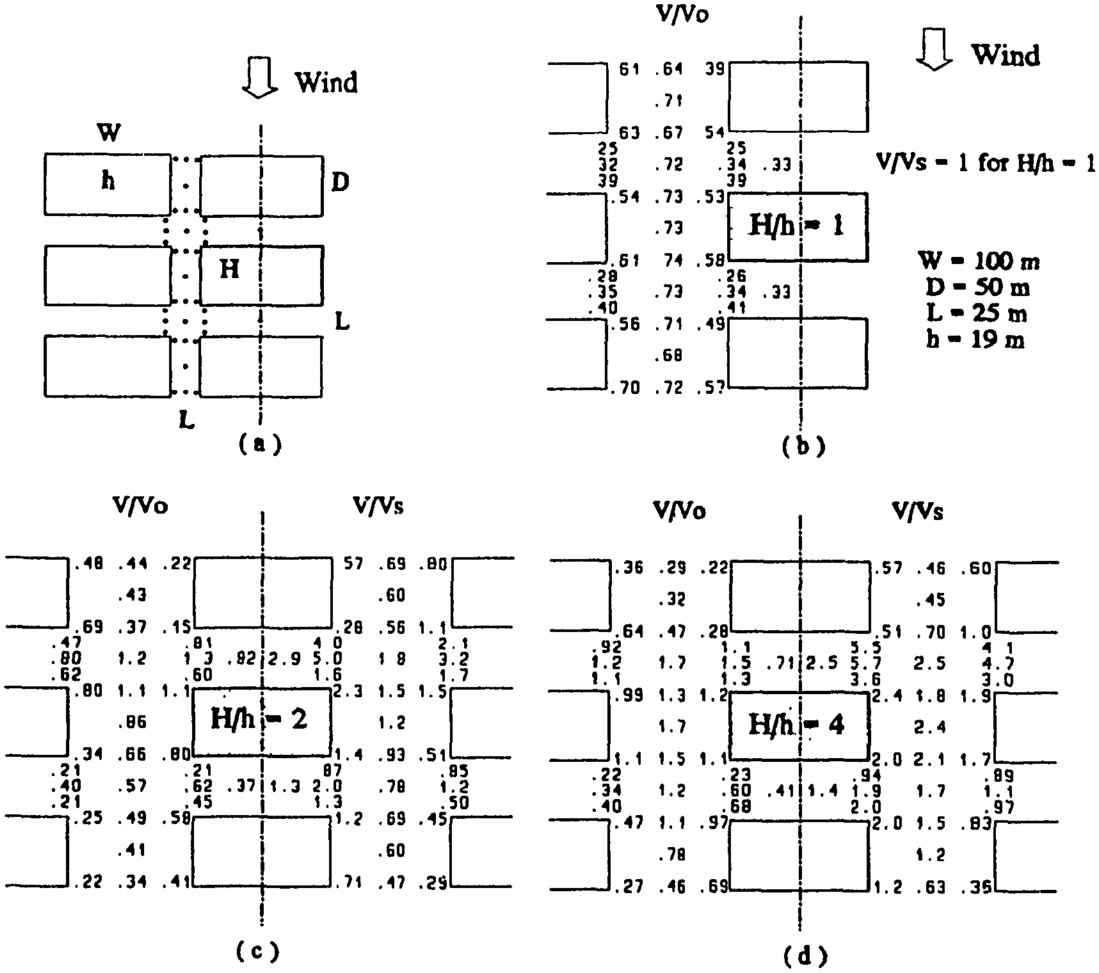

Fig. 5.6.6 Wind-speed ratios distributed around buildings standing among uniform street blocks.

flows at both the street level ($\overline{V}_S/V_O$) and higher levels; the latter may relate to the non-dimensional height difference $(H\text{-}h)/b$. A tentative relation is given as follows:

$$(V_M/V_O)^2 = C_1(\overline{V}_S/V_O)^2 + C_2\left(\frac{H-h}{b}\right)^{C_3} \tag{5.6.4}$$

where b is the height of speed measurement, and C_1, C_2 and C_3 are constants determined by experimental data. By using the linear regression technique, constants (C_1, C_2, C_3) are

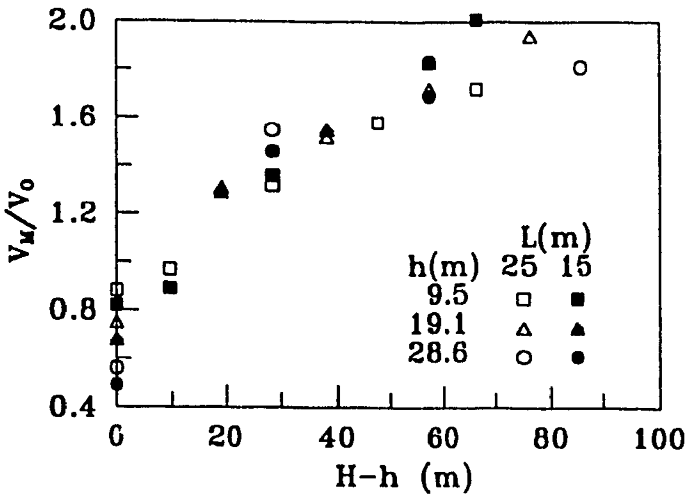

Fig. 5.6.7 Variation of maximum wind-speed amplification with the height difference.

calculated as (2.0, 0.12, 0.88) for data of the present study. These constants are also applicable for other cases from the literature when the measurement heights (ranging from 2 to 10 m) are taken into account for the wind-speed prediction. The agreement of predicted speeds with measured data is shown in Fig. 5.6.8. A more accurate empirical relation may be expected if a wider range of wind-tunnel results are obtained and analyzed.

While the highest wind speed normally takes place around the windward corners of a tall building, the vortex flow in front of the tall building is also critical in some building cases. The speed ratio V_F/V_O at the central point in front of the main buildings in Fig. 5.6.6 is 0.33, 0.82 and 0.71 for H/h=1, 2 and 4, respectively. More wind-tunnel data are summarized in Fig. 5.6.9 for the speeds in front of tall buildings against the height difference of buildings. The speed ratio jumps from its lowest value at H-h=0 to the maximum at H-h=h to $2h$. After reaching the maximum, the speed decreases slightly

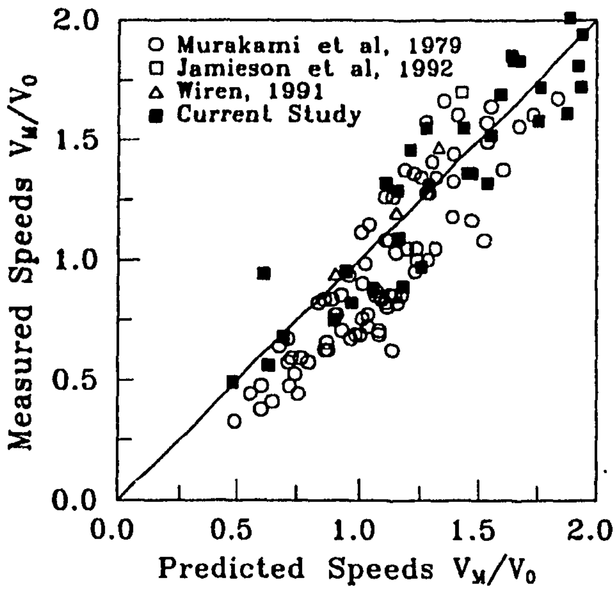

Fig. 5.6.8 Comparison of measured and predicted wind speeds around tall buildings with uniform surroundings.

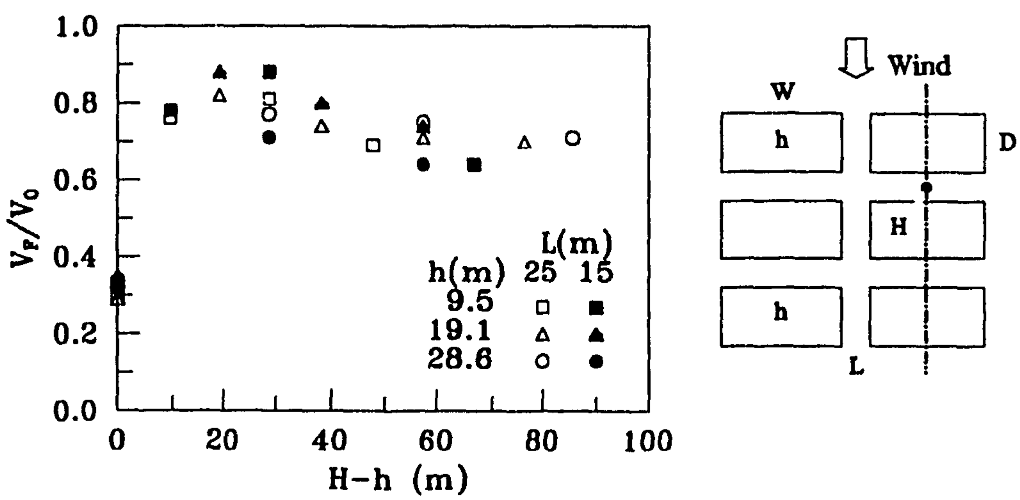

Fig. 5.6.9 Variation of wind speeds in front of tall buildings with height differences.

for any additional increase in the height difference for all cases tested. One possible explanation to this phenomenon is that as the height difference becomes larger , the high level air flow tends to move laterally around the tall building, instead of vertically down to the street level. In addition, the intensity, size and position of front vortices depend not only on the height difference, but also on the distance between buildings. See Section 5.1 for further explanations.

5.6.4 Other Considerations

For all building models discussed so far, the wind flow is parallel, or perpendicular, to streets. Actual winds, however, may come from any direction. For oblique wind directions, the blockage ratio, hence the wind speed, is expected to change. Take uniform street blocks with h=H=19 m and L=25 m for example. When W=100 m and D=50 m, wind speeds on along-wind streets decrease from about 0.7 to 0.4 as the wind direction changes from 0° to 22.5°, as shown in Fig. 5.6.10. Under the same circumstance, the wind speeds on cross-wind streets do not change much, except at the centre of blocks where wind speeds are more than doubled. When the wind angle becomes 45°, wind speeds on both streets are higher than those for 22.5° or even for 0° over some zones. This is also true for the street arrangement with W=50 m and D=100 m, for which, oblique winds (22.5° and 45°) provide higher speeds in general. This appears contradictory to the well-known guidelines that suggest street blocks be oriented diagonally to prevailing winds for the best protection of pedestrians. However, this finding is limited to uniform blocks with buildings of relatively low heights. More measurements are required to study the speed variation with the incident angle for different configurations of street blocks.

In built-up cities, a tall building may be located at the corner or midway of a

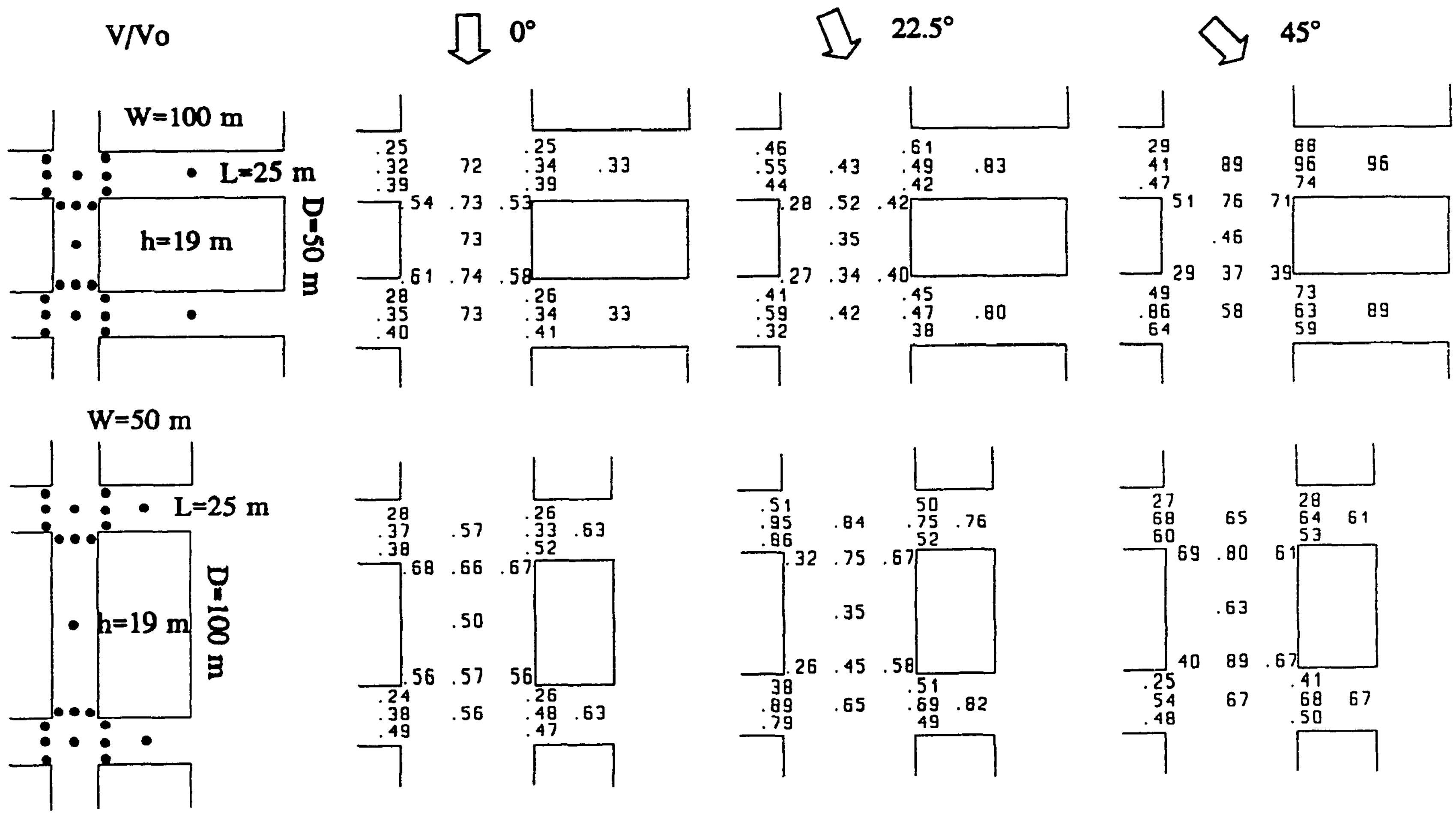

Fig. 5.6.10 Effect of wind incidence on wind speeds around uniform street blocks.

block, instead of possessing the entire block. Consequently, its impact on the wind environment may be different on nearby streets. Figure 5.6.11 provides two examples of wind speed distribution along the central line of an adjacent street when the tested tall building has different dimensions and locations, but h=9.5 m and L=25 m for all cases. The main building tested is equally divided into two parts with heights H_1 and H_2. When

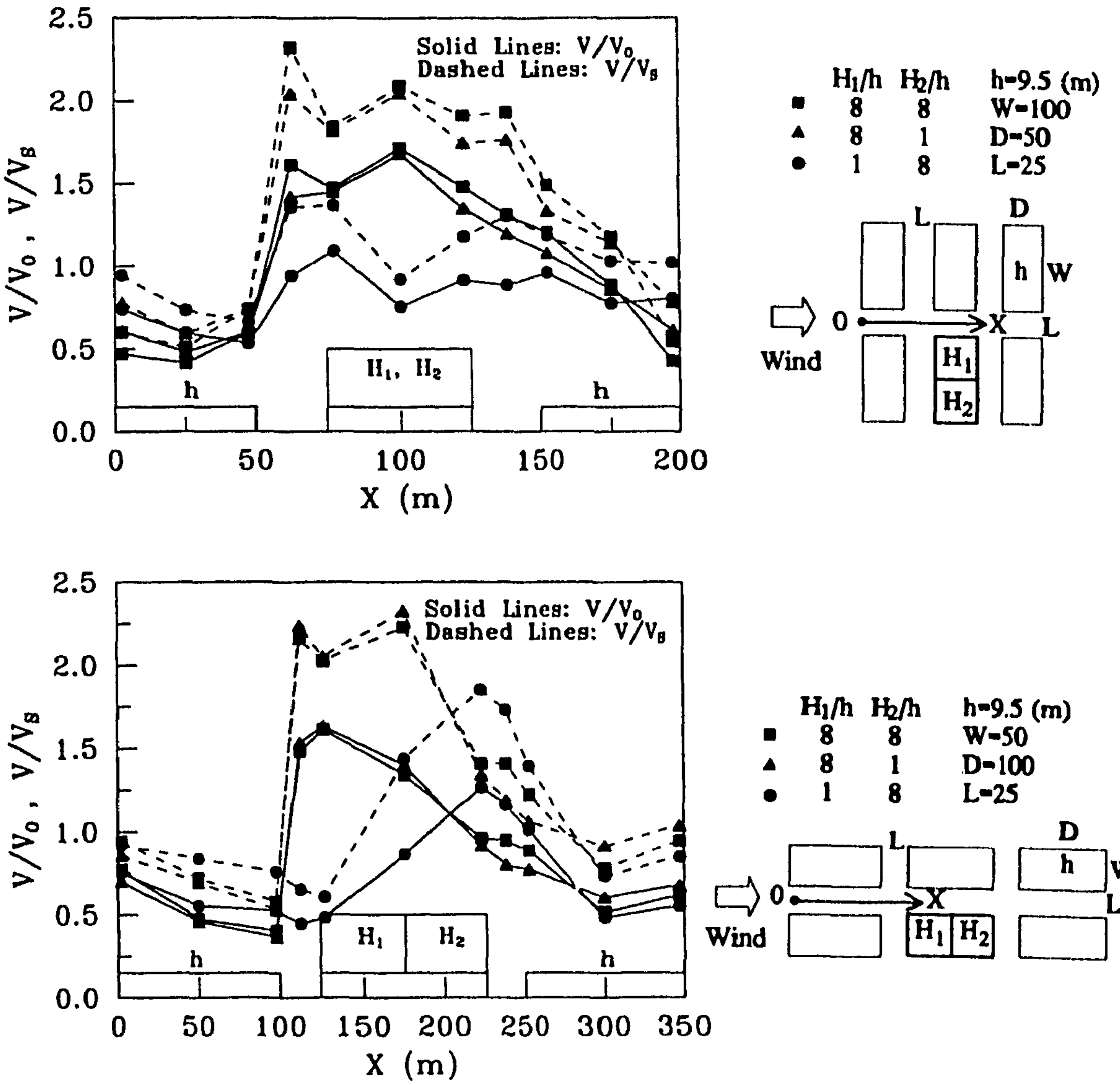

Fig. 5.6.11 Effect of tall building locations within a block on wind speeds along adjacent streets.

the two parts have the same height $H_1/h=H_2/h=8$, i.e. a single building covering the entire block, both speed ratios get values higher than other cases. More specifically,

(a) If the tall building with a half width of the block is located nearer the street where the measurements take place ($H_1/h=8$ and $H_2/h=1$), the speed ratios decrease slightly in comparison to the case of $H_1/h=H_2/h=8$. When such a building is moved to the far side of the block ($H_1/h=1$ and $H_2/h=8$), the maximum values of the two speed ratios drop significantly with (V/V_O, V/V_S) equal to (1.7, 2.3), (1.7, 2.0) and (1.1, 1.3) for the three cases, respectively.

(b) When the windward width $W=50$ m, the slender building can be moved along the wind direction within the same block. If the slender building covers the front half of the block ($H_1/h=8$ and $H_2/h=1$), it induces high wind speeds on the street similar to those with the tall building covering the entire block. On the other hand, when the slender building is drawn backwards ($H_1/h=1$ and $H_2/h=8$), wind speeds are reduced by a noticeable amount (from 1.6 to 1.3 for V/V_O). The location where the maximum speed occurs is also moved downstream accordingly.

The speed drops in both cases demonstrate the efficiency of a setback, or a large podium, on wind reduction in the design of high-rise buildings.

5.7 SUMMARY

In this chapter, wind flows around two- and multi-building models are discussed. These models consist of two buildings in tandem, side-by-side and staggered combinations relative to incident winds, building-enclosed courtyards with and without openings, and tall buildings surrounded by street blocks. The wind flows around two or more buildings are considered as the interaction of flows around respective isolated buildings, estimated by the influence scales and relative locations of buildings. Conclusions are drawn for these models based on the current wind-tunnel experiments and the literature information.

For two tandem buildings, the down-washing flow in front of the downstream building is modified by the presence of the upstream building. The extent of modification could be assessed by a function of the relative height and the relative distance, which is provided in contour form. For side-by-side models, the wind flow is channelled into the gap between buildings. The influence scales and distance between the two buildings determine the intensity of interaction of corner streams around the buildings. When two buildings are staggered, the sheltering effect and the pressure-short-cutting effect must be considered in addition to the front vortex and the channelled flow. These two effects may become more significant for multiple buildings, around which some kind of superposition of flow patterns around isolated and two-building models may be applicable.

For a courtyard enclosed by buildings, the inside wind conditions vary with the height of the windward building and the along-wind length of the courtyard. If one or more openings are designed for a yard, there will be high-speed winds at the openings for certain orientation. The inside wind environment, on the other hand, may also be changed significantly depending upon the orientation and location of openings - a windward opening makes the reattachment of jumping-over flow rather unlikely and other openings work in the opposite way for all tested cases.

For uniformly distributed street blocks, a blockage ratio is defined by the windward dimensions of buildings and streets. The average wind speed over along-wind streets can be estimated by such a blockage ratio; When a tall building is surrounded by uniform blocks, the maximum speed amplification is a function of the height difference of the tall building from surroundings, the blockage ratio of surrounding blocks and the measurement height. Empirical equations have been suggested for the assessment of wind conditions for several cases. Further experiments have been carried out for the effects of wind direction and location of the tall building within a street block.

It should be pointed out that the pedestrian-level wind conditions in a built-up region are influenced not only by the adjacent buildings, but also by the meteorological records and upstream terrains. Some architectural details of building design may also affect the local wind conditions as well. More information regarding these aspects is presented in the next chapter.

CHAPTER 6

URBAN MICROCLIMATIC WIND CONDITIONS

In the two preceding chapters, wind mechanisms has been studied for several simplified building models ranging from isolated tall buildings to street blocks. Both the speed amplification and the spatial extent of building-induced winds at the pedestrian level have been parameterized with the characteristics of building models and approach winds, based on wind-tunnel experiments and theoretical analyses.

On the other hand, the urban microclimatic wind conditions are also affected by other elements such as the regional meteorological data, the roughness and topography of surrounding terrains, the configuration of adjacent buildings as well as the architectural details of buildings under investigation. Besides an objective estimation of wind speeds and their frequencies of exceedance, a subjective diagnosis can also be performed by conforming the wind discomfort criteria established by scientific research and/or the design guidance formulated by city authorities. Appropriate remedial actions may be necessary to consider in practical cases for improving the wind environmental conditions. An evaluation of the wind conditions is incomplete if any of the above-described elements is not properly taken into account.

In this chapter, the major elements affecting the urban microclimatic wind conditions are identified and discussed in detail. A case study is provided to illustrate the entire process for the wind evaluation. The knowledge discussed in this chapter along with the wind mechanisms presented in Chapters 4 and 5 constitutes the basis for a knowledge-based system developed for the preliminary evaluation of wind conditions at the pedestrian level.

6.1 INFLUENCE ELEMENTS

As mentioned previously, the development of wind profiles from a weather station to a built-up site is affected by a number of elements, including the roughness and topography of upstream terrains, the configuration of surrounded buildings and the features of main building under consideration. They are sketched in Fig. 6.1.1.

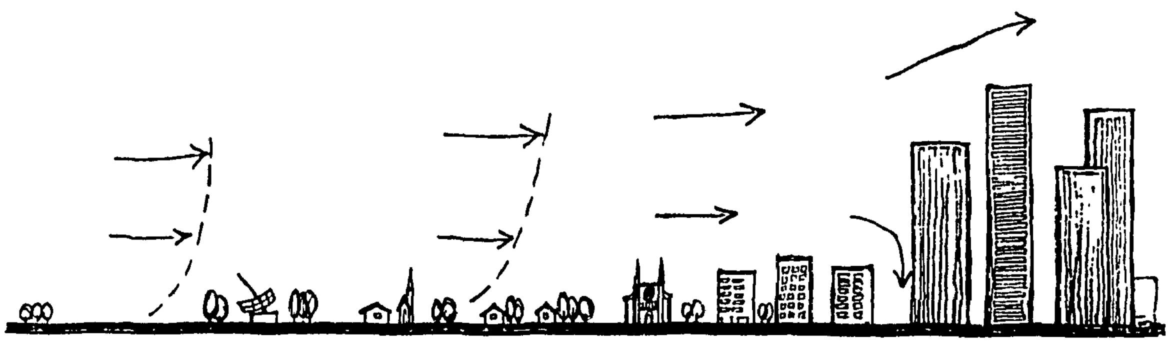

Fig. 6.1.1 Evolution of wind profiles influenced by numerous elements.

Over an open, smooth land like an airport where the meteorological data are recorded, the wind speed near ground increases rapidly with the elevation. The increase in the general roughness over suburban and city terrains retards the low part of atmospheric boundary layer. When it finally arrives at the main building under investigation, the wind flow may be deflected by the building and its surroundings. Significant variations in wind speed usually take place at the pedestrian level.

Symbolically, wind speeds recorded at a weather station, $V_o(\theta_i)$, and experienced at a built-up site (V_i) can be related by a vector of modification factors f_i in this study:

$$V_i = f_i \times V_o(\theta_i) \tag{6.1.1}$$

where θ_i denotes a sector of 22.5° in the 16-point compass system.

Note that V_i is the wind speed induced by $V_o(\theta_i)$, but not necessarily in the sector θ_i. For instance, a down-washing flow may induce a reversed drift in front of buildings; a pressure difference around buildings may create transversal streams; and hills and valleys may also deviate the wind flow off its original course. Generally, the value of f_i varies with the wind direction due to the asymmetry and non-uniformity of buildings and their surroundings. Within the same sector θ_i, however, f_i is assumed to be a constant for a given location regardless of the magnitude of $V_o(\theta_i)$, provided that the effect of Reynolds Number is insignificant for the pedestrian-level wind patterns.

In the following sections, the meteorological records, as the basis for pedestrian wind evaluation, are analyzed first. Then the modification factor for a given building in a built-up site is determined by integrating contributions made by the terrain roughness, the building configuration and the architectural details of relevant buildings.

6.2 METEOROLOGICAL DATA

Meteorological data are usually available at a nearby weather station for a considerably long period of time. They consist of averaged speeds over a certain time interval measured at 10 meters above the ground. An example of organized meteorological records is shown in Table 6.2.1 with hourly wind speed records from Dorval airport in Montreal

Table 6.2.1 Number of observations of classified wind speeds in 16 compass directions.

		Wind Speed Class (km/h)									
i	Sector	1-10	11-20	21-30	31-40	41-50	51-60	61-70	71-80	81-90	Total
1	N	6182	3864	934	144	17	1	1	0	0	11143
2	NNE	6934	10296	3618	923	178	31	14	9	0	22003
3	NE	4614	9083	4749	1421	308	83	19	4	0	20281
4	ENE	2363	3362	1142	210	30	5	0	0	0	7112
5	E	3051	2499	398	43	2	0	0	0	0	5993
6	ESE	3386	2511	614	68	2	0	0	0	0	6581
7	SE	4962	4904	1837	359	31	2	0	1	0	12096
8	SSE	5057	6117	2109	438	38	6	0	0	0	13765
9	S	4890	3666	591	71	2	0	0	0	0	9220
10	SSW	5670	6976	1678	281	42	0	0	0	0	14647
11	SW	8634	13640	6937	2196	386	69	24	6	1	31893
12	WSW	9018	14715	9706	3744	816	177	39	9	0	38224
13	W	7732	12265	8249	3172	570	89	18	4	0	32099
14	WNW	4826	6271	3317	986	139	18	3	0	0	15560
15	NW	4528	3732	1233	234	19	3	0	0	0	9749
16	NNW	4538	2427	655	73	1	3	0	0	0	7697
										Calm	13689
							Total for All Directions				271752

Note: Data are derived from hourly records during the period of January 1, 1960 to December 31, 1990 at Dorval Airport, Montreal.

for 31 years. They are grouped by speed classes (in km/h) in 16 compass directions.

In contrast to the absolute number of occurrences, relative frequencies of wind-speed exceedance are more informative in practice. Let $P_i(>V_o(\theta_i))$ denote the probability of speed exceedance defined by the ratio of the occurrence number of wind speeds higher than $V_o(\theta_i)$ in the sector θ_i to the total number of observations for all directions, the data in Table 6.2.1 can be presented by the so-called wind roses as shown in Fig. 6.2.1.

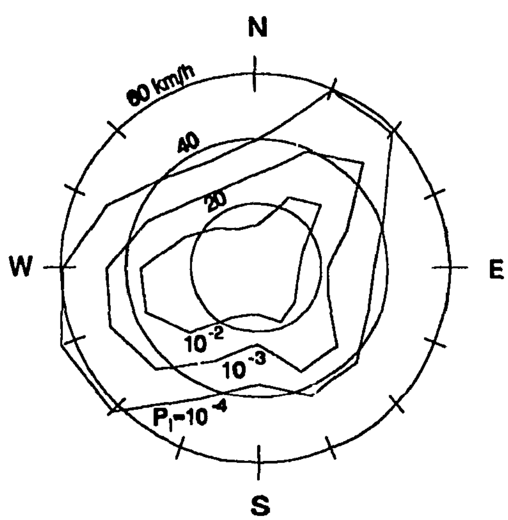

Fig. 6.2.1 Wind roses drawn from data recorded at Dorval Airport, Montreal.

To apply these data, the total exceedance frequency of speeds $V_o(\theta_i)$ which may induce V_i higher than, for example, 5 m/s at a built site can be calculated. Even for this simplest case, interpolation and approximation are required for the discrete wind data. In some realistic situations, a number of frequencies of exceedance of wind speeds are required for given seasons and time periods for several locations around buildings. Therefore, it is desirable to represent these wind records by a series of well-known probability functions in the domain of interest.

The Weibull distribution has been found to be suitable for describing the probability of natural wind speeds (Isyumov and Davenport, 1975a). For each wind direction, the exceedance probability of wind speeds higher than $V_o(\theta_i)$ can be approximated by

$$P_i(>V_o(\theta_i)) = p_i e^{-(\frac{V_o(\theta_i)}{c_i})^{k_i}} \qquad i = 1,2,\cdots,16 \tag{6.2.1}$$

where p_i is the accumulated probability for sector θ_i. Constants c_i and k_i determine the shape of the probability curve. Values of these constants can be estimated by using simple regression technique and they constitute 16 continuous functions convenient for numerical calculations.

In some applications, it may be of interest to estimate frequencies for a group of seasons or time periods. For instance, the City of Montreal stipulates different wind guidelines for summer and winter daylight hours. Accordingly, different probability constants are expected for specific time periods or data sets, as given in Table 6.2.2 with $V_o(\theta_i)$ in m/s. As indicated by p_i values, the wind is more likely coming from SW, WSW and W as well as NNE and NE, especially in winter days. A large c_i or a small k_i value suggests a long tail in speed distribution, i.e., relatively high likelihood of strong winds. With these constants, the frequency of exceedance can readily be evaluated using Eqs. 6.1.1 and 6.2.1. For example, if the threshold wind speed is V_T in m/s, the exceedance probability of wind speeds at the site for all 16 directions can be calculated by

$$P(>V_T) = \sum_{i=1}^{16} p_i e^{-(\frac{V_T}{f_i \times c_i})^{k_i}} \tag{6.2.2}$$

A case study is evaluated with the modification factor $(f_i)_{i=1,2,\ldots,16}$=(0.3, 0.3, 0.4, 0.6,

Table 6.2.2 Weibull constants for three specific time periods estimated from meteorological records for 31 years at Dorval airport, Montreal.

		p_i (%)			k_i			c_i (m/s)		
i	Sector	A.H.	S.D.	W.D.	A.H.	S.D.	W.D.	A.H.	S.D.	W.D.
1	N	4.10	3.37	3.70	1.51	1.81	1.31	3.34	3.58	3.37
2	NNE	8.10	6.08	9.28	1.05	1.55	1.14	3.11	4.05	3.84
3	NE	7.46	6.02	9.33	1.30	1.61	1.33	4.47	4.68	5.00
4	ENE	2.62	2.68	2.87	1.69	1.63	1.87	4.29	4.02	4.85
5	E	2.21	2.27	2.32	1.62	1.53	1.69	3.23	2.98	3.48
6	ESE	2.42	2.64	2.44	1.79	1.85	1.82	3.69	3.72	4.04
7	SE	4.45	5.05	4.18	1.81	1.00	1.91	4.35	2.29	5.03
8	SSE	5.07	5.66	4.39	1.76	1.98	1.89	4.33	4.29	5.14
9	S	3.39	4.32	2.42	1.57	1.92	1.46	3.14	3.43	3.20
10	SSW	5.39	8.43	3.93	1.62	1.76	1.51	3.80	3.96	3.85
11	SW	11.74	14.98	10.15	1.26	1.90	1.35	4.17	5.12	5.18
12	WSW	14.07	12.60	16.22	1.40	1.40	1.63	5.06	4.54	6.72
13	W	11.81	10.67	15.61	1.45	2.00	1.66	5.02	5.60	6.46
14	WNW	5.73	5.65	5.16	1.83	1.91	2.26	3.10	5.22	6.39
15	NW	3.59	3.80	2.43	1.67	2.11	1.83	3.97	4.64	4.79
16	NNW	2.83	2.81	1.99	1.43	1.41	1.65	3.07	3.31	3.52

Data Sets: A.H. = All Hours and all seasons;
S.D. = Summer Daylight hours: 6:00 to 22:00 from April to September;
W.D. = Winter Daylight hours: 8:00 to 18:00 from October to March.

0.7, 0.6, 0.5, 0.5, 0.4, 0.4, 0.3, 0.6, 0.5, 0.4, 0.4, 0.2) for a location south of a high-rise building at downtown Montreal. By using Eq. 6.2.2 along with the Weibull constants in Table 6.2.2, the all-hours $P(>5\ \mathrm{m/s})$ will be 3.7% at the site, compared with 16.4% at the airport; for the latter a power-law profile of α=0.16 is assumed and f_i=0.77 is used for converting the wind speeds recorded at the height of 10 m to that at the height of 2 m.

Similar calculations of exceedance probabilities could be performed for other specified time periods, threshold speeds and modification factors. In addition, this method can be applied for other cities as long as the meteorological data are available.

6.3 TERRAIN ROUGHNESS

Usually, a weather station is located at an open grass land like an airport far from densely built cities. At such an *ideal* site, wind flow is free of the influence of large individual obstacles, but affected by the uniform surface roughness. At the other end of the problem, the building to be evaluated may be erected at a downtown core approached by wind flows retarded by upstream terrains and further affected by individual buildings.

Between the open country land and the downtown site are upstream terrains. The retardation by roughness elements on the terrains is diffused via mechanical and thermo-dynamic mixing throughout the atmospheric boundary layer up to several hundred meters or higher above the ground. The wind speed increases with the elevation whereas the shear stress induced by ground roughness vanishes near the top of boundary-layer wind flows. Over a uniform, long fetch, the wind profile can be approximated by the *Logarithmic Law*:

$$V(z) = \frac{u_*}{\kappa} \ln\left(\frac{z - z_d}{z_o}\right) \qquad (6.3.1)$$

where $V(z)$ is the wind speed at the height of z from ground, u_* is known as the shear velocity of the flow and κ is the von Kármán's constant equal to 0.4. The surface roughness length z_o is a measure of eddy size at the ground with a value varying not only with the height of obstacles, but also with their density and distributions. Typical z_o values are 0.03 m at a grass covered open plain (airport) and around 1 m at the centres of large cities. The classifications of terrains according to the roughness lengths have been proposed by several researchers. Table 6.3.1 gives an example after Wieringa (1992).

The value of z_d indicates the vertical displacement of zero plane of wind profile caused by obstacles. Typically, z_d is 70 to 80% of the height of the large roughness elements such as trees or houses and it could also be reasonably estimated by a relation given by Helliwell (1972):

$$z_d = \overline{h} - \frac{z_o}{\kappa} \qquad (6.3.2)$$

where $\overline{h}$ is the general roof-top level.

It is worth noting that thermodynamic forces may affect the stability of boundary layer flows. Over the same terrain, wind flow may have different profiles in day time and night time due to the differences in ground temperature and temperature gradient. Mechanical forces, however, usually dominate during the periods of strong winds. Also noted that the logarithmic law is only valid over a uniform, long fetch (5 to 20 km for example), where a complete flow mixing can be achieved.

Table 6.3.1 Classification of terrains and roughness lengths, after Wieringa (1992).

z_o (m)	Landscape Description
1: 0.0002 Sea	Open sea or lake (irrespective of the wave size), tidal flat, snow-covered flat plain, featureless desert, tarmac and concrete, with a free fetch of several kilometres.
2: 0.005 Smooth	Featureless land surface without any noticeable obstacles and with negligible vegetation; e.g. beaches, pack ice without large ridges, morass, and snow-covered or fallow open country.
3: 0.03 Open	Level country with low vegetation (e.g. grass) and isolated obstacles with separations of at least 50 obstacle heights; e.g. grazing land without windbreaks, heather, moor and tundra, runway area of airports.
4: 0.10 Roughly open	Cultivated area with regular cover of low crops, or moderately open country with occasional obstacles (e.g. low hedges, single rows of trees, isolated farms) at relative horizontal distances of at least 20 obstacle heights.
5: 0.25 Rough	Recently-developed "young" landscape with high crops or crops of varying height, and scattered obstacles (e.g. dense shelter belts, vineyards) at relative distances of about 15 obstacle heights.
6: 0.5 Very rough	"Old" cultivated landscape with many rather large obstacle groups (large farms, clumps of forest) separated by open spaces of about 10 obstacle heights. Also low large vegetation with small interspaces, such as bushland, orchards, young densely-planted forest.
7: 1.0 Closed	Landscape totally and quite regularly covered with similar-size large obstacles, with open spaces comparable to the obstacle heights; e.g. mature regular forest, homogeneous cities or villages.
8: ≥ 2 Chaotic	Centres of large towns with mixture of low-rise and high-rise buildings. Also irregular large forests with many clearings.

In addition, there is a bottom limit of height to which the logarithmic law can be applied. For example, $z>20z_o+z_d$ is suggested as the minimum requirement for the wind flow out of the influence of individual elements. The upper limit, on the other hand, is proportional to the surface shear velocity and could be as high as a few hundred meters over a built-up city.

There are several ways to relate wind profiles of the logarithmic law in different roughness regimes. One is the approximation presented by Simiu and Scanlan (1986):

$$\frac{u_{*1}}{u_{*2}} = \left(\frac{z_{o1}}{z_{o2}}\right)^{0.0706} \tag{6.3.3}$$

Based on the roughness length z_{o1} and wind speeds at a height of 10 m above an airport, the shear velocity u_{*1} could be calculated using the logarithmic law. By knowing the roughness length of the second terrain (z_{o2}), Eq. 6.3.3 gives the corresponding shear velocity (u_{*2}). Then a new speed profile is obtained over the second terrain where the logarithmic law is valid as well.

Another commonly used empirical relation for describing the profile of atmospheric boundary layer flow is the *Power Law*. The first presentation of the mean wind profile was proposed much earlier than the logarithmic law by Hellman (1916) as follows:

$$\frac{V(z_1)}{V(z_2)} = \left(\frac{z_1}{z_2}\right)^{\alpha} \tag{6.3.4}$$

where the speed ratio is related to the elevation ratio of a power function with the exponent equal to α. The typical α values are 0.16 for the open country terrain, 0.28 for the residential suburbs and woodlands, and 0.40 for the centre of large cities (Davenport, 1965). Wind speeds in two different roughness regimes could be related by assuming that the geostrophic speeds are the same over both sites, i.e.:

$$V_2(\delta_2) = V_1(\delta_1) \tag{6.3.5}$$

where δ_l and δ_2 are the gradient heights of boundary layers over the two sites, respectively. Applying the power law for both sites and using Eq. 6.3.5, one obtains:

$$V_2(z_2) = (\frac{z_2}{\delta_2})^{\alpha_2}(\frac{\delta_1}{z_1})^{\alpha_1} V_1(z_1) \tag{6.3.6}$$

The power law has been widely used in structural design and due to its simplicity the exponential index becomes one of the most consequential parameters in wind-tunnel simulation for different exposures. For the lower atmosphere, however, the logarithmic law is regarded as a superior representation of strong wind profiles.

Additional aerodynamic concepts of importance to atmospheric boundary layer flows and pedestrian-level winds can be found in the literature. Refer to Panofsky and Townsend (1964), Taylor (1969) and Jensen (1978) for internal boundary layer; Jackson (1975) and Lemelin et al (1988) for the wind flow over escarpments and hills; and Hinze (1959) and Panofsky and Dutton (1984) for atmospheric turbulence.

This section has discussed how to link the wind records at a weather station with the wind profiles over different terrains. A model landscape of built-up areas features a city in the centre surrounded by suburbs and then by open countries. Meteorological records are usually taken at one station on open country far from the city and they could be assumed representative for the country areas embracing the suburbs and the city from all directions. This is true when similar flat, smooth fetches prevail. Between the open country and the built site are terrains of 10 kilometres or wider, over which the wind profiles are fully developed and can be described by Eq. 6.3.3 by the logarithmic law, or

Eq. 6.3.6 by the power law. The next step is then to convert the wind speeds over upstream terrains to those above and around buildings at built-up sites.

6.4 MAIN BUILDING AND IMMEDIATE SURROUNDINGS

In the boundary-layer wind tunnel studies on pedestrian wind conditions, upstream terrains can be simulated with different boundary-layer generating devices for appropriate mean and turbulence wind profiles. Around the main building, buildings and structures are scaled on a plate within a radius of 300 to 1000 m, depending on the dimensions of wind tunnel and the geometric scale of experiments. Farther upstream terrains may also be simulated by adding more scaled objects out of the pla'.' in the wind direction.

To normalize the wind speeds at the pedestrian level, three reference heights may be used, namely the gradient height, the roof height of main building and the pedestrian level.

In most consultation projects for wind environmental conditions, the wind speed at gradient height or a height clear of any interference of building models is commonly employed as the reference. The gradient height of boundary layer flow could be determined by the measurement of speed profiles or, sometimes, at an imaginary height based on experience. A single height is usually considered for all wind directions regardless of the variation in building density. Such a wind speed is assumed to be equal to that at the gradient height over the upstream terrain and to that over the weather station, even though the gradient height increases with surface roughness. In an actual case, however, the gradient height of boundary-layer flow over a city may vary from 400 to 1000 m under different mechanic and thermal conditions. This uncertainty is ignored in most wind-tunnel tests, but may bring difficulties to the proposed computerized evaluation; for instance, if a ground-level wind speed is referenced to the geostrophic speed, what should the gradient height be? More critically, disturbances created by the change in roughness from suburbs to the city (usually an abrupt change not far enough from measurement locations in a wind tunnel) can be hardly transferred to the top of the boundary layer; and the pedestrian-level wind conditions are affected more directly by the lower part of boundary flow obstructed by buildings. Therefore, it is desirable to link the pedestrian-level wind speed to the reference at a lower level.

When wind-tunnel studies are carried out for simple building models, as presented in the last two chapters and a large portion of the literature, the gradient-height speeds are seldom employed. Instead, the other two reference heights are found more convenient and informative. If the proposed building is erected well above its surroundings, the speed at building height could be considered not being affected by the surroundings and it has the same speed of the oncoming flow at the same height. The ratio of speed at the pedestrian level to that at the building height provides an accurate and direct indication of the wind intensity.

Using the same pedestrian level as the reference height is even more convenient for simplified wind-tunnel tests. The reference wind speeds are measured at locations of interest when the new building is not in place. The ratio of speeds before and after the building presence shows the speed amplification caused by the new building. However, such a ratio may become obsolete as soon as surroundings are brought into their positions, since the reference speeds appraise the sheltering effect of surroundings, but not the intensity of oncoming winds.

Compared with the data referenced to the gradient height from scattered consultation projects, more results are available from parametric studies referenced to the building height or the pedestrian level. Overspeed ratios based on the last two reference heights can be converted to each other by knowing the features of approach flows, which are supposed to be unaffected by individual obstacles before hitting the building under investigation. However, this is not the case in the real world when surrounding buildings are present and the surrounding-induced new profiles of wind speeds have to be re-evaluated. It leads to a proposal for two new parameters to be used in the computer system for describing the wind profiles over built-up sites.

According to Theurer et al (1992), obstacles like buildings on the ground only affect the lower part of local atmospheric flow field. The disturbances of such an internal boundary layer extend to two to three times of the average building heights, beyond which the influence of local buildings is insignificant. The reference height would better be out of the disturbed wind flow. As illustrated in Fig. 6.4.1, a new reference height could be defined by

$$Z_r = \max(H, 2\bar{h}) \tag{6.4.1}$$

where H is the height of the main building under investigation, and $\bar{h}$ is the average height of upstream buildings. At the reference height Z_r,

$$V_1(Z_r) = V_2(Z_r) \tag{6.4.2}$$

and the overspeed ratios referenced to the building height or the pedestrian height can be converted into ratios for the reference height Z_r:

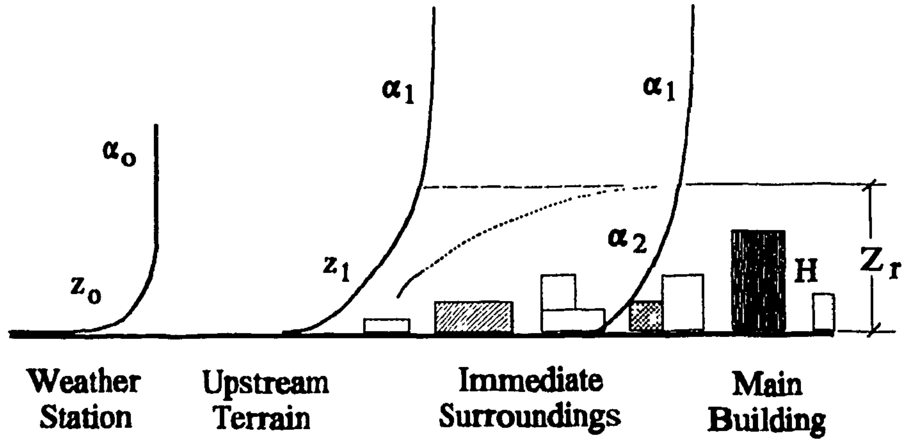

Fig. 6.4.1 Boundary layer flow approaching the building of interest.

$$K_Z = \left(\frac{H}{Z_r}\right)^{\alpha} K_H \tag{6.4.3a}$$

$$K_Z = \left(\frac{b}{Z_r}\right)^{\alpha} K_b \tag{6.4.3b}$$

where K_Z, K_H and K_b are ratios of ground-level wind speed to the reference speeds at the reference height Z_r, the building roof height H and the measurement height b, respectively. The values of K_H and K_b can be found from the literature and have been organized in the current study for various simplified building models. The value of K_Z is always lower than K_H and K_a since $Z_r \geq H$ and $Z_r > b$. By using these formulas, wind speeds at the pedestrian level could be estimated. If there are no major surrounding obstacles, $\alpha = \alpha_l$ can be assumed for the power law.

Due to the sheltering effect created by surroundings, the pedestrian wind speeds or K_Z values are expected lower than those calculated by using $\alpha = \alpha_1$, i.e. a higher α value is anticipated to be appropriate for Eqs. 6.4.3a and 6.4.3b. In Fig. 6.4.1, the boundary layer lower than Z_r is disturbed by the upstream blocks. In the lower portion of boundary layer, the wind flow is too complex for any analytical solutions due to the interactive disturbances from individual buildings. The wind profiles change with measurement locations, but, on average, the speed increases with the elevation. Suppose the power law can be nominally applied over the built-up site with $\alpha=\alpha_2$, the lower part of the last two adjacent wind profiles in Fig. 6.4.1 can be described by:

$$\left(\frac{V(b)}{V(Z_r)}\right)_1 = \left(\frac{b}{Z_r}\right)^{\alpha_1} \tag{6.4.4a}$$

$$\left(\frac{V(b)}{V(Z_r)}\right)_2 = \left(\frac{b}{Z_r}\right)^{\alpha_2} \tag{6.4.4b}$$

where subscriptions 1 and 2 denote the approach wind and the flow right in front of the main building, respectively. Since $V(Z_r)_1=V(Z_r)_2$, Eqs. 6.4.4a and 6.4.4b yield:

$$\alpha_2 = \alpha_1 + \ln\frac{V(b)_2}{V(b)_1} / \ln\left(\frac{b}{Z_r}\right) \tag{6.4.5}$$

here the ratio of ground-level wind speeds $V(b)_2/V(b)_1$ can be estimated by the blockage ratio R_B defined Section 5.6 for the uniform street blocks. Considering $V(b)_2$ as the average speed on the along-wind street and $V(b)_1$ as the speed in the oncoming wind, Eq. 5.6.3 can rewritten as:

$$\frac{V(b)_2}{V(b)_1} = 1 - 0.9 R_B^{\,0.4} \tag{6.4.6}$$

Usually, the power law exponent over suburban terrain α_1 is in the range of 0.20 to 0.30. It could also be related to surface roughness by coupling two wind profiles presented by Eqs. 6.3.1 and 6.3.4:

$$\alpha_1 = \frac{z}{(z - z_d)\ln[(z - z_d)/z_o]} \tag{6.4.7}$$

where z_o and z_d are the roughness length and the vertical displacement of zero plane, z is a typical height in the boundary layer to which the logarithmic and power laws are to be applied, for example, $z=Z_r$. See Panofsky and Dutton (1984) for the detailed derivation.

In summary, a reference height Z_r, an exponent α_2, and their relationships with the pedestrian wind speeds are proposed in order to facilitate the evaluation of wind conditions around buildings in built-up areas. Relations are also established for making use of wind-tunnel experimental results within a computerized environment. The entire process consists of the following procedures: (1) probability analysis of local meteorological records for wind exceedance in all directions; (2) prediction of wind profiles over upstream terrains by using the logarithmic law; (3) estimation of the reference height Z_r and the exponent α_2 over immediate surroundings; (4) conversion of the overspeed ratios to the reference height Z_r by using α_2; and (5) combination of the derived overspeed ratios and the reference wind speeds for actual wind intensities at the pedestrian level in built-up sites.

Yet, another factor of importance to local wind environment has to be taken into account. It is the aerodynamic impact of architectural details of the main buildings and surroundings, including remedial actions for improving wind conditions.

6.5 ARCHITECTURAL DETAILS AND REMEDIAL ACTIONS

Building models discussed in Chapters 4 and 5 are all of rectangular cross sections and flat surfaces, that are clearly unfavourable when the ground-level wind environment is concerned. In contrast, buildings with circular sections or rounded corners promote crosswise wind flows. Also, buildings with tapered or set-backed facades tend to reduce the down-washing effect which causes windy conditions to pedestrians. In addition, some architectural details associated with buildings, such as canopies, arcades, pavilions, fences, screens and trees, are effective for the reduction of wind speeds as well.

Numerous measures can be taken to reduce the wind speeds at ground level and they are classified into three categories according to the design stage suitable for the implementation, namely prior, during and post design. Prior to the detailed design, the orientation and location of buildings could be selected, if possible, in order to avoid any direct exposure of larger surfaces of the building to the prevailing winds. The relative position of the building vis-a-vis its surroundings is also of influence. For example, designers must not plan two or more buildings at critical distances that may significantly amplify the front vortices, corner streams and other aerodynamic effects, see Chapter 5.

During the process of building design, a better wind environment may be achieved by adopting favourable building geometry and dimensions, and by carefully arranging and protecting pedestrian-accessible areas. Generally, large surfaces directly exposed to the wind flow likely cause the windy environment at ground level. Decisions made prior and during the design stage are consequential to the future performance of the building with respect to the pedestrian-level wind conditions.

After the original design is complete and even after the building construction, there may still be room for improving the wind conditions. The potential impact, however, is complicated and, in most cases, limited both at the speed reduction and at the effective area. At this stage, it is a difficult task to choose a most promising remedy due to several reasons. Firstly, a measure may be very effective for migrating the wind from some directions, but not of influence on the wind from others; secondly, the spatial impact of a remedy is usually localized - for certain cases, the reduction of wind speeds at one region may increase speeds at others; and thirdly, the function of a remedial action is highly dependent not only on the main building, but also on the surroundings.

It is even more difficult to quantify the aerodynamic efficiency of remedial measures. Some typical remedial actions and their potential efficiency are organized in Appendix G based on the literature information. In this section, an attempt is made to establish *Utilities* for selected remedial actions. Regardless of the building dimensions and surroundings, aerodynamic effects which may cause high wind speeds around buildings can be rooted to three flow mechanisms, namely front vortex, corner stream and wake turbulence. Each flow mechanism is associated with the wind direction relative to the building and the area of interest. Table 6.5.1 provides the utility values for selected remedial measures. The greater the utility value, the higher the potential aerodynamic efficiency of a remedy. For a given remedial action, utility values vary with the flow mechanisms (or wind directions). The overall aerodynamic efficiency of a remedy is calculated as the sum of utility values for every flow mechanisms weighted by the relative frequencies of wind exceedance for the specific case under consideration.

It should be mentioned that all utility values in the table are generated from the literature information and the current findings on numerous building projects and parametric studies. Specific building configurations may behave differently and remedies may have utilities differing from these typical values.

Table 6.5.1 Aerodynamic utility values of remedies for three flow mechanisms.

Remedial Actions	Flow Mechanisms: Front Vortex	Corner Stream	Wake Turbulence
Height reduction	75	85	30
Re-orientation	70	70	40
Large podium	65	65	40
Tapered or setback building	70	70	50
Rounded or chamfered corners	60	70	30
Arcade, roof or pavilion	80	65	60
Large canopy at low height	75	40	40
Tree or bush planting	50	50	60
Screen, fence or wall	30	60	40
Vertical surface projections	40	40	70

Nevertheless, the aerodynamic effects of architectural details and remedial actions should be taken into consideration as a further modification on wind speeds derived from the evaluation process summarized at the end of previous section. Some typical cases are organized in the knowledge base for remedy implementations with the potential speed reductions, derived from several studies carried out by a number of researchers in the last two decades. The selection of remedial measures is also affected by economic, architectural and functional constraints of the building project. These can be incorporated in the utilities by a multi-objective decision making process. Detailed information on the utility values and aerodynamic weights are described in the next chapter.

6.6 WIND DISCOMFORT CRITERIA

Once obtained, the pedestrian-level wind speeds and their exceedance frequencies are compared with the established wind discomfort criteria to determine whether the resulted wind conditions are acceptable for given pedestrian activities.

As described in Section 2.3, the wind discomfort criteria specify the (dis)comfort levels for certain wind speeds with threshold frequencies for various human activities. A number of criteria and guidelines have been established from full-scale observations and wind-tunnel experiments and they are presented in Appendices B and C. Examples provided in this section are two criteria established by Davenport (1972) and Melbourne (1978) and the guidance for urban microclimate authorized by the City of Montreal.

One of the earliest criteria was proposed by Davenport (1972) based on Beaufort Scales. Extensive sets of activities and comfort categories are specified for several occurrence frequencies as listed in Table 6.6.1.

Table 6.6.1 Comfort criteria for windiness proposed by Davenport (1972).

		Beaufort Scale for Relative Comfort Level			
Activity	Areas Applicable	Perceptible	Tolerable	Unpleasant	Dangerous
Walking fast	Sidewalks	5 (7.4)	6 (9.9)	7 (12.4)	8 (15.1)
Strolling, skating	Parks, entrances Skating rinks	4 (5.5)	5 (7.4)	6 (9.9)	8 (15.1)
Standing, sitting - short exposure	Parks, plaza areas	3 (3.5)	4 (5.5)	5 (7.4)	8 (15.1)
Standing, sitting - long exposure	Outdoor restaurants Bandshells, theatres	2 (1.9)	3 (3.5)	4 (5.4)	8 (15.1)
Representative criteria for acceptability			<once/wk	<once/m	<once/yr

Numbers in parentheses are mean speeds in m/s at 2 m above the ground, 80% of the medium speeds of corresponding Beaufort Scales at the reference height of 10 m. The criteria are tentative for air temperatures higher than 10 °C. At lower temperatures, the relative comfort level might be expected to be reduced by one Beaufort number for every 20 °C reduction in temperature.

The other criteria were suggested later by Melbourne (1978) for peak gust speeds occurring once a year during daylight hours. The human activities are similar to those in Davenport's criteria. The peak gust speed is evaluated by $V_p=\bar{V}+3.5V_{rms}=2\bar{V}$ for a turbulence intensity of 30%. The once-per-year occurrence corresponds to probabilities of 0.05-0.1% for daylight hours, estimated by the annual number of storms and the probability distribution of strong winds. The criteria were shown graphically in Fig. 2.3.1 and the contents are listed in Table 6.6.2.

Table 6.6.2 Wind discomfort criteria for daylight hours, Melbourne (1978).

Activity	$\bar{V}$ (m/s)	V_p (m/s)	$P(>V)$
Stationary long exposure	5	10	once/yr
Stationary short exposure	6.5	13	once/yr
Walking	8	16	once/yr
Unacceptable for any activity	11.5	23	once/yr

The unacceptable wind speed is specified as 15.1 m/s for one occurrence per year by Davenport (1972) and as 11.5 m/s for one daylight occurrence per year by Melbourne (1978). The acceptable speeds given by Davenport are 3.5, 5.5 and 7.4 m/s of one occurrence per week for long exposure, short exposure and walking, respectively. The corresponding wind speeds suggested by Melbourne are 5, 6.5 and 8 m/s of one occurrence per year for daylight hours only. Considering wind speed distributions and the temperature reduction in Davenport's criteria (the comfort level is reduced by one Beaufort number for every 20 °C reduction in temperature), these threshold speeds in two criteria may be quite compatible. Although there is still an argument on the comparability (Melbourne, 1978) and the incomparability (Ratcliff and Peterka, 1989) between existing discomfort wind criteria, the real problem in implementation is how to correctly interpret the specifications employed in different criteria, such as exceedance frequencies and occurrence numbers of daylight and all hours for the wind probabilities as well as the Beaufort scales, and mean, gust, peak and effective speeds at 2 or 10 m height for the wind speed. See Appendix B for more details on this subject.

Usually, the local climate, the perceptivity or sensitivity of inhabitants to the wind environment and other facts have to be considered when these criteria are applied. For this reason. more and more city authorities are in the process of establishing their own guidelines for city planning and building design with respect to the building-induced urban microclimate. For instance, the guidance of City of Montreal specifies:

(1) the acceptable mean wind speeds are 4 m/s for winter and 6 m/s for summer;
(2) with exceedance frequencies not higher than 5% for rest areas, 15% for dense pedestrian regions and 25% for fast-walking zones.

These criteria and guidelines have been coded into the knowledge base accessible to the computer system for a preliminary subjective evaluation of wind conditions in the urban environment at the pedestrian level.

The relevant knowledge described in this chapter has been used as the knowledge base for a computer system developed for evaluating the pedestrian-level wind conditions around buildings. The body of knowledge and its implementation procedures are in certain aspects different from those of conventional wind-tunnel consultations, the latter are more restrictive for the following reasons: (1) Wind-tunnel tests may be carried out only for selected wind directions rather than all azimuths due to both financial and time constraints of the project; consequently, all meteorological information is not taken into consideration, see Section 6.2; instead, wind speeds and their exceedance frequencies are examined for each tested direction independently; (2) It is extremely time-consuming, or sometimes impossible, to test many design alternatives and remedial actions which may result in different wind conditions from those of an original design.

However, the wind-tunnel experimentation is still regarded as one of the most reliable approaches to the pedestrian-level wind studies. Therefore, it deserves more detailed explanations regarding the experimental procedure and the data analysis. The following case study provides a typical wind-tunnel evaluation of the wind environmental conditions around a proposed building complex in a built-up area. This case study will be used for the comparison between results derived from the wind-tunnel experiments and the developed computer system.

6.7 A CASE STUDY

A building complex, sketched in Fig. 6.7.1, is to be built at a corner of two main streets in the City of Montreal. The main building (A) consists of a 20 storey tower at the corner

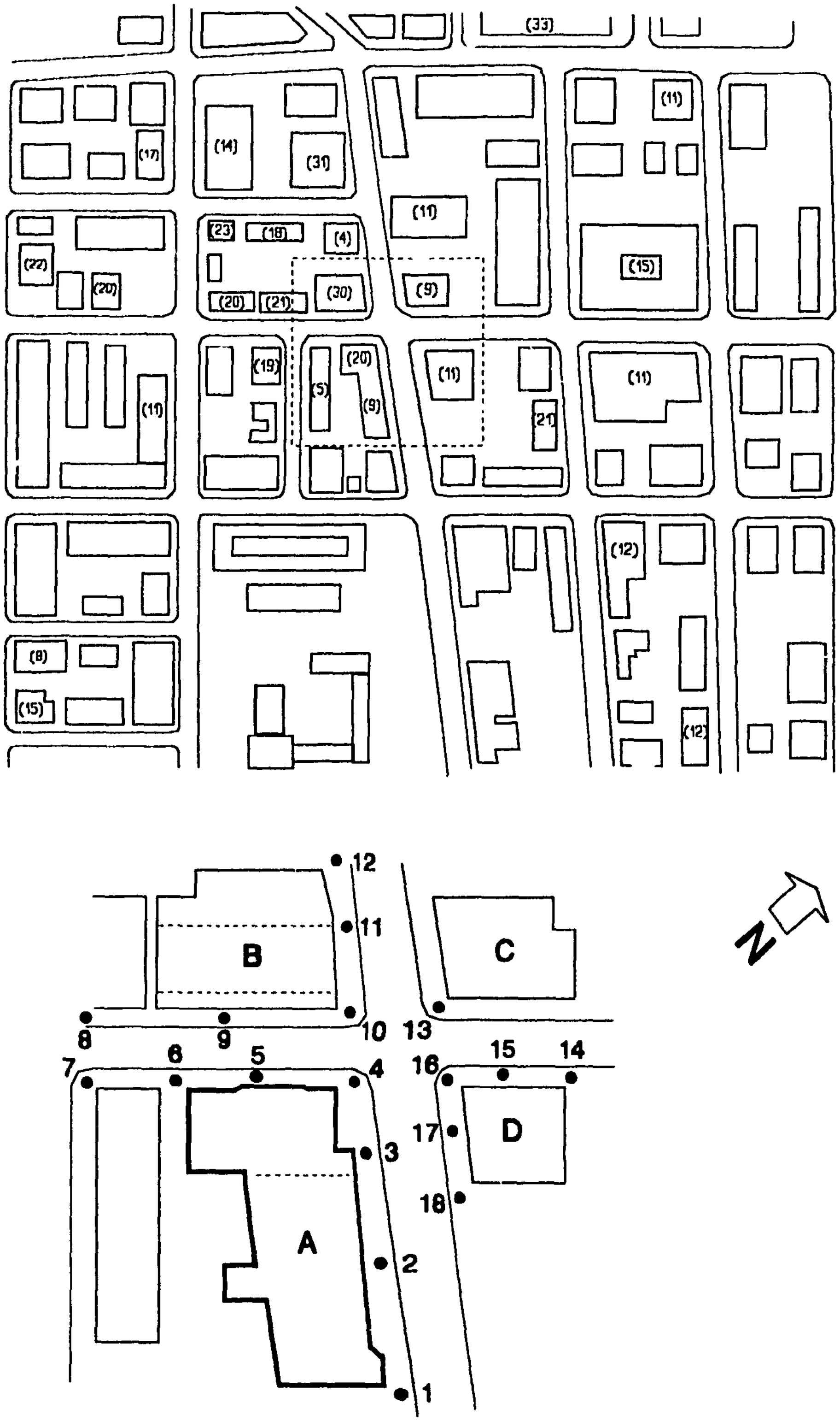

Fig. 6.7.1 Plan view of the building and its surroundings for the case study.

and a lower lever building development along a street. Numbers in parentheses indicate the storeys of the large buildings in the area with generally taller buildings from west, and lower buildings from southeast relative to the complex.

A 1:500-scale model of the proposed building and surrounding blocks is mounted on the turntable of the boundary-layer wind tunnel. The proposed building **A** is located at the centre of the model plate of 450 m in radius, similar to the plan shown by the top graph in Fig. 6.7.1. For simplicity reasons, farther terrains are simulated by the same suburban features with the power law exponent equal to 0.28. As shown in the figure, there are 18 measurement locations along sidewalks around the proposed building and three other buildings at the same intersection. On each location, the mean wind speeds are detected by Irwin's sensors at an equivalent height of 2 m for six selected wind directions NNE, NE, SE, SW, WSW and W. Such a selection is made for directions prone to speedy winds, based on flow aerodynamics and meteorological considerations. The reference wind speed is measured by a Pitot tube at an equivalent height of 300 m above the ground. Although slight differences are found for reference wind speeds for different wind directions, the average speed is used as a nominal reference speed for normalizing all measurement results.

Table 6.7.1 lists mean pedestrian-level speeds at all 18 locations for the nominal reference speed of 12.9 m/s at 300 m above the ground. Tested in the experiment are three building configurations: Model I with the existing buildings; Model II with the new complex in place; and Model III with the new complex of a reversed plan, i.e. with the tower at the middle block and the lower development around the street corner.

For all three models, high wind speeds are observed at locations around the tall

Table 6.7.1 Measured wind speeds in m/s at 18 positions around building models for 6 wind directions.

Direction	NNE			NE			SE			SW			WSW			W		
Model	I	II	III	I	II	III	I	II	III	I	II	III	I	II	III	I	II	III
No. 1	2.8	4.8	4.0	4.4	4.4	4.2	2.4	4.1	8.4	4.1	4.4	2.7	3.7	2.9	2.9	2.7	2.3	2.4
2	3.1	2.9	3.4	3.1	2.4	3.4	3.6	2.2	3.8	2.6	2.4	2.3	3.3	2.1	2.5	3.0	2.1	3.0
3	3.7	3.8	2.8	2.4	2.7	3.0	4.5	2.7	3.7	2.6	3.2	2.2	3.2	2.7	2.6	4.4	3.1	3.6
4	6.6	4.2	3.5	3.6	2.7	2.7	7.1	3.5	5.1	2.5	3.6	2.9	3.5	2.5	2.5	4.2	3.2	3.0
5	6.2	7.0	6.3	3.3	2.9	2.6	5.6	4.7	4.7	2.9	3.2	3.4	2.6	2.2	2.4	4.7	3.7	3.3
6	4.8	5.9	6.0	2.5	2.6	2.7	6.0	5.2	4.4	3.7	3.7	**4.8**	2.8	2.5	3.2	5.1	3.9	3.9
7	3.8	5.0	4.1	3.6	2.5	4.1	4.3	5.5	5.4	4.3	4.1	3.8	3.0	2.9	3.3	4.3	3.7	3.6
8	6.5	**6.9**	6.2	3.0	3.0	2.9	5.2	4.9	5.0	**4.8**	**4.7**	4.1	2.5	2.7	2.5	2.9	2.5	2.5
9	6.1	5.9	5.8	2.7	3.0	3.0	3.8	5.3	5.3	2.9	4.2	4.5	2.9	2.7	3.1	2.8	2.6	3.0
10	**7.7**	6.8	**6.9**	**4.5**	**4.5**	**4.8**	**7.7**	**7.7**	6.8	2.6	3.1	3.2	3.4	3.2	3.1	5.8	4.9	5.2
11	2.9	3.5	3.6	2.8	2.8	2.7	4.8	3.9	4.6	2.5	2.4	2.4	5.0	5.1	4.8	**6.9**	**6.8**	6.7
12	3.5	3.6	3.9	3.5	3.6	3.2	7.4	5.3	**7.4**	2.5	2.9	2.7	4.9	4.9	4.9	6.8	6.8	6.8
13	3.9	4.2	4.0	3.2	3.0	2.8	6.5	5.4	6.8	2.6	3.1	3.2	**6.7**	**6.7**	**6.5**	6.8	6.6	**6.8**
14	2.5	2.4	2.5	3.9	3.9	3.7	3.5	2.7	3.2	2.0	2.7	2.9	3.7	3.6	3.7	2.8	2.9	2.7
15	3.3	3.2	3.5	2.2	2.3	2.2	4.4	3.8	4.9	2.4	3.9	3.6	3.4	3.2	3.3	4.0	3.7	3.5
16	5.5	5.1	5.3	2.9	2.9	2.3	6.6	5.2	5.5	2.8	2.8	2.8	6.2	6.1	5.7	5.7	5.7	5.8
17	3.0	3.6	3.3	2.3	2.9	2.5	3.5	3.3	3.5	2.4	4.1	2.7	4.5	4.3	4.1	3.5	3.6	3.4
18	3.2	3.2	3.9	3.1	2.8	2.9	3.4	3.5	4.7	2.6	2.8	2.6	3.2	2.7	2.6	3.1	2.5	2.6

Notes: (1) Refer to Fig. 6.7.1 for wind directions and measurement locations;
(2) The wind speed at 300 m above ground is 12.9 m/s for all cases;
(3) Mean speeds at 2 m are listed for all points and the maxima are highlighted for each case; and
(4) Building models I = existing building configuration without the new building,
II = new building of original design with the tower at street corner, and
III = building of reversed plan with the tower at middle block.

building **B**, most likely at location 10. The expected channelling effect is not evident for wind directions NE and SE due to tall upstream buildings, but higher wind speeds are detected when the street orientation is somewhat angled with the wind direction, for instance, the NNE wind. For the tested directions, SE wind creates the most serious wind impact on the ground level regardless of building models, owning to the generally low building arrangements over the SE side.

It appears that the construction of a new complex has intricate effects on the existing wind environment depending on the measurement locations and wind directions. The overall impact, however, is insignificant for areas around the complex itself and around adjacent buildings. This phenomenon could be attributed to the tall building **B**, which induces a dominating flow field over the region under investigation. Due to the same reason, the change of building plan (Model III), which is supposed to reduce the wind intensity around the block corner, is also insignificant. However, those speeds shown in Table 6.7.1 consider only the effects caused by building aerodynamics and meteorological data should also be used to derive the actual wind conditions on these locations.

The annual maximum hourly wind speeds for each sector can be obtained using the weather data with an approximate probability $P(>V_o)=10^{-3}$ for daylight hours as suggested by Melbourne (1978). The wind speeds can be determined for each direction based on the daylight data drawn from meteorological records such as those in Table 6.2.1. The wind speed V_c is then converted into the reference wind speed at 300 m over the tested site for this case study:

$$V_{300} = V_o\left(\frac{300}{10}\right)^{0.16}\left(\frac{300}{500}\right)^{0.28} = 1.49\,V_o \qquad (6.7.1)$$

where the gradient height and the power law exponent are assumed to be 300 m and 0.16 over the airport, and 500 m and 0.28 over the tested area, respectively. The difference of V_{300} from the nominal reference speed (12.9 m/s) should be adjusted to obtain the real wind speed occurring once a year during daylight hours based on the measured wind speeds:

$$V_{predicted} = \frac{V_{300}}{12.9}V_{measured} \qquad (6.7.2)$$

Final results are shown in Table 6.7.2 which presents the annual hourly maximum speeds for daylight hours at corresponding locations. After the above adjustment, SE wind becomes much less severe due to the lowest speed at the airport. In contrast, the WSW and W wind turns out to be much more significant. At several locations, the wind speeds in certain directions are higher than 8 m/s, the maximum mean speed acceptable for walking, but there is no location with the wind speed higher than 11.5 m/s, which is characterized as dangerous for any activities.

To display the results graphically, the wind speeds around the corners of the intersection are shown in Fig. 6.7.2 for the six tested wind directions for Model I and II. The wind speeds are circularly scaled in 5, 6.5, 8 and 11.5 m/s, corresponding to the threshold speeds suggested by Melbourne (1978) for different human activities. For Models I and II, there is no apparent difference due to the dominant character of Building **B** in the area with the exception of Location 4, where wind speeds are generally reduced by the presence of the proposed building.

Table 6.7.2 Estimated wind speeds with the exceedance frequency of 0.001.

Direction	NNE			NE			SE			SW			WSW			W		
Uo (m/s)	9.4			11.1			8.6			11.4			11.9			11.7		
Model	I	II	III	I	II	III	I	II	III	I	II	III	I	II	III	I	II	III
No. 1	3.1	5.2	4.4	5.6	5.6	5.4	2.4	4.1	8.3	5.4	5.8	3.6	5.1	4.0	4.0	3.6	3.1	3.2
2	3.4	3.2	3.7	4.0	3.1	4.4	3.6	2.2	3.8	3.4	3.2	3.0	4.6	2.9	3.5	4.1	2.8	4.1
3	4.0	4.1	3.1	3.1	3.5	3.8	4.5	2.7	3.7	3.4	4.2	2.9	4.4	3.7	3.6	5.9	4.2	4.9
4	7.2	4.6	3.8	4.6	3.5	3.5	7.0	3.5	5.0	3.3	4.8	3.8	4.8	3.5	3.5	5.7	4.3	4.1
5	6.8	7.6	6.9	4.2	3.7	3.3	5.5	4.7	4.7	3.8	4.2	4.5	3.6	3.0	3.3	6.3	5.0	4.5
6	5.2	6.4	6.5	3.2	3.3	3.5	5.9	5.1	4.4	4.9	4.9	**6.3**	3.9	3.5	4.4	6.9	5.3	5.3
7	4.1	5.5	4.5	4.6	3.2	5.2	4.3	5.4	5.3	5.7	5.4	5.0	4.1	4.0	4.6	5.8	5.0	4.9
8	7.1	**7.5**	6.8	3.8	3.8	3.7	5.1	4.9	5.0	**6.3**	**6.2**	5.4	3.5	3.7	3.5	3.9	3.4	3.4
9	6.6	6.4	6.3	3.5	3.8	3.8	3.8	5.2	5.2	3.8	5.5	5.9	4.0	3.7	4.3	3.8	3.5	4.1
10	**8.4**	7.4	**7.5**	**5.8**	**5.8**	**6.1**	**7.6**	**7.6**	6.7	3.4	4.1	4.2	4.7	4.4	4.3	7.8	6.6	7.0
11	3.2	3.8	3.9	3.6	3.6	3.5	4.8	3.9	4.6	3.3	3.2	3.2	6.9	7.0	6.6	**9.3**	**9.2**	9.0
12	3.8	3.9	4.3	4.5	4.6	4.1	7.3	5.2	**7.3**	3.3	3.8	3.6	6.8	6.8	6.8	9.2	9.2	9.2
13	4.3	4.6	4.4	4.1	3.8	3.6	6.4	5.3	6.7	3.4	4.1	4.2	**9.2**	**9.2**	**9.0**	9.2	8.9	**9.2**
14	2.7	2.6	2.7	5.0	5.0	4.7	3.5	2.7	3.2	2.6	3.6	3.8	5.1	5.0	5.1	3.8	3.9	3.6
15	3.6	3.5	3.8	2.8	2.9	2.8	4.4	3.8	4.9	3.2	5.1	4.8	4.7	4.4	4.6	5.4	5.0	4.7
16	6.0	5.6	5.8	3.7	3.7	2.9	6.5	5.1	5.4	3.7	3.7	3.7	8.6	8.4	7.9	7.7	7.7	7.8
17	3.3	3.9	3.6	2.9	3.7	3.2	3.5	3.3	3.5	3.2	5.4	3.6	6.2	5.9	5.7	4.7	4.9	4.6
18	3.5	3.5	4.3	4.0	3.6	3.7	3.4	3.5	4.7	3.4	3.7	3.4	4.4	3.7	3.6	4.2	3.4	3.5

Notes: (1) Reference wind speeds V_o are determined by the daylight exceedance frequency of 0.001;
(2) The conversion of wind speeds follows Eqs.(6.7.1) and (6.7.2); and
(3) Building models I = existing building configuration without the new building;
II = new building of original design with the tower at street corner; and
III = building of reversed plan with the tower at middle block.

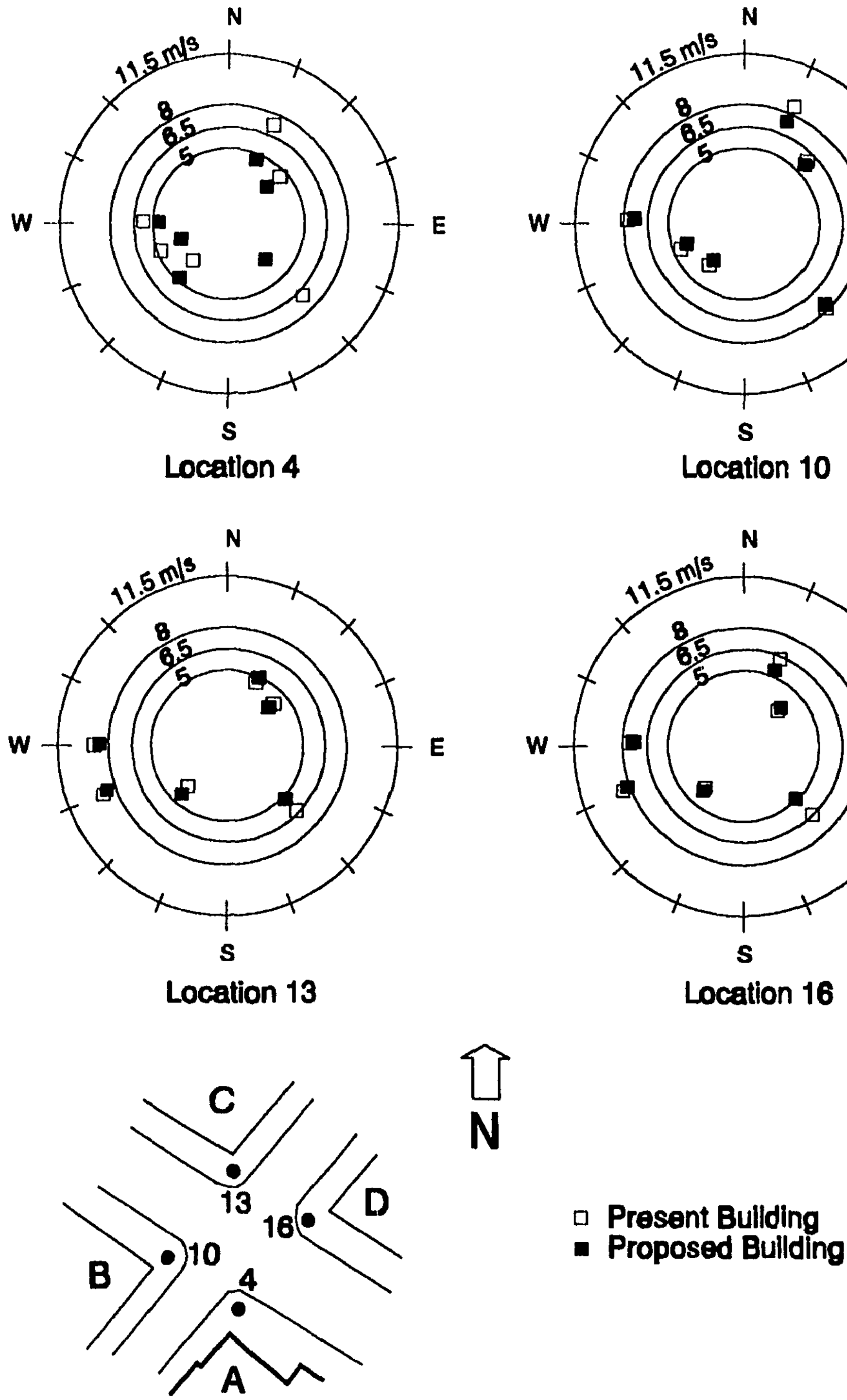

Fig. 6.7.2 Annual hourly maximum speeds around block corners, calculated from wind-tunnel measurements and weather station records for daylight hours.

As shown by the above results, the proposed building complex will not create any serious problems to its surroundings. The wind conditions around buildings **B**, **C** and **D**, however, cannot be really improved unless some effective remedial actions are taken for respective buildings. Suggestions include installing canopies and pavilions or fencing around the buildings. For the efficiency of these remedial actions, more wind-tunnel tests have to be performed.

6.8 SUMMARY

This chapter presents the development and application of procedures essential for obtaining model-study results and utilizing them in design practice. The existing knowledge is classified and organized in pertinent domains such as the weather records, terrain roughness and wind discomfort criteria. New relations and procedures are established in order to facilitate the computerized estimation of wind conditions at the pedestrian level. For instance, the long-term meteorological records from a nearby airport are analyzed and represented by a set of well-known Weibull functions; a nominal reference height and a wind-profile index are also introduced to link the wind profile over the built-up site around the main building of interest with the approach wind flow.

The proposed procedure for linking the weather records and on-site wind speeds focuses on the lower part of the boundary layer which has the direct effect on the pedestrian-level wind conditions. The procedure starts with the meteorological data including wind speeds, wind directions and frequencies of occurrence. These could be represented by probability models like the Weibull distributions with probability constants determined by regression analysis for local weather records. The wind intensity is modified by upstream terrains classified by their roughness lengths which depend upon the height and density of obstacles on terrains. The main buildings and their immediate surroundings play the most important parts in determining the local wind conditions. Also important are architectural details and remedial measures associated with buildings. The entire process was simply presented by Eq. 6.1.1, in which the vector of modification factor f_i could be broken down to:

$$f_i = (f_T \times f_S \times f_B \times f_R)_i \tag{6.8.1}$$

where the factors on the right-hand side of the equation represent the modifications to the meteorological data contributed by the upstream Terrain, the Surroundings, the main Building and the Remedial actions, respectively. The knowledge regarding f_T and f_S has been organized in this chapter, while results of f_B for various simple building models have been presented in Chapters 4 and 5. Some typical remedial actions have also been discussed here and their efficiency (f_R) are shown in Appendix G.

Based on the results derived from the current study and the literature information, a computer system has been developed for the preliminary evaluation of wind conditions and the recommendation for remedial actions. Although the role of wind-tunnel experimentation in the pedestrian wind studies cannot be replaced, the knowledge-based computer system demonstrates advantages in several respects, as will be discussed in the next chapter.

CHAPTER 7

A KNOWLEDGE - BASED COMPUTER SYSTEM

In an attempt to complement traditional approaches, a knowledge-based computer system has been developed for the evaluation of pedestrian-level wind environmental conditions around buildings. This chapter describes the computer system with emphasis on its general architecture and major components. The existing information has been collected systematically from the literature and generalized by further analysis and supplementary experiments, as presented in previous chapters. The knowledge is explicitly encoded in the form procedures with access to tabulated values via database operation within a computerized user-friendly environment. The knowledge-based computer system is expected to act as a consultation tool for building design and city planning at the preliminary stage.

7.1 INTRODUCTION

Traditionally, the evaluation of wind environmental conditions could only be carried out by means of wind-tunnel tests and full-scale measurements, which are known to be relatively expensive and time-consuming. Recent advances in the development of detailed computational techniques offer another avenue to solve the problem. Potentially, the flexibility and low cost of computer simulations would allow wind-environmental evaluation in the initial stages of building design, though further refinements is still needed for the simulation of turbulence characteristics, boundary conditions and architectural details.

However, these methods cannot account for the less formalized aspects of the problem-solving process. Some empirical judgement and modellizations are required for simplifying actual building cases before a solution procedure can be applied. Results obtained from these algorithmic procedures have then to be assessed by the knowledge of experienced wind engineers. Finally, the suggestion of remedial actions in case of unfavourable wind conditions is not a simple deterministic process and it is affected by a variety of constrains.

Knowledge-Based Systems (KBS) are interactive computer programs that incorporate human experience, judgement, rules of thumb and other expertise to provide knowledgeable advice on a wide range of topics. Compared with the conventional programming languages, KBS are more suitable for handling empirical, heuristic or incomplete knowledge non-sequentially and symbolically. Another important feature of KBS is that the domain knowledge is explicit and separate from the inference mechanism of the system. Therefore, the domain knowledge can be expanded independently without disturbing other parts of the system. Because of the ill-structured nature of many wind related design and analysis problems, it is anticipated that the knowledge-based systems will play a major role in wind engineering in the 90's (Reed, 1989).

GURU (Micro Data Base System Inc., 1985 and 1992) is the shell selected for the expert system development. In addition to the general advantages of KBS tools, GURU provides a development environment which integrates the capabilities of a rule-based system, natural language interpreter, data base management, spreadsheet analysis, business graphics, text processing and procedural language programming facilities. To meet the needs and tastes of a different class of users, GURU can be accessed in any of four distinct ways: menu guidance, natural language conversation, command language and customized interface. GURU's programming language allows developers to build customized applications. Hence, GURU is very attractive as a tool for the development of computer systems for the solution of some engineering problems.

7.2 GENERAL ARCHITECTURE OF DEWEN

The knowledge-based system developed is called DEWEN (Discomfort Evaluation of Wind ENvironment). Its general structure is shown by the flow chart in Fig. 7.2.1.

The evaluation of wind conditions around buildings starts with user instructions and queries. All questions appear with explanatory graphs and/or texts on the computer screen. Based on answers to several initial questions, the system will determine if the input building case can be simplified into one of basic building models, or if it is suitable for the evaluation. For a suitable case, further inputs consist of detailed descriptions for all contributing components including the main building's location, orientation, geometry and dimensions, the adjacent buildings, the surrounding street blocks and the farther terrains. They are captured and analyzed in the appropriate stages of the consultation process. If applicable, procedures in the system match the specific building configuration with established flow modules of wind overspeed ratios in the form of formulas and tables. Wind speed variations around buildings are then combined with the local meteorological records that are stored in data bases. A preliminary evaluation is

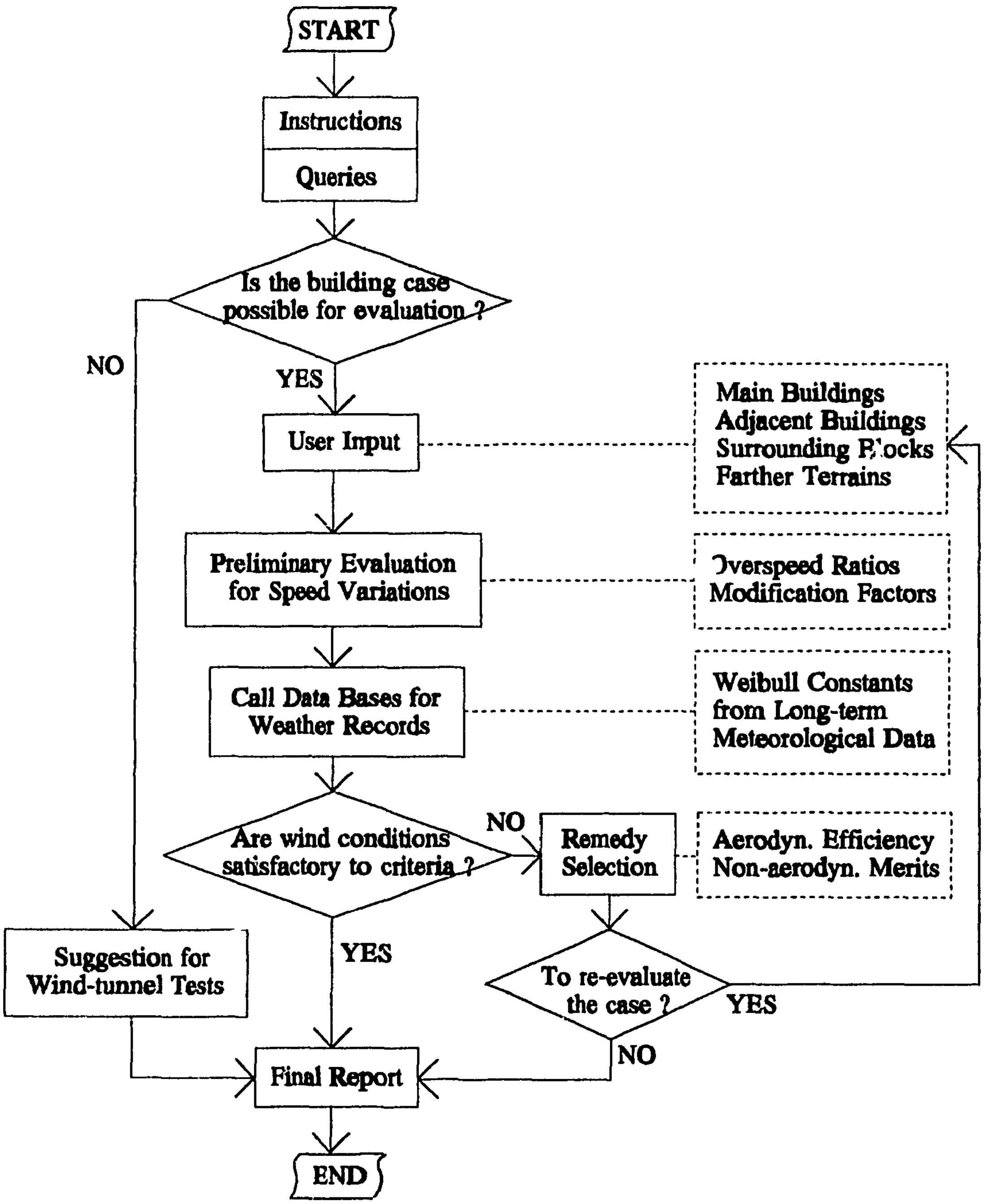

Fig. 7.2.1 General architecture of the knowledge-based system DEWEN.

accomplished with the wind speeds and exceedance frequencies at particular locations around buildings.

These exceedance frequencies for respective threshold speeds are compared with wind discomfort criteria. Then diagnoses are provided with wind speeds and discomfort levels anticipated for given pedestrian activities at various zones around buildings. If the wind conditions are not satisfactory, the selection of remedial actions comes up by the system following the principles of multi-objective decision making with considerations on both aerodynamic efficiency and non-aerodynamics merits of the remedies.

The major components of system DEWEN are discussed in detail in Section 7.3, and they are illustrated in Section 7.4 through a case study. In Section 7.5, a sub-system for the remedy selection is presented.

7.3 DETAILED DESCRIPTION OF MAJOR COMPONENTS

7.3.1 Model Identification

Actual buildings on a built-up site may have countless configurations in terms of dimensions, geometries and relative locations. It is impossible to have a knowledge base including potential pedestrian-level wind conditions for all building types. Broadly, three groups of building models are considered in the current computer system as shown in Fig. 7.3.1 - A: Isolated large buildings; B: Buildings on street blocks; and C: Building-enclosed courtyards.

Model A consists of a few large buildings in the neighbourhood of low buildings. These low surroundings are far apart so that their influence can be neglected. All regions in the vicinity of the large buildings are subject to strong wind flows caused by front vortices, corner streams and other flow mechanisms depending upon the location and the

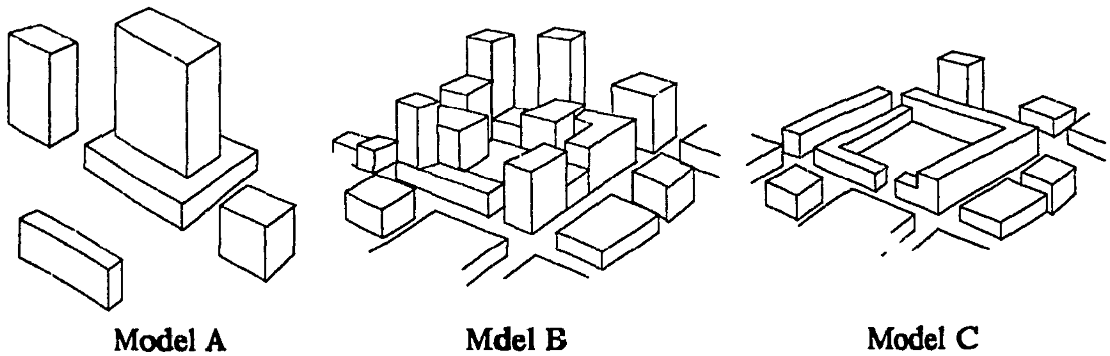

Fig. 7.3.1 Three basic building models in DEWEN.

approach wind direction of interest. The flow interaction may exist, but the spatial extent is assumed to be limited, i.e. isolated or two building models can be applied to the main building and its adjacent large buildings of concern. The simplest case is a flat, rectangular building. The large buildings may also have different cross-sections and various design features such as chamfered corners and setbacks.

Model B considers a number of buildings located within a rectangular block bounded by four straight streets where wind conditions are evaluated. Buildings and structures in the block and adjacent blocks are assumed to have vertically flat surfaces parallel to streets. The impact of other building geometries on the induced wind conditions is complicated by the presence of surrounding buildings and cannot be fully dealt with by the system at the current stage. The farther surroundings are simplified as uniform street blocks provided that there are no significantly large buildings dominating upstream flow patterns. Model B becomes Model A when a single building comprises the entire block and most surrounding buildings are extremely low.

Model C is a courtyard enclosed or partly enclosed by buildings. Buildings in this model are relatively low - say, not higher than 30 m - since hight-rise buildings usually provide shelter to the enclosed yard. The courtyard model is assumed covering an entire street block with flat building surfaces facing four adjacent streets. Adjacent buildings are generally low with a few exceptions of isolated large buildings, which may induce the sheltering effect to the courtyard. Openings may exist for connecting the enclosed space to outside streets. The wind conditions inside courtyards and at openings are regions to be evaluated.

These building model types provide local wind conditions given information about the approach winds. For buildings too complex or too special to be simplified, wind-tunnel tests are suggested. On the other hand, for a building case suitable for the evaluation, further information is inquired by the computer system.

7.3.2 Data Input

Two sets of data are required for the building model itself and its surroundings.

The first set of data assists in specifying the building model. Inputs for Model A include the dimensions, the geometry and the orientation of the main building, heights of adjacent buildings and their distances from the main building. For Model B, the main street block is divided into nine zones (Fig. 7.3.2) and detailed inputs of heights and horizontal dimensions are required for eight outer zones, that determine the wind conditions over adjacent streets. Orientations are also needed for the four sides of the block. In addition, dimensions and relative locations of buildings on eight adjacent blocks are also required when building groups are considered.

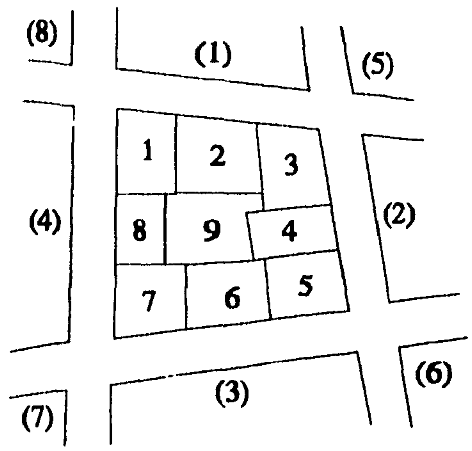

Fig. 7.3.2 The main street block and surroundings for data input of Model B.

To describe a courtyard, data such as averaged heights, lengths and widths of buildings forming four sides of the courtyard are needed for Model C. Based on these data, both external and internal dimensions can be calculated. Types, widths and orientations of openings are effective factors in determining the wind speeds through passages. For adjacent buildings, the sheltering effect caused by a larger upstream building and the channelling effect caused by a cross-street opening can also be evaluated by the computer system. Once specified, the building model is related to overspeed ratios for different regions and wind directions that are in turn modified by surroundings.

The other set of data is for surroundings handled by the same input format for all three models. These data include the averaged block heights and widths, and averaged street widths from two to ten or more street blocks away from the main building in four equally divided angle sectors. Farther city topographies are considered as the upstream terrains classified by the average roughness lengths and obstacle heights determined by the heights and densities of ground obstacles. These data enable the system to evaluate the variations of wind speeds from the meteorological data recorded at a weather station.

7.3.3 Combination with Meteorological Data

In DEWEN, the combination of overspeed ratios and meteorological data is performed by following the procedure proposed in Chapter 6. The Weibull constants are derived and stored in data bases for the time periods of all hours, daylight hours, summer days and winter days for the city where the building locates. At present, this process has taken place only for Montreal. The combination proceeds in the computer system as follows: (1) evaluation of modification factors contributed by all parameters specified in Eq. 6.8.1; (2) extraction of appropriate Weibull constants for given time periods from data bases; and (3) estimation of the exceedance frequency for specified threshold wind speeds using Eq. 6.2.3. The selection of threshold speeds and time periods depends on the wind criteria to be used for criteria conformance.

7.3.4 Conformance of Criteria

Three sets of wind discomfort criteria are encoded in the computer system: the Davenport's criteria (Davenport, 1972), the Melbourne' criteria (Melbourne, 1978) and the City of Montreal Guidelines. The derived wind frequencies of exceedance are compared with these criteria for respective human activities associated with the zones of interest. One or more criteria can be selected for conformation, although different conclusions may be generated due to the incomparability among these criteria.

If the criteria suggest acceptable wind conditions, the system proceeds to the last procedure: generation of final reports with wind speeds and frequencies around buildings. Otherwise, the program turns to remedial selections, for which, a sub-system has been built for both general suggestion and specific decision making for effective remedies.

7.3.5 Suggestions and Report

Remedial suggestions are provided by the computer system through either a single or a multiple objective procedure. The latter considers not only the aerodynamic efficiency of remedies, but also the non-aerodynamic aspects from the economic, functioning and architectural viewpoints, for which detailed descriptions are given in Section 7.5.

The single objective refers to the aerodynamic efficiency of remedies ranging from reducing building height to planting trees. As exemplified in Fig. 7.3.3, general guidelines of remedial actions suitable for the wind-speed reduction are provided if the wind conditions are unacceptable or the building configuration is not suitable for the evaluation. Associated with these suggestions is a data base with applicable building configurations and their potential efficiency.

The final report for a consultation case is generated by DEWEN following a pre-defined scheme using GURU's report-generating, data base and spreadsheet facilities. The report consists of input information of buildings and surroundings, predicted exceedance frequencies for given threshold speeds and corresponding discomfort levels at several locations around buildings, as well as remedial suggestions for unacceptable cases. These could be stored in a data base, shown on the screen and output to a printer.

GENERAL GUIDELINES FOR BUILDING DESIGN

- Avoid tall buildings with large surfaces facing dominant wind directions
- Design buildings with a circular cross section, rounded or chamfered corners
- Increase distances between tall buildings in order to avoid channelling or Venturi effect
- Place tall buildings on large podiums
- Install screens and/or slide doors for passages underneath high-rise buildings
- Protect pedestrian areas by roofs, pavilions, canopies, fences or other wind breaks
- Protect building-enclosed courtyards by reducing inside space or increasing surrounding heights
- Keep pedestrian areas away from tall buildings
- Plant trees or bushes around buildings
- Provide handrails and warning signs for windy areas

Fig. 7.3.3 General suggestions of remedies for wind-speed reduction.

It is worth mentioning that all data, input and output, can be called in by spreadsheet commands. Users can change their input data for design modifications and obtain the output wind conditions in the same spreadsheet file. This makes the evaluation of several design alternatives an easy task.

7.4 A CASE STUDY

The building case presented in Section 6.7 can be simplified into Model B by the computer system. As illustrated in Fig. 7.4.1 (based on Fig. 6.7.1), two narrow blocks, i.e. the block where the proposed building to be erected and its left neighbourhood, are combined as the main block with a similar plan size to surrounding blocks. Wind

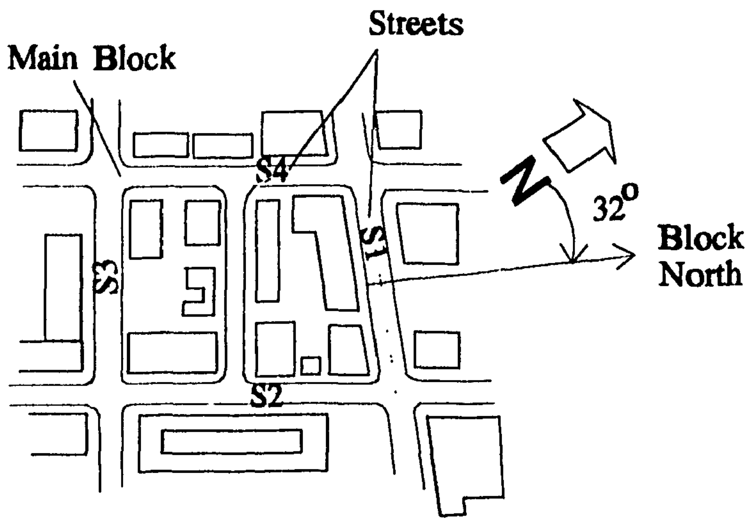

Fig. 7.4.1 Building model evaluated in case study.

conditions on the streets (S1 to S4) around the main block are to be evaluated.

The input data consist of heights, widths, and orientations of the eight outer zones in the main block, dimensions of adjacent blocks and their distances from the main block, averaged distributions of street blocks and terrain roughness in different directions. For comparison purposes, these values are determined in consistence with the wind-tunnel simulation, instead of reproducing the actual topography of the downtown Montreal. As explained previously, data inputs are assisted by explanatory texts and graphs. All input data for the model are stored in a single spreadsheet file defined after the process of data input. Major contents of the spreadsheet file are summarized in Fig. 7.4.2.

All figures in the file are in meters except the wind direction which is in degrees. Based on the user input, the modification factors, f_i in Eq. 6.2.2 as the ratios of local wind speeds at 2 m to those at 10 m recorded at the weather station, are estimated for Model B. Over the four streets, the estimated modification factors are provided by DEWEN for 16 wind directions as in Table 7.4.1.

```
1-  :A    :B    :C    :D    :E    :F    :G    :H    :I    :J    :K    :L    :M    :N
 1|                    ------ - Summary of Input Data
 2|
 3|      ---- Main Block
 4|                    NORTH                 EAST                  SOUTH                 WEST
 5|Height:        67.5  27.5  16.0  12.5   3.0  12.5  12.5  12.5   3.0  12.5  12.5  17.5
 6|Width:         22.5  50.0  35.0  70.0  15.0  70.0  70.0  26.5  43.0  40.0  25.0  70.0
 7|Direction:           32.0              38.0              38.0              38.0
 8|Opening:             Nil
 9|      - -- Adjacent Buildings
10|             NORTH  EAST SOUTH  WEST    NE    SE    SW    NW
11|Height:       12.0  19.0  20.0  90.0  12.5  10.0   6.0  29.0
12|Width:        90.0 125.0  90.0 135.0
13|Depth:        45.0  37.5  25.0  22.5
14|Distance:     22.5  22.5  22.5  27.5
15|      ---- Surrounding Streets
16|             NORTH  EAST SOUTH  WEST
17|Height:       40.0  20.0  20.0  70.0
18|W-E Length:  150.0 150.0 110.0 110.0
19|N-S Length:   75.0  75.0 110.0  90.0
20|      ---- Terrain Roughness
21|                    NORTH  EAST SOUTH  WEST
22|Roughness Length:   0.030 0.030 0.030 0.030
23|Obstacle Height:      2.0   2.0   2.0   2.0
```

Fig. 7.4.2 Input data stored in a spreadsheet file.

Table 7.4.1 Modification factors estimated for four streets and 16 wind directions.

	Streets			
Directions	S1	S2	S3	S4
N	0.25	0.36	0.23	0.36
NNE	0.22	0.41	0.18	0.49
NE	0.21	0.39	0.14	0.46
ENE	0.27	0.41	0.25	0.49
E	0.35	0.34	0.35	0.47
ESE	0.43	0.27	0.44	0.47
SE	0.41	0.23	0.42	0.45
SSE	0.43	0.27	0.44	0.54
S	0.39	0.33	0.33	0.49
SSW	0.35	0.40	0.23	0.47
SW	0.31	0.37	0.15	0.45
WSW	0.36	0.40	0.18	0.47
W	0.31	0.34	0.23	0.35
WNW	0.28	0.28	0.28	0.21
NW	0.27	0.23	0.26	0.11
NNW	0.28	0.33	0.28	0.22

On Street S4 which is channelled by the proposed building and other tall buildings, the modification factors are higher than others for most wind directions due to the channelling effects and front vortices. By combining the modification factors and weather records, the exceedance frequencies for different threshold wind speeds during different time periods can be calculated. For example, the threshold wind speeds in Melbourne's criteria are 5, 6.5, 8, 11.5 m/s for different human activities, and 6 m/s for summer days and 4 m/s for winter days in the city guidelines of Montreal. Exceedance frequencies for these threshold speeds are calculated and presented in Table 7.4.2.

Table 7.4.2 Calculated exceedance frequencies in percent for different threshold speeds and time periods.

	Montreal Guidelines		Melbourne's Criteria			
Time periods	Sum. Day	Win. Day	Daylight Hours			
Speed(m/s)	6	4	5	6.5	8	11.5
Street S1	0.04	3.20	0.48	0.07	0.01	0.00
S2	0.07	5.39	1.07	0.20	0.04	0.00
S3	0.01	0.52	0.04	0.00	0.00	0.00
S4	0.32	9.60	2.47	0.63	0.16	0.01

As a result of criteria conformance against of the City of Montreal Guidelines, all four streets are found acceptable for pedestrian walking in all seasons (P<15%). Frequencies of exceeding 6 m/s in summer are extremely low and suitable for all human activities. During winter day time, Streets S2 and S4 experience exceedance frequencies higher than 5%, the maximum for a long stay which probably will seldom take place on streets in Montreal in winter.

The acceptable frequency in Melbourne's criteria is once a year, corresponding to

0.05% - 0.1% of daylight hours. Higher frequencies are predicted on Streets S2 and S4 which are in the directions of prevailing winds. It should be noted that Melbourne's criteria give much stricter diagnoses; for example, Street S4 is not even suitable for walking based on the daylight frequency of wind speeds exceeding 8 m/s. For all cases, DEWEN provides not only objective exceedance frequencies but also subjective diagnoses based on the set of criteria used. Since the different criteria may give different conclusions, naturally, the final judgement has to be made by the users themselves.

It is interesting to compare the DEWEN predictions and wind-tunnel measurements for such a building model. However, for a given direction, only one wind speed or frequency of wind exceedance is provided for each street by DEWEN. On the other hand, wind conditions could be evaluated at many points over streets in the wind-tunnel tests. For instance, points 1-4 and 16-18 on Street S1 and points 4-10 on Street S4 are selected for the measurements. In the comparison, only the average of wind speeds at all the points of the streets are used. The same reference wind speed at 300 m is assumed equal to 12.9 m/s for both the wind-tunnel test and the computer system. Based on the modification factors provided by DEWEN, the ground-level wind speeds are computed for six wind directions on streets S1 and S4 where wind-tunnel measurements have been carried out.

As shown in Fig. 7.4.3, the computer predicted wind speeds generally follow the measured values. Large discrepancies under several wind directions, such as NNE for Street S1, and NE and WSW for S4, could be caused by the negligence of some complex building details by the system, the mismatch in estimation of actual street densities and the measurement errors in the wind-tunnel experiment.

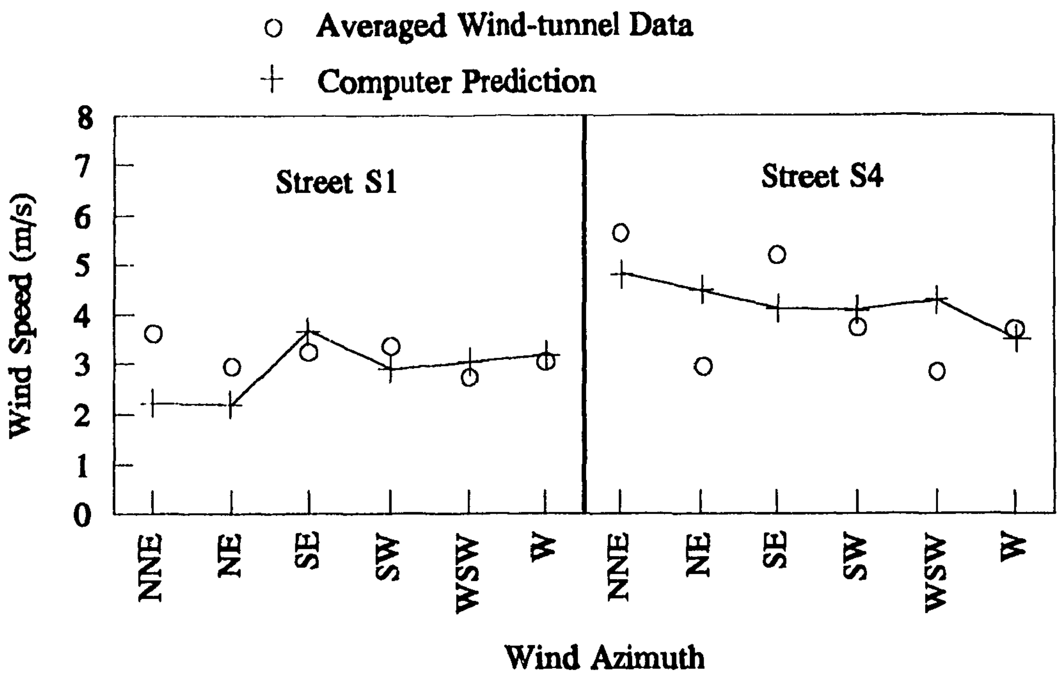

Fig. 7.4.3 Comparison of average of wind speeds measured in the wind tunnel and predicted by the computer system.

7.5 REMEDY SELECTION: MULTI-OBJECTIVE DECISION MAKING

Non-aerodynamic concerns such as financial constraints, aesthetic appearance and functional performance of a building project may have a significant impact on the decision making process. An aerodynamically effective remedy may not be preferred from other viewpoints. The general structure of the decision making process implemented in the KBS for selecting a remedial action accounts for all these concerns. As shown in Fig. 7.5.1, this approach determines the overall utility value for a selected remedy as follows:

$$U_o = W_a \times U_a + W_n \times U_n \tag{7.5.1}$$

where W_n=1-W_a. The major components involved in Fig. 7.5.1 and Eq.7.5.1 are explained below in detail.

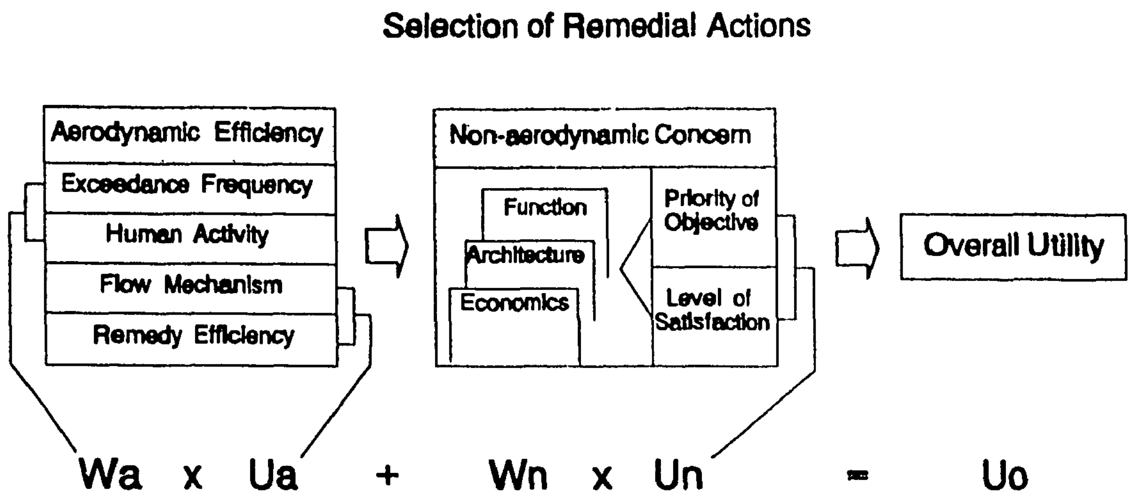

Fig. 7.5.1 General structure of decision making for remedy selections.

7.5.1 Aerodynamic Weight and Utility

The most important objective to be achieved by the implementation of remedial measures is the reduction of wind speeds. The aerodynamic weight (W_a) involved in the decision making process is related to the frequency of exceedance of strong winds and the human activity associated with the evaluated area. For the human activities grouped as: (1) *Long Stationary Exposure*, (2) *Short Stationary Exposure*, (3) *Strolling, Skating* and (4) *Walking Fast*, after Davenport (1972), Table 7.5.1 shows the aerodynamic weight utilized by the system with respect to the frequencies of wind speeds exceeding 5 m/s.

The wind speed of 5 m/s is widely accepted as the onset of discomfort. Wind conditions are classified as *acceptable*, *marginally acceptable* and *unacceptable* according to the frequency of exceedance. No remedial action is necessary for a frequency lower than 5% regardless of human activities. The weight of 0.5 is assumed for *marginally* *acceptable* wind conditions. The heaviest weight assigned in Table 7.5.1 is 0.9 when the higher-than-5 m/s wind happens more than 20% of the time on a site for the long stationary exposure. This is considered unacceptable or even dangerous. In general, the higher the frequency of exceedance, the heavier the aerodynamic weight for a given human activity. After calculating the aerodynamic utilities for all feasible remedial actions (Section 6.5), the system suggests four choices with highest scores of U_a for further examination of their non-aerodynamic features (U_n).

Table 7.5.1 Weight of aerodynamic factors (W_a) assigned for human activities and frequencies of exceedance of mean wind speeds higher than 5 m/s.

Human Activity	Frequency of Exceedance P(>5 m/s) %			
	5-10	10-15	15-20	>20
Long stationary exposure	0.6 (U)	0.7 (U)	0.8 (U)	0.9 (U)
Short stationary exposure	0.5 (M)	0.5 (M)	0.7 (U)	0.8 (U)
Strolling, skating	0.4 (A)	0.5 (M)	0.5 (M)	0.7 (U)
Walking fast	0.3 (A)	0.4 (A)	0.5 (M)	0.6 (U)

Notes: (1) Letters in parentheses represent wind conditions:
A = Acceptable; M = Marginally acceptable and U = Unacceptable; and
(2) No remedial action is necessary for P(>5 m/s) < 5%.

7.5.2 Non-aerodynamic Concerns

The non-aerodynamic concerns in Fig. 7.5.1 consist of economic, architectural and functional requirements which affect the final selection of remedial actions. W_n is automatically determined by the value of W_a since $W_a+W_n=1$. The calculation of U_n is generally based on input of program users. Data at two levels are required by the system. One is the relative priority of the three requirements among themselves. The other is the level of satisfaction of each remedy with respect to those requirements.

The priority is quantified by input numbers from 0 to 100, i.e., from *least importance* to *most importance*. Three priority values are normalized and used as sub-weights for each concern. The level of satisfaction quantifies the performance of each specific remedy from the three different viewpoints (economic, architectural and functional). Proper input values can be supplied graphically by means of a special ruler. The ruler is marked from 0 to 100 by an increment of 25, simply corresponding to *impossible*, *unfavourable*, *feasible*, *favourable* and *excellent*, respectively. For example, if values of level of satisfaction (25, 75, 50) are assigned to a remedy, it means that this remedy is economically unfavourable, architecturally favourable and functionally feasible. Values that are not multiples of 25 can also be used indicating assessments between two marked levels, say the score of 65 representing an evaluation for a remedy between feasible and favourable.

At the current stage, no quantitative relations have yet been built between design alternatives and their non-aerodynamic utilities, although there might be some possibilities to do so. For instance, the impact of reducing the building height or the total floor area may lead to an empirical function on economic utilities. However, due to the lack of pertinent information, the non-aerodynamic utility for a proposed remedy is determined by the computer system based entirely on user's input values.

7.5.3 An Example for Remedy Selection

The selection of remedies with the computer system proceeds in the following steps: (1) determination of the aerodynamic weight (W_a) and aerodynamic utility values (U_a) of remedies from data bases and wind conditions; (2) suggestions based on aerodynamic considerations only; (3) input of general priorities on non-aerodynamic aspects and respective levels of satisfaction for each aerodynamically preferred remedy; (4) calculation of non-aerodynamic utility values (U_n); and (5) combination of utility values for overall recommendations. The consultation process is illustrated by a simple case as shown in Fig. 7.5.2. For clarity, only essential literal content is displayed here and no attempt has been made to show the exact appearance on the computer screen. Underlined text is input data and text in **bold** shows calculated results.

The case is given for a small park next to a high-rise building. Wind speeds at the park are evaluated for 16 wind directions, yielding the frequencies of wind speeds exceeding 5 m/s as 2.5%, 10.1% and 0.3% of the time caused by front vortex, corner stream and wake turbulence of the building, respectively. The total frequency is therefore 12.9%, which assigns an aerodynamic weight W_a=0.7 (Step 1) for the *Long Stationary Exposure* (Table 7.5.1). Based on the wind frequencies of exceedance, relative frequencies for those three flow mechanisms are calculated and coupled with the remedy utilities in Table 6.5.1 to obtain the aerodynamic utility values for all potential remedies. Four most effective remedies are then listed as 1 to 4 aerodynamics suggestions (Step 2). Next, the inputs of general priorities on the economic, architectural and functional concerns are needed for calculating the respective sub-weights. For the four remedies, values of the level of satisfaction are specified for the three non-aerodynamic concerns (Step 3). Non-aerodynamic utility values are evaluated from values of sub-weight and level of satisfaction (Step 4). By calculating and comparing the overall utility values, two final selections are made at the end (Step 5).

```
 CASE STUDY:  Small downtown park next to tall building

------------------ Aerodynamic Concern -----------------------

        Frequencies of Wind Speeds Exceeding 5 m/s

Flow Mechanism              (Normalized Freq.)
 Front Vortex         2.5 %   ( 19.4 %)
 Corner Stream       10.1 %   ( 78.2 %)
 Wake Turbulence      0.3 %   (  2.4 %)
           Total:    12.9 %   (100 0 %)

 Activity:  Long Stationary

      From Table 4: Wa = 0.7

 Remedial Actions                Ua x 0.7
     (From Table 5)
 1  Height Reduction           81.7          57.2
 2  Re-orientation             69.3 x 0.7 = 48.5
 3  Tapered or Setbacked       69.5          48.7
 4  Arcade, Roof or Pavilion   67.8          47.5

--------------- Non-Aerodynamic Concern ----------- -----------

          Econ. Arch. Func.
Priority   80    40    20
Sub-weight .57   .29   .14

                                                           Overall
Actions  Satisfaction Level->  Un   x 0.3        -->   Uo   Ranking
   1        10    40    20     20.1           6.0      63.2    2
   2        40    60    20     42.6 x 0.3 = 12.8      61.3    4
   3        50    30    50     44.3          13.3      62.0    3
   4        70    50    20     57.1          17.1      64.6    1

    Final selections are: 4. Arcade, Roof or Pavilion
                          1. Height Reduction
```

Fig. 7.5.2 A consulting case for the selection of remedies.

One suggestion is to install arcade, roof or pavilion for regions immediately adjacent to the tall building, and the other is to reduce the building height - the aerodynamically most effective action becomes the second choice due to the low scores of level of satisfaction on non-aerodynamic concerns.

7.6 SUMMARY

In order to organize and present the existing knowledge of pedestrian winds, a knowledge-based system has been developed for the evaluation of the pedestrian-level wind conditions around buildings. Three basic building models are implemented in the knowledge base with information necessary for predicting the exceedance frequencies for given wind speeds around buildings. A procedure using the principles of multi-objective decision making is developed and executed in the system for the selection of remedial actions with considerations on both aerodynamic and non-aerodynamic merits of remedies.

The advantage of the knowledge-based system compared with conventional approaches such as wind-tunnel experiments and numerical computations can be summarized as follows: (1) No special knowledge is required for running the program and the complex domain knowledge is accessible to building designers and city planners via a user-friendly interface. (2) A usually time-consuming consultation process can be executed consistently in a very short time period. (3) Such a time-saving feature also makes it feasible to evaluate different design alternatives and remedies at early design stages. (4) The system can be expanded readily as more information of pedestrian-level winds becomes available, since the inference engine of the computer system is independent from the knowledge base and the entire system is designed by a programming language similar to plain English.

However, it should be emphasized that at the current stage, (1) the system is only capable for a preliminary evaluation of the pedestrian-level wind conditions around building configurations very similar to three established models to be specified in the next section; (2) a particular region, such as a building corner area and a building-enclosed courtyard, is evaluated by the system as a whole with only one representative frequency of wind exceedance provided, while the wind-tunnel assessments can be made at many locations; and (3) since DEWEN is one of the first knowledge-based systems in wind engineering, further improvements such as the refinement of user interface, and the validation and expansion of knowledge base are required in several aspects prior to commercialization.

Nevertheless, it has been shown that the knowledge-based approach is applicable for predicting the wind environmental conditions at preliminary design stages. The development of DEWEN bridges sophisticated laboratory findings of pedestrian winds to engineering practices for building design and city planning.

CHAPTER 8

CONCLUSIONS AND RECOMMENDATIONS

An extensive study has been carried out for the pedestrian-level wind conditions around buildings. The objectives and approaches of this study are stated at the beginning of the thesis. After a brief literature review, relevant experimental techniques are compared with respect to pedestrian wind assessments. Various building models are investigated in the boundary-layer wind tunnel to establish relationships between wind speeds and building configurations. These research findings, along with other information, are organized in a knowledge base for a computer system designed for the preliminary evaluation of wind environmental conditions around buildings at the pedestrian level.

In this thesis, a summary is provided at the end of each chapter to highlight the progress of the study, from which, final conclusions can be drawn as follows.

8.1 CONCLUSIONS

(1) Literature Information

The brief literature review discusses the major elements of pedestrian-level wind studies in terms of

- wind flow mechanisms around buildings;
- criteria for the comfort and safety of pedestrians; and
- remedial actions for improving wind environment.

Based on the review, research needs are identified, and specific research approaches and programs are implemented.

(2) Experimental Techniques

For the assessment of pedestrian-level wind conditions,

- a novel technique based on infrared thermography has been developed and applied in wind-tunnel experiments. Results from various measurement techniques such as the LDA, Irwin's sensor and flow visualization, have been compared with respect to the assessment of wind flows around buildings.
- In general, point measurement systems are capable of providing quantitative information about the turbulent wind flow at several points. For a better spatial coverage, these systems may be supplemented by area methods which, however, have their own limitations in supplying quantitative evaluations.
- A logical approach is suggested to use area methods first for identifying windy zones, then to perform point measurements for accurate speeds at selected positions. A table is provided as a quick reference for selecting the proper instrumentation for pedestrian-level wind measurements in addition to any specific requirements of the particular experimental environment.

(3) Isolated Buildings

Isolated, rectangular buildings are considered as bench-mark models in the study. The root cause for wind speed variations is the spatial differences of air pressures. High speed winds may occur at several regions around buildings and governed by respective flow modules.

- In front of a large building, down-washing winds create a strong flow reversal at ground level.
- The horse-shoe vortex wraps round the building base and induces corner streams with speedy winds near windward corners of the building.
- Due to the pressure differences, air flows may be channelled through any passage underneath the building with considerably high speeds.
- In the wake area, where wind speeds are usually low because of the sheltering effect, the reattachment of jumping-over flow may induce a windy zone behind a long building oblique to incident winds.

Extensive experiments have been carried out in the boundary-layer wind tunnel for a range of rectangular buildings with various dimensions.

- Major contributing parameters are identified and examined for both buildings and approach winds.
- The spatial impact of building-induced winds is related to the influence scale defined by the windward dimensions of rectangular buildings.
- The variation of wind speeds is described by the overspeed ratios. Empirical relations between the overspeed ratios and the building dimensions are established for corresponding flow modules.
- In addition to the mean speed, the 3-D wind fluctuation is also investigated around buildings using LDA.
- The impact of wind incidence is demonstrated by the point measurements around rectangular buildings.

(4) Multiple Buildings

Wind flows around two or multiple buildings are considered as a complex interaction of flows around respective isolated buildings with the intensities estimated by influence scales and the relative locations of buildings.

- For two tandem buildings, the down-washing flows in front of the downstream, tall building are modified by the upstream building. The extent of modification could be assessed using the modification function of the relative height and the relative distance.
- For side-by-side models, the wind flow is channelled into the gap between buildings. The speed amplification, or the interaction intensity, is estimated by a function of the influence scales and the distance between buildings.
- When two buildings are staggered, the sheltering effect and the circuit-short-cutting of wind pressure must be considered in addition to the front vortex and the channelled flow. These effects may become more complex for multiple buildings, around which some kind of superposition of flow patterns around isolated and two-building models amy be applied in some cases.
- For a courtyard enclosed by low buildings, the inside wind conditions vary in principle with the height of windward buildings and the along-wind length of courtyard; high-speed winds may occur at the courtyard openings depending on their dimensions and orientations.
- For uniform street blocks, the average wind speed along streets can be estimated using an empirical relation associated with the blockage ratio defined by the windward dimensions of street blocks. When a tall building is erected in a uniformly

built region, the maximum speed amplification is a function of the height difference of buildings, the blockage ratio of street blocks and the height for wind measurement Further experiments are also carried out for the effects of wind direction and location of the tall building within a street block.

(5) Urban Microclimatic Wind Conditions

Procedures, data bases and formulas essential for applying model-study results into practical building cases have been developed. The knowledge has been classified and organized in pertinent domains. For instance,

- the long-term meteorological records from a nearby weather station are analyzed and represented by sets of coefficients of the Weibull functions for several time periods of interest.
- A nominal reference height and a wind-profile index are introduced for coupling the wind profile over a built site to those over the surrounding street blocks, upstream terrains and the weather station. The proposed procedure focuses on the lower part of boundary layer flows, that is believed to have the primary effect on the pedestrian-level wind conditions.
- The selection of remedial actions for the unacceptable wind conditions is handled as a multi-objective decision making problem. Utility values and weights are generated by considering both aerodynamic and non-aerodynamic merits of remedies.

(6) Knowledge-Based Computer System

For organizing and representing the relevant knowledge, a knowledge-based system is developed for the evaluation of pedestrian-level wind conditions around buildings.

- Three basic building models are implemented in the system with information necessary for predicting the frequencies of wind exceedance at several regions around buildings.
- A procedure using the principles of multi-objective decision making is executed in the computer system for the selection of remedial actions.
- Compared with conventional approaches, the knowledge-based computer system with a user-friendly interface is (1) easy to access, run and maintain, (2) time saving, (3) repeatable; and (4) readily expandable.

8.2 SUMMARY OF CONTRIBUTIONS

Contributions of the present study to knowledge in engineering fundamentals and building applications can be summarized as follows:

(1) The development and application of a novel wind-tunnel experimental technique based on infrared thermography demonstrates an effective means for the assessment of wind conditions around buildings.

(2) The establishment of flow modules for various building configurations reveals the wind flow mechanism around buildings and facilitates the estimation of building-induced variation of wind speeds at the pedestrian level.

(3) The organization of knowledge from the literature and the current study along with the proposed procedures for knowledge integration contribute a

comprehensive tool for handling the pedestrian-level wind problems.

(4) The development of a knowledge-based system for the preliminary evaluation of pedestrian-level wind environmental conditions makes the complex domain knowledge available for building engineering applications within a computerized environment.

8.3 RECOMMENDATIONS FOR FUTURE WORK

Research on pedestrian-level winds around buildings has been progressed all over the world for the last 30 years. Studies have been carried out on almost every aspect of the problem, yielding an enormous amount of knowledge as partly shown in this thesis. However, during the course of development of the knowledge-based computer system, some essential information is found missing or incomplete. The knowledge of pedestrian-level winds can be expanded in several fields from the understanding of building aerodynamics to the application of weather records. Some specific research topics are suggested below for further investigation.

(1) Link of Meteorological Data and on-site Wind Speeds

Meteorological data are the basis for evaluation of wind environmental conditions around buildings at a built-up site. Connecting these data with wind speeds and directions on a built-up site involves analyses of weather records, terrain topographics, surrounding blockages and building aerodynamics. Only a few concepts, such as the logarithmic law and the boundary-layer simulation, are widely accepted. New relationships and procedures have to be developed to make use of amplification factors derived from idealized model studies. In the current study, for instance, a detailed procedure is proposed for linking wind speeds around buildings on a built-up site to those over the surroundings, upstream terrains and weather station. The validation for the entire journey of wind-speed development in a boundary-layer wind tunnel is somewhat difficult due to the limitations of experimental scale and measurement techniques. However, examination of each step involved is possible and worthwhile to study in both laboratory and field scales.

(2) Practical Models and Rules

A number of wind modules have been established in the current study. More building models and more practical rules can be developed as research work goes on. Special attention should be paid to the multiple building models including surroundings, the effect of building geometry and architectural details, and the efficiency of remedies as well. Note that the existing building models are mainly extracted from simplified building configurations. Rules of thumb based on actual building cases may be more valuable for building design and city planning.

(3) Assessments of 3-D Turbulence

It is found that pedestrian-level wind speeds vary with time and space to a great extent. As indicated by the measurements using the LDA around rectangular buildings, the selection of measurement locations is critical for both the mean and rms wind speeds at all three directions and hence for the outcome of wind environment evaluations. Practical constraints like the width of sidewalks and the pedestrian accessibility should certainly be taken into account in such a selection. Besides these, no detailed rules or criteria have been established on this issue, although the proposed influence scale of a building is capable of identifying the spatial extent of wind impact and the locations of maximum wind speeds.

At a given location, turbulent wind flow fluctuates with time, that is usually quantified by the mean and rms wind speeds, or their combinations called effective (peak) wind speeds. Most wind-tunnel measurements, however, were performed by using thermal anemometers or other techniques, which are not quite suitable for the 3-D, high-turbulence wind flow near the ground. New techniques have to be developed to define and quantify the effective wind speeds representing the wind impact on pedestrians.

(4) Experimental Techniques

In order to carry out further detailed measurements, improvements are needed for both point and area techniques. The Laser Doppler anemometer and the infrared-thermography technique are promising for pedestrian-level wind measurements with the potential already demonstrated by the current study.

Particle-imaging velocimeter is another technique for turbulence measurements developed in the field of experimental fluid mechanics. According to Adrian (1991), the technique is now capable of providing accurate measurements in two dimensions for a variety of laboratory-scale flows. The technique is particularly powerful for measuring the flow field around complex geometrical configurations. With the advancement of computer techniques for image recording and data processing, extension of the applications of the method to pedestrian wind measurements is anticipated.

(5) Comprehensive Evaluation of Outdoor Environment

Although the mechanical force on a human body is the most important impact created by the pedestrian-level winds, the thermodynamic effect should also be evaluated when comfort is considered. Not only the wind speed, but also the temperature, humidity, solar radiation, clothing, activity and exposure time should be taken into consideration (Soligo et al, 1993). More theoretical and experimental studies are needed to establish new criteria for a comprehensive evaluation of outdoor environmental conditions.

(6) Applications in Snow Drifting and Air Pollutant Dispersion

Accumulation of snow at sidewalks and doorways creates inconvenience to people in winter time. Snow falls are often accompanied by wind storms. Instead of straight falling downwards, snow flakes may follow air movements around buildings. Even on the ground, snow accumulation can be drifted by wind flows from one place to another. The pedestrian-level wind speeds and directions are important factors in the snow drifting.

Dispersion of air pollutants in cities has similar mechanisms, except pollutants can be generated by disparate sources at different heights including the pedestrian level by automobiles, for example. More significantly, the thermal gradient near the ground, the turbulence scale and intensity, as well as the physical and chemical features of pollutants also play important roles in the pollutant dispersion.

The knowledge derived from this study for pedestrian-level winds around buildings can be applied for the prediction of snow drifting and pollutant dispersion with additional information provided.

REFERENCES

Adrian, R.J. (1991) "Particle-imaging techniques for experimental fluid mechanics," *Annu. Rev. Fluid Mech.*, 23, 261-304.

Apperley, L.W. and Vickery, B.J. (1974) "The prediction and evaluation of the ground level wind environments," *Proc. 5th Australasian Conf. on Hydraulics and Fluid Mech.*, University of Canterbury, Christchurch, New Zealand, 175-182.

Arens, E.D. (1981) "Designing for an acceptable wind environment," *Transportation Engrg. J., ASCE*, 107(TE2) 127-141.

Arens, E., Ballanti, D., Bennet, C., Guldman, S. and White, B. (1989) "Developing the San Francisco wind ordinance and its guidelines for compliance," *Building and Environment*, 24(4) 297-303.

Arens, E., Gonzalez, R. and Berglund, L.G. (1986) "Thermal comfort under an extended range of environmental conditions," *ASHRAE Trans.*, 92 (1).

ASHRAE, (1989), *ASHRAE 1989 Fundamentals Handbook*, Chapter 8: Physiological Principles, Comfort and Health.

Aynsley, R.M. (1974) "Effects of airflow on human comfort," *Building Science*, 9, 91-94.

Aynsley, R.M. (1989) "Politics of pedestrian level urban wind control," *Building and Environment*, 24(4) 291-295.

Aynsley, R.M., Melbourne, W.H. and Vickery, B.J. (1977) *Architectural aerodynamics*, Applied Science Publishers Ltd., London, UK.

Baker, C.J. (1978) *Vortex flow around the bases of obstacles*, Ph. D. thesis, Cambridge

University, Cambridge, UK.

Baskaran, A. and Stathopoulos, T. (1989) "Computational evaluation of wind effects on buildings," *Building and Environment*, 24(4) 325-333.

Bellhouse, B.J. and Schultz, D.L. (1966) "Determination of mean and dynamic skin friction, separation and transition in low-speed flow with a thin-film heated element," *J. Fluid Mech.*, 24, 379-400.

Beranek, W.J. (1984) "Wind environment around single building of rectangular shape and wind environment around building configurations," *HERON*, 29(1), Institute for Building Materials and Building Structures, Rijswijk, The Netherlands.

Beranek, W.J. and von Koten, H. (1979) "Visual techniques for the determination of wind environment," *J. Indust. Aerodyn.*, 4, 295-306.

Bicknell, J. and Shaw, A. (1966) "Wind tunnel tests of Eastman Court and the Green Building at M.I.T.," *Wright Brother Facility reports* TR 1027-1029, Dept. of Aerodyn. and Astron., MIT, Boston, MA, US.

Borges, A.R.J. and Saraiva, J.A.G. (1979) "An erosion technique for assessing ground level wind," *Proc. 5th Int.. Conf. on Wind Engrg.*, Fort Collins, Colorado, US, 235-242.

Bottema, M. (1993) *Wind climate and urban geometry*, Ph. D. thesis, Eindhoven University of Technology, Eindhoven, The Netherlands.

Bradbury, L.J.S. (1976) "Measurements with a pulsed-wire and a hot wire anemometer in a highly turbulent wake of a normal flat plate," *J. Fluid Mech.*, 177, 473-497.

Britter, R.E. and Hunt, J.R.C. (1979) "Velocity measurements and order of magnitude estimates of the flow between two buildings in a simulated atmospheric boundary layer," *J. Indust. Aerodyn.*, 4, 165-182.

Carpenter, P., Cenek, P.D. and Jamieson, N.J. (1992) "The inference of city wind ordinances on building design in Wellington, New Zealand," *Proc. ASCE Struct. Cong.'92 X*, San Antonio, Texas, US, 364-367.

Cohen, H., Mclaren, T., Moss, S., Petyk, R. and Zube, E. (1977) "Pedestrians and wind in the urban environment," *UMASS/IME R-77/13*, University of Massachusetts, Amherst, MA, US.

Davenport, A.G. (1961) "The spectrum of horizontal gustiness near the ground in high winds," *J. Royal Meteorol. Soc.*, 87, 194-211.

Davenport, A.G. (1965) "The relationship of wind structure to wind loading," *Proc. Sympo. on Wind Effects on Buildings and Struct.*, Nat. Physical Lab., Teddington, U.K., 1, 53-102.

Davenport, A.G. (1971) "On the statistical prediction of structural performance in the wind environment," *ASCE Nat. Struct. Engrg. Meeting*, Baltimore, Maryland, US.

Davenport, A.G. (1972) "An approach to human comfort criteria for environmental wind conditions," presented at *Colloq. on Building Climatology*, Stockholm, Sweden.

Durgin, F.H. (1989) "Proposed guidelines for pedestrian level wind studies for Boston - comparison of results from 12 studies," *Building and Environment*, 24(4) 305-314.

Durgin, F.H. (1992) "Pedestrian level wind studies at the Wright Brothers Facility," *J. Wind Engrg. and Indust. Aerodyn.*, 41-44, 2253-2264.

Durgin, F.H. and Chock, A.W. (1982) "Pedestrian level winds: a brief review," *J. Struct. Div., ASCE*, 108(ST8) 1715-1767.

Dye, R.C.F. (1980) "Comparison of full-scale and wind-tunnel model measurements of ground winds around a tower building," *J. Wind Engrg. and Indust. Aerodyn.*, 6, 311-326.

Ettouney, S.M. (1977) "Notes on courtyard aerodynamics," *Proc. 6th Course: Airflow and Building Design*, Post Experience Courses in Building Service Engrg., University of Sheffield, UK.

Ettouney, S.M. and Fricke, F.R. (1975) "An anemometer for scale model environmental wind measurements," *Building Science*, 10, 17-26.

Fang, C. and Sill, B.L. (1992) "Aerodynamic roughness length: correlation with roughness elements," *J. Wind Engrg. and Indust. Aerodyn.*, 41-44, 449-462.

Fanger, P.O. (1972) *Thermal Comfort*, Danish Technical Press, Copenhagen, Denmark.

Gandemer, J. (1975) "Wind environment around buildings: aerodynamic concepts," *Proc. 4th Int. Conf. on Wind Effects on Buildings and Struct.*, Heathrow, UK, 423-432.

Gandemer, J. (1979) "Wind shelters," *J. Indust. Aerodyn.*, 4, 371-389.

Garratt, J.R. (1990) "The internal boundary layer - a review," *Boundary-Layer Meteorol.*, 50, 171-202.

Harmon, P. and Sawyer, B. (1990) *Creating expert systems for business and industry*, John Wiley and Sons Inc., NY, US.

Hayes-Roth, F., Waterman, D.A. and Lenat, D.B. (1983) *Building expert systems*, Addition-Wesley Publishing Company, Inc., NY, US.

Helliwell, N.C. (1971) "Wind over London," *Proc. 3rd Int. Conf. on Wind Effects on Buildings and Struct.*, Tokyo, Japan, 23-32.

Hellman, G. (1961) "Über die Bewegung der Luft in den untersten Schichten der Atmoshäre," *Meteorol. Z.*, 34, 273.

Hinze, J.O. (1959) *Turbulence*, McGraw-Hill, NY, US.

Hosker Jr., R.P. (1985) "Flow around isolated structures and building clusters: a review," *ASHRAE Trans.* 91(2b) 1679-1692.

Hunt, J.C.R. (1991) "Industrial and environmental fluid mechanics," *Annu. Rev. Fluid Mech.*, 23, 1-41.

Hunt, J.C.R., Abell, C.J., Peterka, J.A. and Woo, H. (1978) "Kinematical studies of the flow around free and surface-mounted obstacles: applying topology to flow visualization," *J. Fiuid Mech.*, 86, 179-200.

Hunt, J.C.R., Poulton E.C. and Mumford, J.C. (1976) "The effects of wind on people: new criteria based upon wind tunnel experiments," *Building and Environment*, 11, 15-28.

Irwin, H.P.A.H. (1981) "A simple omnidirectional sensor for wind-tunnel studies of pedestrian-level winds," *J. Wind Engrg. and Indust. Aerodyn.*, 7, 219-239.

Irwin, H.P. (1982) "Instrumentation considerations for velocity measurements," *Proc. Int. Workshop on Wind Tunnel Modelling Criteria and Techniques in Civil Engrg. Application*, Cambridge University Press, NY, US, 546-557.

Ishizaki, H. and Sung, I.W. (1971) "Influence of adjacent buildings to wind," *Proc. 3rd Int. Conf. on Wind Effects on Buildings and Struct*, Tokyo, Japan, 145-152.

Isyumov, N. (1978) "Studies of the pedestrian level wind environment at the Boundary Layer Wind Tunnel Laboratory of the University of Western Ontario," *J. Indust. Aerodyn.*, 3, 187-200.

Isyumov, N. and Davenport, A.G. (1975a) "The ground level wind environment in built-up areas," *Proc. 4th Int. Conf. on Wind Effects on Buildings and Struct*, Heathrow, London, UK, 403-422.

Isyumov, N. and Davenport, A.G. (1975b) "Comparison of full-scale and wind tunnel wind speed measurements in the Commerce Court Plaza," *J. Indust. Aerodyn.*, 1, 201-212.

Isyumov, N., Helliwell, S., Rosen, S. and Lai, D. (1985) "Winds in cities: effects on pedestrians and the dispersion of ground level pollutants," presented at *6th Colloq. on Indust. Aerodyn.*, Aachen, Germany.

Jackson, P.S. (1976) "A theory for flow over escarpments," *Proc. 4th Int. Conf. on Wind Effects on Buildings and Struct.*, Heathrow, UK, 33-40.

Jackson, P.S. (1978) "The evaluation of windy environments," *Building and Environment*, 13, 251-260.

Jamieson, N.J., Carpenter, P. and Cenek, P.D. (1992) "The effect of architectural detailing on pedestrian-level wind speeds," *J. Wind Engrg. and Indust. Aerodyn.*, 41-44, 2301-2312.

Jensen, N.O. (1978) "Change of roughness and the planetary boundary layer," *Quart. J. Royal Meteorol. Soc.*, 104, 351-356.

Kamei, I., and Maruta, E. (1979) "Study on wind environmental problems caused around buildings in Japan," *J. Indust. Aerodyn.*, 4, 307-331.

Lawson, T.V. (1978) "The wind content of the built environment," *J. Indust. Aerodyn.*, 3, 93-105.

Lawson, T.V. (1980) *Wind effects on buildings*, Applied Science Publishers Ltd., London, UK.

Lawson, T.V. and Penwarden, A.D. (1975) "The effects of wind on people in vicinity of buildings," *Proc. 4th Int. Conf. on Wind Effects on Buildings and Struct*, Heathrow, UK, 605-622.

Lee, B.E. (1977) "Aerodynamic effects of building groups," *Proc. 6th Course: Airflow and Building Design,* Post Experience Courses in Building Service Engrg., University of Sheffield, UK.

Lee, B.E. and Hussain, M. (1979) "The ground level wind environment around the Sheffield University Arts Tower," *J. Indust. Aerodyn.*, 4, 334-341.

Leene, J.A. (1992) "Building wake effects in complex situations," *J. Wind Engrg. and Indust. Aerodyn.*, 41-44, 2277-2287.

Lemelin, D.R., Surry, D. and Davenport, A.G. (1988) "Simple approximations for wind speed-up over hills," *J. Wind Engrg. and Indust. Aerodyn.*, 28, 117-127.

Letchford, C.W. and Ginger, J.D. (1993) "Wind environment assessment: a case study in the Brisbane CBD," presented at *3rd Asia-Pacific Sympo. on Wind Engrg.*, Hong Kong, Dec., 1993.

Livesey, F.M. (1991) *The impact of new development on pedestrian level winds*, M.E.Sc. thesis, The University of Western Ontario, London, Ontario, Canada.

Melaragro, M. (1982) *Wind in architectural and environment design*, Van Nostrand Reihold Company, NY, US.

Melbourne, W.H. (1978) "Criteria for environmental wind conditions," *J. Indust. Aerodyn.*, 3, 241-249.

Melbourne, W.H. and Joubert, P.N. (1971) "Problems for wind flow at the base of tall buildings," *Proc. 3rd Int. Conf. on Wind Effects on Buildings and Struct.*, Tokyo, Japan, I.11-1-I.11-10.

Merati, P., Wigeland, R. and Nagib, H. (1979) "Control of adverse wind near buildings," presented at *ASCE Annual Convention and Exposition*, Atlanta, GA, US.

Meroney, R.N. (1988) "Bluff-body aerodynamics influence on transport and diffusion," presented at *Int. Colloq. on Bluff Body Aerodyn. and Its Applications*, Kyoto, Japan.

Micro Data Base Systems Inc. (1985 and 1991) *GURU Reference Manual and User's Guide*, Lafayette, Indiana, US.

Morkovin, M.V. (1972) "An approach to flow engineering via functional flow modules," *Beitrage zur Stromungsmechnik, A. Walz 65th Anniversary Volume, Deutsch Luftund Raumfahrt Forschungsvericht*, paper 72-27.

Murakami, S. (1990) "Numerical simulation of turbulent flowfield around cubic models: current status and applications of k-ε model and LES," *J. Wind Engrg. and Indust. Aerodyn.*, 33, 139-152.

Murakami, S. and Deguchi, K. (1981) "New criteria for wind effects on pedestrians," *J. Wind Engrg. and Indust. Aerodyn.*, 7, 289-309.

Murakami, S., Iwasa, Y. and Morikawa, Y. (1986) "Study on acceptable criteria for assessing wind environment at ground level based on residents' diaries," *J. Wind Engrg. and Indust. Aerodyn.*, 26, 1-18.

Murakami, S. and Kunio, F. (1983) "Turbulence characteristics of wind flow at ground level in built-up area," *J. Wind Engrg. and Indust. Aerodyn.*, 15, 133-144.

Murakami, S., Shoda, T. and Kobayashi, N. (1975) "Wind effects on air flow in half-enclosed spaces," *Proc. 4th Int. Conf. on Wind Effects on Buildings and Struct.*, Heathrow, UK, 433-446.

Murakami, S., Uehara, K. and Komine, H. (1979) "Amplification of wind speed at ground level due to construction of high-rise building in urban area," *Proc. 3rd Colloq. on*

Indust. Aerodyn., Aachen, Germany, 55-77.

Oke, T.R. (1988) "Street design and urban canopy layer climate," *Energy and Buildings*, 11, 103-111.

Panofsky, H.A. and Townsend, A.A. (1964) "Change of terrain roughness and the wind profile," *J. Royal Meteorol. Soc.*, 90, 147-155.

Panofsky, H.A. and Dutton, J.A. (1984) *Atmospheric turbulence*, John Wiley and Sons, NY, US.

Paterson, D.A. and Apelt, C.J. (1986) "Computation of wind flows over three-dimensional buildings," *J. Wind Engrg. and Indust. Aerodyn.*, 24, 193-213.

Peterka, J.A. and Cermak, J.E. (1975) "Turbulence in building wakes," *Proc. 4th Int. Conf. on Wind Effects on Buildings and Struct*, Heathrow, UK, 447-463.

Peterka, J.A., Meroney, R.N. and Kothari, K.M. (1985) "Wind flow patterns about buildings," *J. Wind Engrg. and Indust. Aerodyn.*, 21, 21-38.

Penwarden, A.D. (1973) "Acceptable wind speeds in towns," *Building Science*, 8, 259-267.

Penwarden, A.D., Grigg, P.F. and Rayment, R. (1978) "Measurements of wind drag on people standing in a wind tunnel," *Building and Environment*, 13, 75-84.

Penwarden, A.D. and Wise, A.F.E. (1975) "Wind environment around buildings," *Building Research Establishment report*, Dept. of Environment, Building Research Establish., H.M.S.O., London, UK.

Perry, A.E. (1982) *Hot-wire anemometry*, Oxford University Press, NY, US.

Plate, E.J. (1982) *Engineering meteorology* (ed.) Elsevier Science Publishers Company, Amsterdam, The Netherland.

Ratcliff, M.A. and Peterka, J.A. (1989) "Comparison of pedestrian wind acceptability criteria," *Proc. 6th US Nat. Conf. on Wind Engrg.*, University of Houston, TX, US, 1, C5-12-C5-21.

Reed, D.A. (1990) "Expert systems in wind engineering," *J. Wind Engrg. and Indust. Aerodyn.*, 33, 487-494.

Sanada, S., Iwasa, Y. and Yoshida, M. (1980) "Full-scale measurement of environmental wind in the Shinjuku New Metropolitan Center," *J. Wind Engrg. and Indust. Aerodyn.*, 6, 291-309.

Shoda, T., Murakami, S., Keda, K. and Uehara, K. (1979) "Wind tunnel experiments on strong wind around buildings and on sheltering effect of windbreaks, Part II, Experimental studies on air flow around buildings (VIII)," *Trans. of Arch. Assoc. of Japan*, 234 (In Japanese).

Simiu, E., and Scanlan, R.H. (1986) *Wind effects on structures*, 2nd ed., John Wiley and Sons, NY, US.

Soligo, M.J., Irwin, P.A. and Williams, C.J. (1993) "Pedestrian comfort including wind and thermal effects," presented at *3rd Asia-Pacific Sympo. on Wind Engrg.*, Hong Kong, Dec., 1993.

Stathopoulos, T. (1984) "Design and fabrication of a wind tunnel for building aerodynamics," *J. Wind Engrg. and Indust. Aerodyn.*, 16, 361-376.

Stathopoulos, T. (1985) "Wind environmental conditions around tall buildings with chamfered corners," *J. Wind Engrg. and Indust. Aerodyn.*, 21, 71-87.

Stathopoulos, T., Bedard, C. and Wu, H. (1992) "Building-induced winds at pedestrian level," presented at *CIB-92 World Building Cong.*, Montreal, Canada.

Stathopoulos, T. and Saathoff, P. (1989) "Pedestrian wind environmental criteria for the City of Montreal," *A report prepared for the City of Montreal*, Centre for Building Studies, Concordia University, Montreal, Canada.

Stathopoulos, T. and Storms, R. (1986) "Wind environmental conditions in passages between buildings," *J. Wind Engrg. and Indust. Aerodyn.*, 24, 19-31.

Stathopoulos, T. and Wu, H. (1992) "Knowledge-based strategies for the assessment of pedestrian-level winds," *Proc. ASCE Struct Cong. '92 X*, San Antonio, Texas, US, 368-371.

Stathopoulos, T. and Wu, H. (1993) "Generic models for pedestrian winds in built-up regions," *Proc. 3rd Asia-Pacific Sympo. on Wind Engrg.*, Hong Kong, Dec., 1993, also accepted for publication by *J. Wind Engrg. and Indust. Aerodyn.*, 1994.

Stathopoulos, T. and Wu, H. (1994) "A Low-cost wind tunnel facility for the visualization of air flow around buildings," *Int. J. Engrg. Educat.*, in press.

Stathopoulos, T., Wu, H. and Bedard, C. (1992) "Pedestrian-level winds around buildings: a knowledge-based approach," *J. Wind Engrg. and Indust. Aerodyn.*, 41-44, 2377-2388.

Stein, B. and Reynolds, J.S. (1992) *Mechanical and electrical equipment for buildings*, 8th ed., John Wiley and Sons, NY, US.

Taylor, P.A. (1969) "On wind and shear stress profiles above a change in surface roughness," *J. Royal Meteorol. Soc.*, 95, 71-91.

Theurer, W., Baechlin, W. and Plate, E.J. (1992) "Model study at the development of boundary layer above urban areas," *J. Wind Engrg. and Indust. Aerodyn.*, 41-44, 437-448.

To, A.P., Lam, K.M. and Thung, D.T.K. (1993) "Evaluation of pedestrian level wind environment around a row of tall buildings," *Proc. 3rd Asia-Pacific Sympo. on Wind Engrg.*, Hong Kong, Dec., 1993.

Uematsu, Y. and Yamada, M. (1991) "Application of infrared thermography to the evaluation of pedestrian-level winds around buildings," presented at *Int. Conf. on Exp. Fluid Mech.*, Chengdu, China.

Uematsu, Y., Yamada, M., Higashiyama, H. and Orimo, T. (1992) "Effects of corner shapes of high-rise buildings on the pedestrian level wind environment with consideration for mean and fluctuating wind speeds," *J. Wind Engrg. and Indust. Aerodyn.*, 41-44, 2289-2300.

White, B.R. (1992) "Analysis and wind-tunnel simulation of pedestrian level winds in San Francisco," *J. Wind Engrg. and Indust. Aerodyn.*, 41-44, 2353-2364.

Wieringa, J. (1992) "Updating the Davenport roughness classification," *J. Wind Engrg. and Indust. Aerodyn.*, 41-44, 357-368.

Williams, C.D. and Wardlaw, R.L. (1992) "Determination of the pedestrian wind environment in the City of Ottawa using wind tunnel and field measurements," *J. Wind Engrg. and Indust. Aerodyn.*, 41-44, 255-266.

Wilson, D.J. (1989) "Airflow around buildings," *ASHRAE Handbooks 1989 Fundamentals*, 14.1-14.18, ASHRAE Inc. Atlanta, GA, US.

Wiren, B.G. (1975) "A wind tunnel study of the wind velocity in passages between and through buildings," *Proc. 4th Int. Conf. on Wind Effects on Buildings and Struct*, Heathrow, UK, 465-475.

Wiren, B.G. (1991) "A wind tunnel study of wind speeds near the ground in a group of block-type buildings," *Research Report*, The National Swedish Institute for Building

Research, Gävle, Sweden.

Wise, A.F.E. (1971) "Wind effects due to groups of buildings," *Phil. Trans. of Royal Society (London)* A269, 469-485.

Wise, A.F.E., Sexton, D.E. and Lillywhite, M.S. (1965) "Air flow round buildings," *Proc. Urban Plng. Research Sympo.*, Ministry of Public Building and Works, Building Research Station, London, UK, 71-91.

Wu, H. and Stathopoulos, T. (1993a) "Wind-tunnel techniques for the assessment of pedestrian-level winds," *J. Engrg. Mech., ASCE*, 119(10) 1920-1936.

Wu, H. and Stathopoulos, T. (1993b) "Infrared thermography for assessing the impact of pedestrian-level winds," *Proc. 3rd Asia-Pacific Sympo. on Wind Engrg.*, Hong Kong, Dec., 1993.

Wu, H. and Stathopoulos, T. (1994) "Further experiments on Irwin's surface wind sensor," *J. Wind Engrg. and Indust. Aerodyn.*, 51, in press.

Wu, H., Stathopoulos, T. and Bedard, C. (1991) "Generation of a knowledge base for the evaluation of the wind environment around buildings," *Proc. 4th Int. Conf. on Computing in Civil and Building Engrg.*, Tokyo, Japan, 243.

Wu, H., Stathopoulos, T. and Bedard, C. (1993a) "Computer-based building design and pedestrian-level wind conditions," *Proc. ASCE/5th Int. Conf. on Computing in Civil and Building Engrg.*, Anaheim, CA, US.

Wu, H., Stathopoulos, T. and Bedard, C. (1993b) "A knowledge-based system for predicting and improving pedestrian wind conditions," submitted to *Civ. Engrg. Sys.*

APPENDIX A

WIND EFFECTS ON PEOPLE

The wind flows at pedestrian level may affect human activities to different degrees depending upon various natural and human factors. Table A-1 summarizes the wind effects on pedestrians according to the well-known *Beaufort Scale*. The wind speeds listed in the table are mean values at 2 meters above the ground, rather than 10 meters as usually used with the Beaufort Scale or at weather stations. Other weather factors, such as the air temperature, sunshade, humidity etc., have to be taken into account if they are not typical of a temperate climate. Additionally, the dress, activity, age, and physical and psychological state of individuals may also affect the assessment of wind effects.

The table is plotted from the following sources: Melbourne and Joubert (1971), Davenport (1972), Penwarden (1973), Lawson and Penwarden (1975), Hunt et al (1976), Jackson (1978), Murakami, et al (1980), Murakami and Deguchi (1981) and recent wind-tunnel experiments at the Centre for Building Studies, Concordia University.

Table A-1 Wind effects on people.

Beaufort Scale	Speed (m/s)	Wind Effects on People
0 Calm	0	Calm
1 Light air		No noticeable wind
2 Light breeze	2	Wind felt on face
3 Gentle breeze		Clothing flaps, hair disturbed, newspaper difficult to read
	4	
4 Moderate breeze		Hair disarranged, dust and paper raised
	6	
5 Fresh breeze		Force of wind felt on body
	8	Control of walking begins to be impaired, violent flapping of clothes, progress into wind slightly slowed
6 Strong breeze		
	10	Umbrellas used with difficulty
7 Near gale	12	Blown sideways, inconvenience felt walking into wind, hair blown straight, difficulty to walk steadily, noise on ears unpleasant
	14	
8 Gale		Almost halted into wind, uncontrolled tottering downwind, difficult with balance in gusts
	16	Impossible to open eyes continuously, tears falling, unbalanced, grabbing at supports
9 Strong gale	18	People blown over in gusts
	20	Whole body bends windward, earache, headache, breathing difficult
	22	Cannot stand

APPENDIX B

SUMMARY OF DISCOMFORT WIND CRITERIA

Based on field observations and wind-tunnel experiments, several sets of discomfort criteria for pedestrian-level winds have been developed. These are summarized in this section in their original format. Additional information is supplied in parentheses for comparison purposes. Following each criteria, some brief explanations are also provided.

1. Davenport (1972)

		Beaufort Scale for Relative Comfort Level			
Activity	Areas Applicable	Perceptible	Tolerable	Unpleasant	Dangerous
Walking fast	Sidewalks	5 (7.4)	6 (9.9)	7 (12.4)	8 (15.1)
Strolling, Skating	Parks, Entrances Skating rinks	4 (5.5)	5 (7.4)	6 (9.9)	8 (15.1)
Standing, Sitting - short exposure	Parks, Plaza areas	3 (3.5)	4 (5.5)	5 (7.4)	8 (15.1)
Standing, Sitting - long exposure	Outdoor restaurants Bandshells, Theatres	2 (1.9)	3 (3.5)	4 (5.5)	8 (15.1)
Representative criteria for acceptability			< once/wk	< once/m	< once/yr
	all hours %		1.5	0.3	0.02

Notes:

(1) Beaufort Scales are suggested for extensive sets of activities and comfort categories;

(2) Numbers in parentheses are the mean speeds in m/s at 2 m above the ground, which is 80% of the medium speeds at the reference height of 10 m for corresponding Beaufort Scales;

(3) The criteria are tentative for temperatures higher than 10 °C. At lower temperatures, the relative comfort level may be expected to be reduced by one

Beaufort number for every 20 °C reduction in temperature; and

(4) For evaluating the effect of local turbulence, Isyumov and Davenport (1975a) revised these criteria by introducing an effective speed defined as $V_e=\bar{V}+1.5V_{rms}$. The exceedance probabilities are also provided.

2. Penwarden (1973)

Mean speed (m/s)	Perception
5	Onset of discomfort
10	Definitely unpleasant
20	Dangerous

Notes:

(1) Only mean wind speeds are suggested for human perception; and

(2) No exceedance probabilities and human activities are specified.

3. Lawson and Penwarden (1975)

Activity	Beaufort #	$\bar{V}$ (m/s)	V_e (m/s)	$P(>V)$ %
Acceptable for covered areas	2	(2.7)	(4.6)	< 4
Acceptable for standing areas	3	(4.4)	(7.4)	< 4
Acceptable for walking	4	(6.4)	(10.9)	< 4
Unacceptable	6	(11.1)	(19.0)	> 2

Notes:

(1) Beaufort scales are converted into wind speeds at 2 m high (in parentheses), which were 80% of the speeds at 10 m. Utilized for each Beaufort range is the uplimit of wind speeds rather than the medium values used by Davenport (1972); and

(2) 3-second gust speeds V_e are estimated by $V_e=\bar{V}+2.5V_{rms}=1.7\bar{V}$.

4. Penwarden and Wise (1975)

$P(\bar{V}>5$ m/s$) < 10$ %	No complaints
$P(\bar{V}>5$ m/s$) > 20$ %	Remedial action required

Notes:
(1) Based on the survey of business in a shopping centre;
(2) $\bar{V}$ is the mean wind speed at pedestrian level; and
(3) The criteria can be simplified as a single sentence:
"Wind conditions are acceptable if $\bar{V}$>5 m/s less than 20% of the time."

5. Hunt, Poulton and Mumford (1976)

Activity	$\bar{V}$ (m/s)	V_e (m/s)	$P(>V)$ %
Tolerable conditions and unaffected performance	6	9	10
Safe and sure walking	9	13	1

Notes:
(1) Equivalent speeds V_e are related to mean and rms speeds by $V_e=\bar{V}+3V_{rms}$.

6. Cohen, Mclaren, Moss, Petyk and Zube (1977)

Activity area	Hourly Mean (m/s)	All hour Occurrence %	Daily Occurrence %
All pedestrian areas - limit for safety	9.1	0.1 (10 h/yr)	0.2
Major walkways, especially principal egress path for high-rise buildings	9.1	0.1	0.2
Other pedestrian walkways, including streets and arcade shopping areas	6.4	5	10
Open plazas and park areas walking, strolling activities	3.6	15	30
Open plaza and park sitting areas, open-air restaurants	2.3	20	40

Notes:
(1) Only mean speeds are included; and
(2) Based on an extensive field study for urban environment.

7. Melbourne (1978)

Activity	$\bar{V}$ (m/s)	V_e (m/s)	$P(>V)$
Stationary long exposure	5	10	once/yr
Stationary short exposure	6.5	13	once/yr
Walking	8	16	once/yr
Unacceptable for any activity	11.5	23	once/yr

Notes:

(1) Annual peak gust speed $V_e=\bar{V}+3.5V_{rms}=2\bar{V}$ for a turbulence intensity of 30%; and

(2) The once-per-year occurrence corresponds to probabilities of 0.05-0.1% for daylight hours and 0.025-0.05% for all hours, estimated by the number of storms per annum and the probability distribution of wind speeds.

8. Murakami and Deguchi (1981)

Effects	Wind Speeds (m/s)
No effect	< 5
Some effect	5 - 10
Serious effect	10 - 15
Very serious effect	> 15

Notes:

(1) Speeds are 3-second average based on wind tunnel tests and field observations; and

(2) Neither occurrence probabilities nor human activities are specified.

9. Murakami, Iwasa and Morikawa (1986)

Activity	Exceedance probability $P(>V_d)$ % for V_d = 10	15	20 m/s
Long & short-term stationary exposure	10	0.8	0.08
Strolling	22	3.6	0.6
Walking	35	7	1.5

Notes:

(1) Derived from a two-year survey of residents living near a high-rise building in Tokyo; and

(2) These criteria are expressed in terms of daily maximum gust wind speed V_d. The use of such a wind speed makes it difficult to compare with others.

10. Soligo, Irwin and Williams (1993)

(a) **Wind Force Criteria**

Category	Gust Wind Velocity (m/s)	Frequency
sitting	0 - 4.7	≥ 80%
standing	0 - 6.9	≥ 80%
walking	0 - 8.9	≥ 80%
uncomfortable	> 8.9	> 20%
severe	≥ 24.4	0.15%

(b) **Thermal Comfort Criteria**

The Pierce Two-Node Model (ASHRAE, 1989) for heat balance of a human body is used by considering temperature, humidity, solar radiation, wind speed, clothing, activity, exposure time and regulatory mechanisms that can maintain thermal comfort even under otherwise uncomfortable conditions.

(c) **Wind Chill Criteria**

Wind Chill Index (WCI) (Arens et al, 1986) is utilized to determine an equivalent wind chill temperature:

$$T_{eq} = -0.04544\ (\mathrm{WCI}) + 33^{\circ}\mathrm{C}$$

The minimum T_{eq} is -20°C, translating to a maximum WCI of 1166 kcal/(m^{2}h).

Notes:

(1) These three criteria should be studied concurrently. In order to pass overall comfort in any given hour, all three individual comfort components must pass for that hour;

(2) The wind force criteria, based on authors' experience and literature information, consider safety and comfort levels for various pedestrian activities; and

(3) The frequency of 0.15% corresponds to four occurrences per year, assuming 3 hour events and 24 hours per day.

APPENDIX C

WIND ORDINANCE, CITY BY-LAWS AND GUIDELINES

Listed in this appendix are wind ordinance, guidelines and by-laws for building design and city planning at several cities over the world.

AUSTRALIA

Australian cities like Melbourne, Sydney and Brisbane use the criteria proposed by Melbourne (1978), although specific legislation does not exist. Generally, a wind effect assessment is required for most new developments. This may require a wind-tunnel test or merely a letter from a wind engineering consultant.

BOSTON

The Boston Planning Department in 1986 specified that a wind-tunnel study is required to assess the wind environment conditions near new developments:

(1) for any new building higher than 150 ft;

(2) for any new building higher than 100 ft and at least two times higher than adjacent buildings; and

(3) for other buildings in special circumstances.

CALGARY

Wind environment is considered in Section 42.1 of the city by-laws which states that adverse pedestrian level winds should be mitigated. Consideration of the wind environment near new developments is a discretionary process. For a small building, only a letter from a wind engineering consultant may be required in the environmental review process.

MONTREAL

The City of Montreal in 1992 established the following requirements for the wind environment induced by buildings:

(1) A brief study of the microclimatic impact is required for buildings with the height ranging from 23 m to 44 m and by 1/3 higher than its surroundings in a radius of 50 m; and

(2) A detailed laboratory study is required for all buildings higher than 44 m.

Wind discomfort criteria were also introduced for the evaluation of wind environmental conditions:

(1) the acceptable mean wind speeds are 4 m/s for winter and 6 m/s for summer;

(2) with exceedance frequencies not higher than 5% for rest areas, 15% for dense pedestrian regions and 25% for fast-walking zones.

OTTAWA

The following recommendations regarding the wind environment were made by the Ottawa Planning Branch in 1977:

(1) Wind environment should be considered in the building permit approval process.

(2) Wind tunnel and full scale studies should be conducted to establish the existing

wind conditions in the downtown core and at specific sites.

(3) In the downtown core, the wind environment should be considered under the following conditions:

   (a) open pedestrian areas such as malls, mini-parks, square etc., not including sidewalks.

   (b) buildings adjacent to open pedestrian areas.

   (c) mid-block buildings if the height is at least 1.67 times the average height of surrounding buildings.

(4) The above criteria should be modified, if necessary, after completion of the base data study.

(5) Adopt wind environment guidelines specified by the Toronto Planning Board in 1974.

(6) Consider wind tunnel testing for buildings outside the downtown core.

SAN FRANCISCO

San Francisco adopted a wind ordinance in 1985. Criteria are expressed in terms of the equivalent speed $V_e = \bar{V} + 3V_{rms}$

AREA	V_e (kph)	$P(>V_e)$
public seating areas	11	0.10
areas with substantial pedestrian use	18	0.10
All areas	42	0.0001

If existing conditions exceed these guidelines, attempts must be made to reduce wind speeds if feasible.

TORONTO

Guidelines were introduced in 1974, which were the same as those specified by Isyumov and Davenport (1975a). The following recommendations were also made:

(1) All buildings shall be designed so that wind conditions within the wind impact area meet the guidelines at all levels of public activity.

(2) Where existing conditions exceed any of the guidelines, the builder should consider modifying the form, height or site location of the new building to improve the wind conditions.

(3) Where existing conditions exceed any of the guidelines and they cannot be mitigated by modifying the new building, the builder should provide wind screens, canopies, covered walkways, etc. to provide adequate protection.

(4) Consider the inclusion of calm places (especially in winter) and breezy places (summer) in the design of new projects.

(5) Consider how ground level air quality can be improved in the design of new projects.

(6) Include wind speed indicators visible to public such as weather vanes, flags etc.

(7) New projects that do not require a boundary layer wind tunnel study should meet the intent of the guidelines.

(8) The city should identify those areas where existing conditions exceed 8 on the Beaufort scale more than once a year and (a) provide adequate protection (in the

form of wind screens) for areas in the public realm or (b) ensure that adequate protection is provided for areas in the private realm.

APPENDIX D

EFFECT OF WIND DIRECTION

Rules of thumb, extracted from the literature and the present study, are utilized in the knowledge-based system DEWEN to facilitate the evaluation of pedestrian-level wind conditions around buildings. Their applicability, however, requires further verification. Appendices D - G summarize some rules, empirical relations and additional explanations on building-induced winds. This appendix discusses the effect of wind direction on the influence scale and the overspeed ratio around isolated buildings.

D.1 Effective Influence Scale

In Section 4.2, an influence scale is introduced for rectangular buildings normal to the approach wind. When a building surface is angled to wind flow, the actual blockage, and thus the effective influence scale of the building, will change with the wind direction and the building geometry.

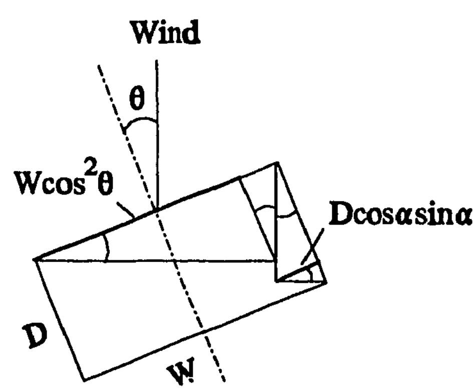

As illustrated at right, the change in blockage is caused by the building area directly exposed to the wind. The projected building width, $W\cos\theta$ and $D\sin\theta$, has the direct impact on the wind flow. In addition, oblique building surfaces may promote transversal air flows, that reduces the down-washing effect on pedestrian-level wind patterns. Therefore, the effective width of a rectangular building may become:

$$W_e = (W\cos\theta + D\sin\theta)\cos\theta$$

where W and D are lengths of windward and side walls, respectively, and θ is the wind incidence. Such an effective building width can then be used with the building height for calculating the effective influence scale.

Note that, for a rectangular building, the effective width W_e has a maximum value at $\tan 2\theta = D/W$ when corner streams are likely to have the highest wind speed around one side of the building, left as in the graph. In contrast, the flow separation around the right side may be migrated to the downwind corner and the intensity of corner streams at this wind direction may be lower than that at $\theta=0°$.

D.2 Variation of Overspeed Ratios with Wind Direction

For an isolated, rectangular building, the following formulas are used in DEWEN to describe the directional variation of overspeed ratios from those at $\theta=0°$, when all modification factors have a value equal to one. These relations are derived for $|\theta|<45°$ from the present study and some previous reports, the latter are specified in the respective notes.

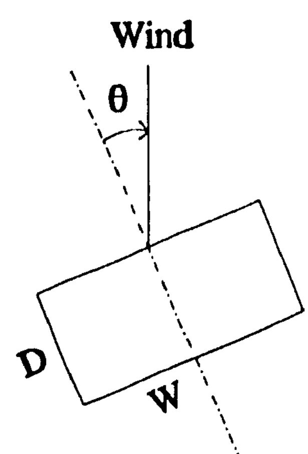

Front Vortex: $1 - 0.2\sin|4\theta|$

Pass-through Flow: $2.17\cos\theta - 1.07\cos^2\theta - 0.1$

Wake Turbulence: $1/\cos^2\theta$

Corner Streams: $1 \pm 0.15 sin(4\theta)$

Notes:

(1) The speed of reversed vortex flow in front of a building decreases about 20% when $|\theta|=22.5^{\circ}$, and bounces back for any further increase of the incident angle owning to the increasing presence of transversal flow, see Penwarden and Wise (1975).

(2) For incident angles from 0° to 45°, the expression for pass-through flow provides similar values (from 1 to 0.9). When the wind is perpendicular to the passage, no significant wind drift is expected inside the passage - 20% of the wind speed at $|\theta|=0^{\circ}$ may be used (Penwarden and Wise, 1975, and Wiren, 1975).

(3) When $|\theta|=45^{\circ}$, the blockage effect of a large building to its wake area is assumed to reduce to a half of that when $|\theta|=0^{\circ}$, i.e. the mean wind speed doubled.

(4) Corner streams should be considered for both sides of the building, with one side (left as in this figure) increasing and the other (right) decreasing for an oblique building. More comprehensive models may be derived using the effective building width and the formula for wind speeds of corner streams (Kamei and Maruta, 1979 and Murakami et al, 1979, Stathopoulos, 1985).

(5) For the gap flow between two side-by-side buildings, $1 + 0.2 sin|4\theta|$ is used as the angle function (Wiren, 1975 and Stathopoulos and Storms, 1986).

(6) All these formulas are also used for the tandem building models.

APPENDIX E

MODIFICATION FUNCTION FOR TANDEM BUILDINGS

This appendix presents an approximation for the modification function for tandem buildings..

The wind flow pattern between two buildings in tandem position has been studied in Section 5.1. The wind speed between the buildings is considered as a modification of that in front of the isolated, downstream building. Results shown in Fig. 5.1.2 could be represented by the modification functions referenced to the overspeed ratio for the isolated, downstream building. The following functions can obtained from the experimental data for describing the effects of the height of front building and the distance between buildings:

$$M_h = 1.6 - 3.8(h/S - 0.4)^2 \qquad \text{when } h/S \leq 0.8$$

$$M_L = 1 + 5(L/S - 0.4)\exp(-(L/S + 0.3)^2) \qquad \text{when } L/S \geq 0.4$$

These two functions correspond to some most critical combinations of tandem buildings as described in Section 5.1. The maximum value is 1.6 occurring at h/S=0.4 for M_h or at L/S=0.84 for M_L. In addition, M_h=1 when h/S=0 or 0.8 and M_L=1 when L/S=0.4 and ∞. Due to the difficulties in measurements and other reasons, there is a lack of data at regions h/S>0.8 and L/S<0.4, where the blockage effect is dominant and the modification functions decrease with an increasing h/S and a decreasing L/S. Based on the these considerations, a general form of modification function is proposed for tandem buildings as the follows:

$M(h/S,\ L/S) = min(M_h,\ M_L)$ when h/S≤0.8 and L/S≥0.4

$M(h/S,\ L/S) = min(1,\ (1 - exp(-25(L/S)^3))S/h)$ Otherwise

This function is a good approximation for the modification function for tandem buildings. Such a function results in the following contours very similar to those in Fig. 5.1.5.

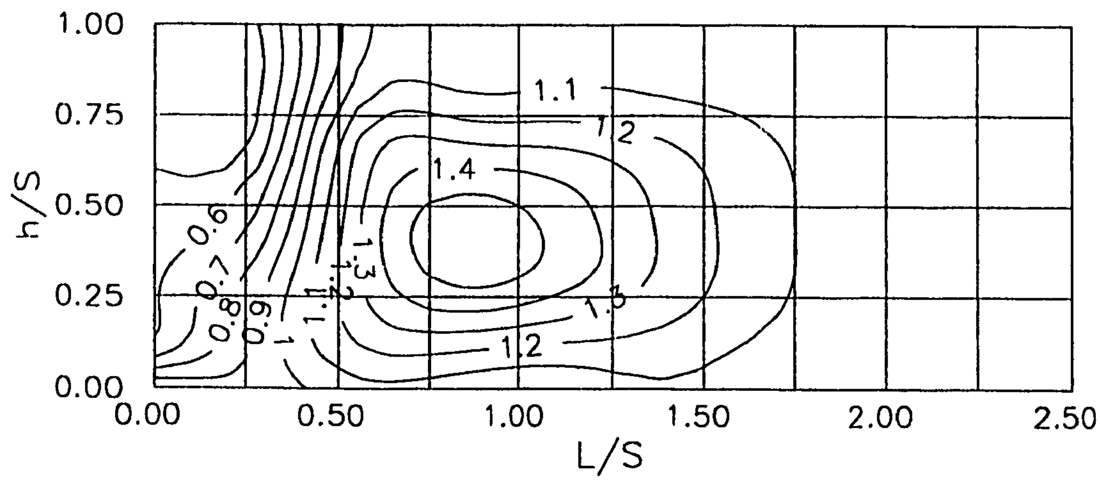

APPENDIX F

WIND CONDITIONS INSIDE COURTYARDS AND OVER OPENINGS

In the computer system DEWEN, Model C refers to a courtyard enclosed or partly enclosed by relatively low buildings. Inside a courtyard, wind conditions are dependent in principle upon the along-wind dimensions of the yard and buildings - see Gandemer (1975) and Ettouney (1975) as well as the distribution of reduced temperatures inside courtyards and the calculated overall impact presented in Section 5.5.

F.1 Inside Courtyards

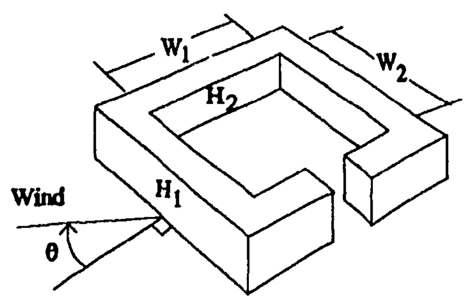

Set W_1 as the average along-wind length of the yard, H_1 as the average height of windward buildings and θ as the wind angle, the average overspeed ratio K can be estimated by

$K = 1 + 0.3|\sin 2\theta|$ when $W_1/H_1 \geq 6$

$K = 0.4 + (W_1/H_1 - 1)(0.12 + 0.06|\sin^2\theta|)$ when $1 < W_1/H_1 < 6$

$K = 0.4$ when $W_1/H_1 \leq 1$

where $|\theta| \leq 45°$.

The wind speed inside a yard may also be affected by the cross-wind dimensions as well - a wider yard has a higher exposure to the wind flow. Therefore,

$$M_1 = 0.4+0.1 W_2/H_2 \qquad \text{and} \qquad 0.5 \le M_1 \le 1$$

where W_2 and H_2 are the average cross-wind length of yard and height of side buildings. In addition, the wind field could be modified by a large upstream building. For a building with the height h and the distance L in front of the windward building of the courtyard, the modification factor is

$$M_2 = L/h \quad \text{and} \quad 0.5 \le M_2 \le 1$$

By combining above factors, the overall overspeed ratio inside a courtyard is evaluated by

$$K_{CT} = K\, M_1\, M_2$$

If there is an opening with buildings, the air flow near the opening will be greatly accelerated. On the other hand, the increasing ventilation through the opening to the yard may lift the air pressure level inside, and consequently reduce the chance of reattachment of the jumping over flow. As the combined result, the average wind speeds inside the yard are expected to be unchanged, unless two or more openings form a channel across the yard along the prevailing wind directions.

F.2 Over Openings

Usually, one or more openings may be designed for building-enclosed courtyards. Over the opening, wind speeds may increase significantly, depending on the opening type, wind direction and building dimensions. The following relations are based on the results of Wiren (1975), Gandemer (1975) and the current study for buildings up to eight storey high.

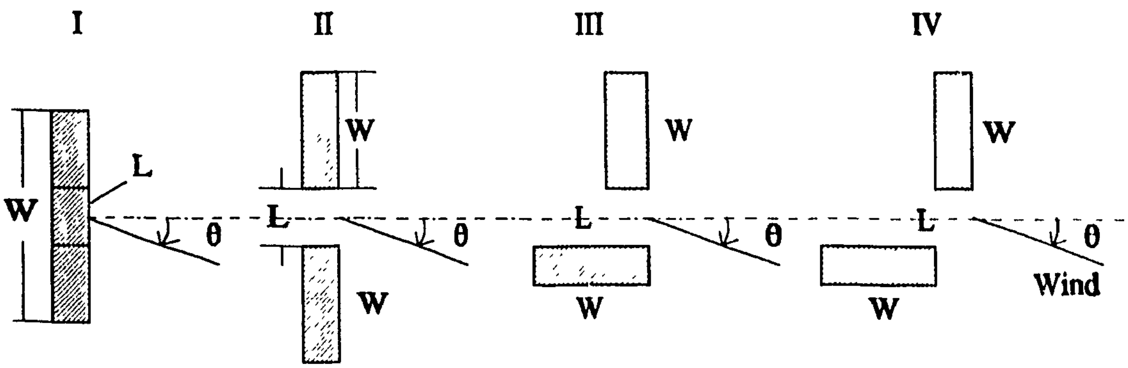

Type I

$K = (1 + 0.03H)f(\theta_1)$

where H = building height

$f(\theta_1) = 1$ when $|\theta_1| \leq 30^\circ$

$f(\theta_1) = 1.25 - \theta/120$ when $30^\circ \leq |\theta_1| \leq 90^\circ$

and $\theta_1 = |\theta - 180^\circ|$ when $90^\circ < \theta \leq 270^\circ$

$\theta_1 = 360^\circ - \theta$ when $\theta > 270^\circ$

Type II

$K = [1 + (35 + H)/100]f(\theta_1)g(L,W)$

where $f(\theta_1)$ is defined as above, and

$g(L,W) = (4W/15L^2)^{1/8}$ is the dimensional factor referenced to the standard buildings of W=60 m and L=4 m.

Type III

$K = [(1.45 - \theta_1/600) + Hsin(2\theta_1 + 10)/48]g(L,W)$

where $\theta_1 = 360^\circ - \theta$ when $\theta > 270^\circ$

and $g(L,W)$ is defined as in Type II.

Type IV

$K = [1 + sin(2\theta)(H/200)^{1/2}]g(L,W)$

where $g(L,W)$ is defined as in Type II.

For Types I and II where the opening is located at the middle of a street block, the blockage effect of a cross-street large building can be evaluated in a way similar to that for the inside wind conditions. If there is an opening with the building across street, forming a channel with the opening of interest, then wind speeds through the opening may be 25% higher than the value provided by above formulas.

The courtyard size also plays an important role in determining the wind speeds through an opening. For all opening types, the modification factor is

$M = 0.2W/H + 0.4$ and $0.5 \leq M \leq 1$

where H is the averaged building height and W is the averaged yard width. A small plan size of courtyard reduces the wind speeds not only over the yard but also through openings.

APPENDIX G

EFFICIENCY OF TYPICAL REMEDIAL ACTIONS

Some typical remedial actions and their efficiency are listed below. See the references for more details.

- Lawson and Penwarden (1975)

  For high efficiency, canopies should be installed at first-floor level. A 6-8 m canopy with 1-2 m parapet may reduce ground-level wind speeds to 1/3.

- Penwarden and Wise (1975)

  A windward canopy may reduce wind speeds on sidewalks to 30% if it is longer than 12 m, to 50% if longer than 6 m, and has no effect if shorter than 4 m. In contrast, a downwind canopy makes no impact on wind flow around a building in any case.

- Wiren (1975)

  For the gap flow between two buildings (24 m in height), a saddle roof with a slope of 2:3 at 4 m height may reduce wind speeds by 20%. For a passage underneath a building, on the other hand, an extended passage can only reduce the wind speeds by 6% to 9%.

- Lee and Hussain (1979)

  Instalment of a pavilion reduces the speed of front vortex to 60%.

- Murakami et al (1979)

  If the maximum mean speed of corner streams around a building of square cross section is 1.0, wind speeds for other buildings with the same height and the same cross-section area are 1.1 for a triangular building with one of surfaces normal to the incident wind, 1.1 for a rhombus building, 0.9 or 1.0 for a hexagonal building with a corner or a surface towards the wind, and 0.9 for an octagonal section regardless of wind direction.

- Stathopoulos (1985)

  The effect of a chamfered corner is significant for the reduction of influence area of speedy wind, but not for the wind speed itself.

- Isyumov et al (1986)

  Around building corners, wind speeds may be reduced 22% at podium and 23% in arcade. At mid-block, the reductions may be 21% and 48%, respectively.

- Stein and Reynolds (1992)

  A strip or belt of trees or shrubs can be used as a wind break. Its efficiency in percent is suggested below for different top profiles, belt densities and distances from the wind break.

Efficiency of Top Profile for Shelter Belts	
High	Irregular Top Profile
Medium	Even Top Profile
Low	Pitched Top Profile

Density of Belt	Average Wind Speed Reduction (%) over First 46m	91m	137m	274m
Very Open	18	24	25	18
Open	54	46	37	20
Medium	60	56	48	28
Dense	66	55	44	25
Very Dense	66	48	37	20